DEVELOPING A BIOMIMETIC IN VITRO MODEL FOR VOCAL FOLD TISSUE ENGINEERING

by

Tanaya Walimbe

A Dissertation

Submitted to the Faculty of Purdue University

In Partial Fulfillment of the Requirements for the degree of

Doctor of Philosophy

Weldon School of Biomedical Engineering

West Lafayette, Indiana

December 2018

THE PURDUE UNIVERSITY GRADUATE SCHOOL
STATEMENT OF COMMITTEE APPROVAL

Dr. Preeti Sivasankar, Co-Chair

Department of Speech, Language, and Hearing Sciences, Purdue University

Dr. Alyssa Panitch, Co-Chair

Department of Biomedical Engineering, University of California, Davis

Dr. Sarah Calve

Weldon School of Biomedical Engineering, Purdue University

Dr. Stacey Halum

Department of Speech, Language, and Hearing Sciences, Purdue University

Approved by:

Dr. George Wodicka

Head of the Graduate Program

Dedicated to Vaishali Walimbe, my Mom and biggest supporter

ACKNOWLEDGMENTS

Attaining my PhD. would not have been possible without the help, support, and encouragement of numerous people who made this journey at Purdue worthwhile. To all, I want to express my most heartfelt thanks.

Firstly, I would like to thank my advisor and mentor Dr. Preeti Sivasankar for her personal and financial support during my PhD. Thank you for being an invaluable guide and mentor to me through all the unpredictable phases of my PhD, and for always having faith in me even when I didn't. This work would not have been possible without you pushing me to ask the right questions and teaching me to critically analyze my own work. I would also like to acknowledge Dr. Alyssa Panitch, my co-advisor, for all of her technical expertise and support that allowed me to pursue my interest in the field of tissue engineering and drug discovery. This work would not have been successful without your patient guidance, critical suggestions and commitment to excellent research. I have truly become a better scientist learning from fantastic role models like my two co-advisors.

I would also like to extend a special thanks to my committee member Dr. Sarah Calve, who has been an unofficial co-advisor to me over the past two years, and has graciously adopted me into her lab so I may be able to complete all my experiments on time. I thank you for your constant invaluable suggestions, critique, and support. I also want to thank my fourth committee member Dr. Stacey Halum for her probing scientific questions that helped guide the direction of my research.

Numerous other people have contributed to this journey, some through technical assistance and intellectual engagement, and others through moral support and friendships. Among these, I would first like to thank Claire for being such an invaluable source of positive

energy and support to me through this time. Thank you for being my best friend and closest lab colleague, and for all your collaborative efforts and helpful advice through this time. Juan Martin, I have enjoyed sitting next to you and troubleshooting all the different twists in our projects together for these past years. Thanks for being a wonderful, always-smiling lab partner to me. Jim, thanks for teaching me how to critically think and solve problems during the formative years of my PhD. You and Maggie have been excellent writing companions during my qualifying exam. Meghan, Divya, Pooja, and all my other friends, thank you for all your conversations and for just being amazing friends in general. I would also like to thank my friends Kapoor, Shrey and Saumya for all the fun times at Purdue and Champaign and for treating me like family. My various roommates – Ankita, Kelly, Elizabeth (and Grim and Trace) and Sneha, thank you for making living at Purdue such a memorable and happy experience for me.

I would also like to thank all the past and present members of the Panitch, Sivasankar, and Calve labs for their support and friendship. They have taught me the true power of collaborations and enabled me to do better research. I would also like to acknowledge my funding sources – the National Institutes of Health/National Institute on Deafness and other Communication Disorders R01DC011759, for providing me with funding for pursuing this research. Additionally, I would also like to thank Tammy Siemers and Sandy May for all the behind the scenes work that they do. Thank you for offering me all the professional and administrative advice and for always ensuring that all the right paperwork is filled out.

A special thanks also goes to Dr. John Paderi and Dr. Kate Stuart, who gave me the invaluable opportunity at Symic Bio to gain practical experience in the startup world of drug development. The scientists at Symic taught me that your passion for doing something good in

the world can go very far, if you work hard and commit to doing the best you can. I am grateful for my experiences there.

And on a more personal note, I would like to thank my Mom and my sister for their unwavering love, staunch support, and constant faith in me. I would not be where I am today without them. I would also like to thank the rest of my family members – my dad, grandma and grandpa, and my uncle for their love and support. Finally and most importantly, I would like to thank Aatithya, who has persevered with me through all highs and lows for these past five years. I am grateful for your extreme patience and encouragement that enabled me to get through this monumental phase in life.

TABLE OF CONTENTS

LIST OF FIGURES

ABSTRACT

Author: Walimbe, Tanaya. PhD.
Institution: Purdue University
Degree Received: December 2018
Title: Developing A Biomimetic In Vitro Model for Vocal Fold Tissue Engineering
Committee Chair: Preeti Sivasankar, Alyssa Panitch

Vocal fold scarring is the fibrotic manifestation of most common pathological voice disorders. Voice disorders lead to direct healthcare costs of over $200 million annually and significantly reduce quality of life for patients. Despite advances in understanding the pathophysiology of vocal fold scarring, effective treatments for scarring and fibrosis remain elusive. The wound-healing cascade associated with vocal fold injury involves complex signaling interactions between cells and their extracellular matrix (ECM), which remain largely unexplored due to the lack of a physiologically relevant preclinical model to study them. Traditional preclinical models do not capture the complex 3D microenvironment of the vocal folds, and the use of stem cells or fibroblasts alone in models has resulted in poor reproducibility and predictability of in vitro models. Toward this end, this work describes the development of a preclinical model that strives to take into account cellular interactions between fibroblasts and epithelial cells and achieve a balance in the native vocal fold 3D environment to function as an in vitro model.

Since a major shortcoming of current in vitro models is the lack of a standardized epithelial fibroblast coculture, initial work focused on developing a coculture system between commercially available tracheal epithelial cells and vocal fold fibroblasts in an *in vitro* setting that would provide more accurate information about the disease pathophysiology and help design better targeted treatments. We designed a healthy and disease state coculture model that can be induced into a fibroplastic state to overexpress stress fibers using TGFβ1. We also demonstrated that both cell types maintained phenotype in the healthy and disease state coculture models.

To further transfer this model in a physiologically relevant 3D system, follow-up research characterized 3D matrices to mimic the native ECM of the vocal folds by using natural biomimetic materials found in the vocal folds such as hyaluronic acid, type I collagen, and type III collagen. We hypothesized that the ability to control the viscoelastic and structural

characteristics of the scaffold in combination with presenting relevant biological cues to cells will result in a better biomimetic scaffold. This research is expected to lay effective groundwork for developing a functional tissue engineered 3D coculture model that retains the reproducibility necessary to serve as a viable diagnostic and therapeutic screening platform.

1. INTRODUCTION

1.1 Motivation

Voice disorders affect between 3-9% of the US population.[1] Dysphonia or difficulty in speaking is severely detrimental to the quality of life of at least 25% of Americans who consider voice as an indispensible part of their work life. The point prevalence rate reported for dysphonia according to a recent study was, however, at 0.98%,[2] implying that even today, a large part of the affected population was not getting the required treatment for their voice problems. Moreover, the direct economic impact of treating laryngeal disorders is estimated between $178 million and $294 million annually,[3] which excludes the research and development cost of prescription drugs, pegged at around $2.6 billion.[4] While a lot of progress has been made recently in current treatment options, treatment of the resulting scar tissue formed due to various voice disorders remains elusive. One specific area that requires attention is the lack of physiologically relevant preclinical models that can screen therapeutics efficiently and predict outcomes in human clinical trials. While animal models are an asset to preclinical studies, the fact that animals do not phonate similarly to humans combined with the variation in vocal fold microstructure between animals and humans result in low predictability of outcomes in humans. Animal models are also slow and expensive to use. An in vitro model of human origin could allow for improved screening of therapeutics and would have the potential to significantly reduce the cost of therapeutic development, as well as increase the speed at which treatments can be made available to patients. This perspective serves as the primary motivation for developing an in vitro model of human origin for the vocal folds.

1.2 Vocal Fold Composition

The vocal folds are mechanically active soft tissues in the larynx that can self-sustain oscillations ranging from 100Hz to 1000Hz in response to airflow in order to produce sound.[5, 6] The ability to sustain small amplitude, high frequency oscillations can be attributed to the anisotropic, layered structure of vocal fold tissue. True vocal folds consist of 5 distinct layers: a stratified squamous epithelium that overlies the heterogeneous, three-layered lamina propria, and

the thyroarytenoid muscle.[7] The epithelial-lamina propria interface contains a basement membrane zone with anchoring fibers that attach the basal cells of the epithelium to collagen IV and laminar proteins.[8] The lamina propria is ECM rich, loose, non-muscular tissue of the vocal folds that is subdivided into three layers known as the superficial (SLP), intermediate (ILP), and deep (DLP) layers of the lamina propria (figure 1-2).[9]

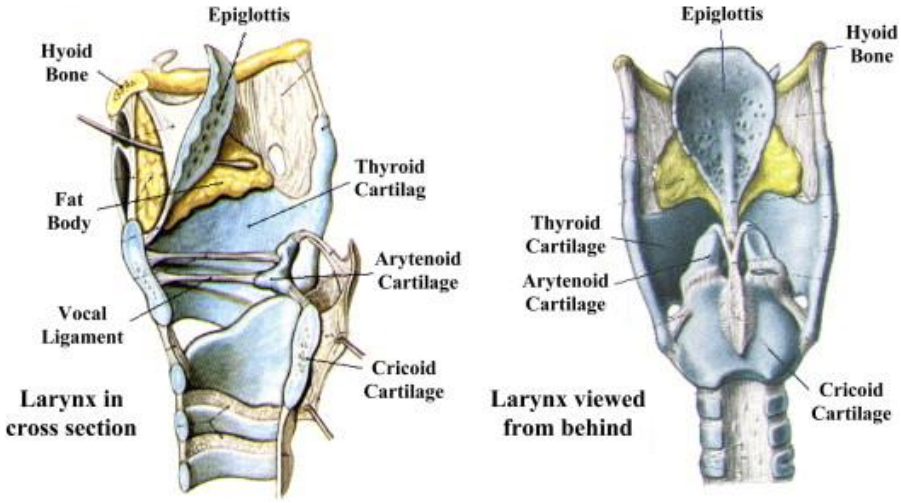

Figure 1-1 Anatomy of the human larynx.
Adapted from Miri et al.[10]

Collagen and elastin are the most abundant fibrous proteins in the lamina propria.[8, 11] Collagen (predominantly type I and type III[12]) constitutes 43% by weight of the total protein in the ECM, and modulates the tensile strength of vocal folds; whereas elastin constitutes 8.5% by weight of the total protein in the ECM and contributes to elasticity and elongation of the vocal folds.[8, 13-15] Histological staining for collagen fibers shows an increase in thickness and density of fibers from the SLP to the DLP.[15-17] Histological staining for elastin reveals that mature, dense, longitudinally aligned elastin fibers are present in the ILP and only minor elastin staining is seen in the DLP. [14, 18]

Apart from these fibrous proteins, the vocal fold ECM also consists of interstitial glycosaminoglycans and proteoglycans such as hyaluronic acid (HA), decorin, fibromodulin, and versican.[8, 19] HA is found dispersed throughout the lamina propria, but is slightly more concentrated in the ILP.[13, 20] It acts as the major modulator of viscoelasticity and osmosis in the vocal folds. It is also involved in migration and wound healing.[21] Other proteoglycans like decorin, which is found mostly in the SLP, and fibromodulin, found mostly in the ILP and DLP,

help in modulating collagen fibrils in the vocal folds by thinning the fibrils and delaying their formation into thicker fibrils, thus supporting the layered structure of the lamina propria.[22, 23] Variations in the lamina propria composition due to gender and age have also been noted with male vocal folds containing higher concentrations of HA and collagen as compared to female vocal folds.[17, 24]

The cellular composition of the lamina propria consists of sparsely dispersed cells such as fibroblasts, myofibroblasts and macrophages.[25] Fibroblasts make up the bulk of the cells in the vocal folds and are essential to generating and maintaining ECM composition. Myofibroblasts are differentiated fibroblasts that stain positively for muscle-specific actin, and are instrumental in injured vocal fold repair.[8] Macrophages are confined to the SLP, and are sparsely distributed. Given that macrophages are mostly associated with wound healing, they may help regulate microscopic damage present in healthy vocal folds due to constant vibration.[25] The regenerative capacity of the vocal folds, however, is limited, leaving them susceptible to permanent irreversible damages, affecting the quality of voice due to altered tissue biomechanics.

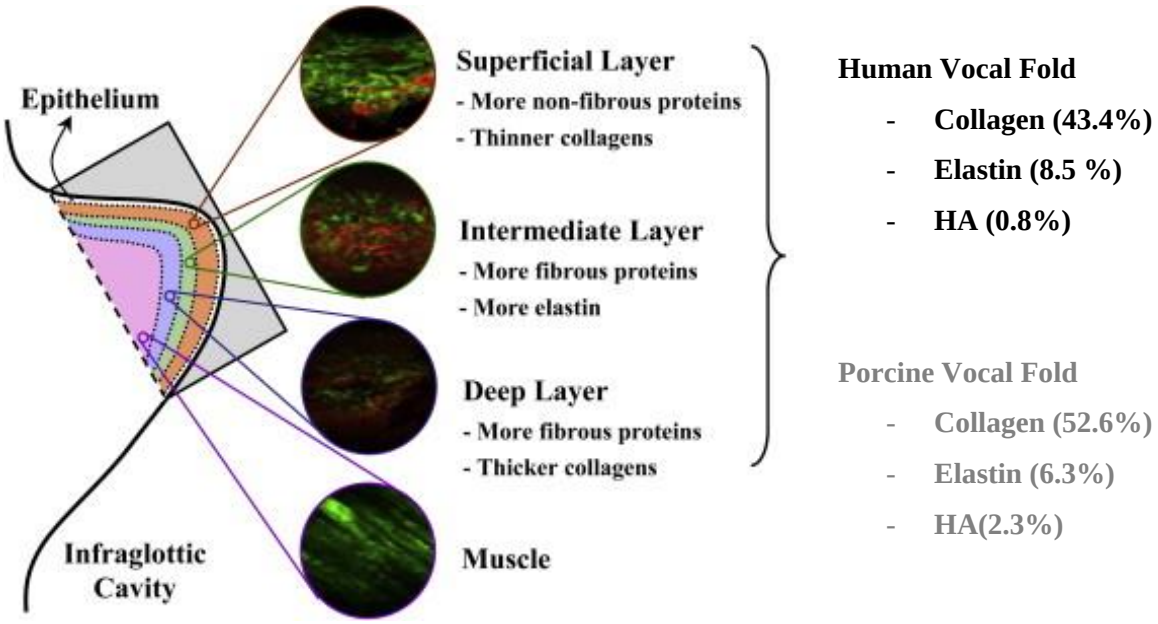

Figure 1-2 Vocal Fold Composition.

The vocal folds consist of multiple layers – an epithelial layer followed by the underlying lamina propria, below which lies the thyroarytenoid muscle. The lamina propria is further subdivided into the superficial, intermediate and deep layer, all of which have different ECM compositions. Adapted from Miri et al.[10]

1.3 Vocal Fold Biomechanics

An understanding of vocal fold cover (epithelium, SLP and ILP)[8] biomechanics provides the foundation required for designing a tissue-engineered model that closely mimics vocal fold dynamics.[26] Viscoelastic properties of the vocal folds are quantified by a complex shear modulus, which is an additive measure of the elastic modulus and the dynamic viscosity.[27] Chan and Titze conducted experiments on human larynges using a parallel plate rotational rheometer with frequencies ranging from 0.01 to 15 Hz and found that the elastic modulus of the mucosa varied from 10-1000 Pa, and the dynamic viscosity decreased monotonically as frequency increased.[27] A follow up study using a controlled strain rheometer allowed for frequency measurements up to 50 Hz[28] and results were comparable to lower frequency data. In order to measure viscoelasticity at physiologically relevant frequencies, alternative strategies have used simple linear, rather than rotational rheometry, allowing for measurements between frequencies of 1-200 Hz. Consistent with prior results elastic moduli were between 20 – 1000 Pa and dynamic viscosity decreased with increasing frequency.[29] Torsional wave analysis, which accounts for anisotropic variations in soft tissue at phonation frequencies,[30] shows that the elastic modulus of excised human larynges (age 60-90) lies between 160 -1600 Pa. Ideally, an elastic modulus within this range should be targeted for tissue engineered scaffolds.

1.4 Vocal Fold Scarring

Damage to the vocal folds and ensuing voice disorders can result from a variety of factors including intubation,[31] phonotrauma,[1] chemical irritants in the environment,[5] and laryngopharyngeal reflux.[1]

Vocal fold lesions that disrupt ECM organization can alter the viscoelastic properties of the vocal folds and result in a hoarse, unsustainable phonation quality.[32] Local macrophages and myofibroblasts are able to repair minuscule damage due to vocal fold edema and inflammation caused by acute phonotrauma.[8, 25] However, when constant damage to the vocal folds occurs, either due to direct injury or external trauma and overuse, permanent pathologic changes can ensue. Chronic, detrimental exposures combined with the high mechanical stresses during phonation can cause permanent changes to vocal fold tissue composition and

biomechanics, which manifest downstream as scarring.[8] Scarred vocal folds suffer from incomplete or compromised mucosal wave formation due to the elevated viscous properties of the tissue and excess collagen deposition[32, 33] leading to an unsustainable phonation quality.

1.4.1 Pathophysiology of Vocal Fold Scarring

A large number of animal models have been studied to understand the biochemistry of scarring.[34-37] Changes in the ECM microstructure and loss of homeostasis are implicated in scarring. Disruption in collagen I deposition is the most common feature of scarring, with studies showing an increase in collagen I and procollagen I levels.[34, 38, 39] Histologically, collagen I loses its longitudinal organization and is instead seen dispersed in disorganized, thick bundles throughout the vocal folds.[34-36, 40, 41] Elastin production is decreased and a loss of organization of fibers in the ILP could explain the decreased pliability of the tissue.[34, 37]

Reduced levels of decorin, which inhibit collagen fibrillogenesis[33, 35], combined with lower expression levels of fibromodulin, which delay collagen synthesis,[33, 42] result in elevated collagen fibril formation, thus decreasing vocal fold flexibility. Fibronectin, which acts as a modulator of inflammation and cell migration during wound healing, is elevated for as long as 6 months post-injury, enhancing migration of fibroblasts and dysregulating collagen morphogenesis.[34, 38, 43] Cellular response includes high density of myofibroblasts as seen through staining for muscle specific actin in scarred tissue. These cells produce collagen continuously, thus adding to the increased tissue stiffness[37], and making phonation difficult.

Optimum levels of HA are responsible, in part, for wound healing processes and scarless wound healing in fetuses.[5] Significant reduction of HA reported in rabbit and pig models[44, 45] could explain the formation of excessive scar tissue and increased stiffness. At the same time, no changes in HA content have been reported in other models.[34, 37] In a recent study, elevated levels of hyaluronan synthase, which synthesizes HA, were reported during the early stages of scarring in rats; while elevated levels of hyaluronidase, which digests HA, were reported 2 months post injury. Combined, these findings could explain advancement to scarring due to loss of HA in later stages of wound healing.[46] Reduction in the shock absorbing properties of the vocal folds due to changes in HA composition could also be responsible for altered biomechanics and poor healing of the tissue.

Since scarring is a macroscopic manifestation of multiple diseases and is known to vary depending on extent of injury and wound healing, treatment is challenging, with methods varying from medical to surgical intervention. But as of yet, no gold standard for treatment has emerged. Tissue engineering provides an attractive alternative to surgery, as it tries to promote wound healing to aid in restoring ECM homeostasis and normal vocal outcomes.

1.5 Tissue Engineering for the Vocal Folds

Tissue engineering can be defined as the application of scientific and engineering principles to the construction, development and maintenance of biological substitutes for living tissues using a structure-function relationship.[47] The aim of tissue engineered vocal fold therapy is to restore native ECM and biomechanical properties that are lost in scarring as well as to suppress progression of scarring using a combination of scaffolds, regulatory signals and cells.

Traditionally, injectable fillers such as Teflon, polydimethylsilicone (PDMS), calcium hydroxypalpitate (CaHA, or Radiesse® Voice) or biological materials such as fat and bovine collagen have been used for treatment of vocal fold scarring in order to increase bulk of the tissue and improve glottal closure.[5, 48, 49] While improvement in rheological properties and glottal closure are observed post-injection, these therapies are more supportive rather than regenerative as they do not repair associated damage with scarring and may also result in long-term complications such as chronic inflammation, implant migration, granuloma formation and quick resorption times.[48, 49] These complications necessitated the development of alternative tissue engineered treatments for the restoration of normal vocal fold function. Type I Collagen or gelatin are heavily explored as biomaterials for tissue engineering applications due to its biocompatibility, nontoxicity, nonantigenic and hemostatic nature. HA, due to its non-immunogenicity, non-antigenicity, innate biocompatibility, tunable viscoelastic properties, and ease of modification, is also one of the most widely researched vocal fold tissue engineering materials. The following sections focus on the roles of collagen and HA in the vocal folds, and their biomaterial based use in vocal fold tissue engineering.

1.5.1 Collagen in the vocal folds

Collagen is the most abundant protein in the human body, accounting for 90% of the total dry weight. In the vocal folds, it exists in high concentrations at approximately 43% of the total protein[15], and plays a pivotal role in imparting unique structural and functional mechanistic properties to the vocal fold lamina propria. There are 28 different types of collagen, among which the vocal fold lamina propria consists predominantly of fibrillar collagen type I and collagen type III. Each fibrillar collagen molecule is composed of 3 parallel polypeptide α-chains that coil to form a triple helix. Type I collagen is a heterotrimer composed of two identical α1 chains, $(\alpha1\ (I))_2$, and one distinct α2 chain, (α2(I)), whereas type III collagen is a homotrimer of three α1 chains $(\alpha1\ (III))_3$. A single collagen molecule, known as tropocollagen, is approximately 300nm in length and 1.5 nm in diameter, and is arranged laterally relative to its neighboring molecules with a regular spacing of 67 nm. This banding pattern is known as the D-periodicity of collagen. Denatured collagen does not associate to form the native D-banding pattern. Although type I and type III collagen are similar molecules with regular D-banding, type I collagen fibrils are thicker (150 nm – 300 nm) in diameter, whereas type III collagen fibrils are thinner (25 nm - 100 nm) in diameter. Fibrils formed by both collagen molecules are stabilized by hydrogen bonds, giving them their characteristic tensile strength, but type III collagen is additionally stabilized with disulfide bonds.

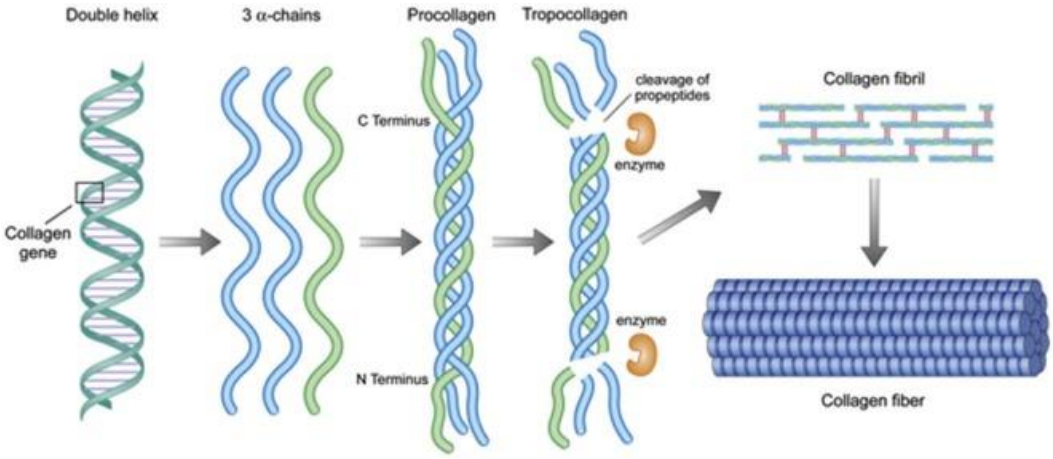

Figure 1-3 Structure of collagen

Collagen contains 3 α chains that assemble into a triple helix known as procollagen. Removal of the N-terminus and C-terminus procollagen peptides results in the formation of tropocollagen.

Tropocollagen molecules self assemble through covalent crosslinking with a D banding pattern of 67 nm to form collagen fibrils, which can further aggregate to form collagen fibers. Image from Tang et al., 2017.[50]

In the vocal fold lamina propria, type III collagen is distributed throughout, whereas type I collagen is found in the superficial and deep layers.[12] Type III collagen constitutes over 40% of the adult LP total collagen[15, 51] and is known to soften collagen type I fibrils[52], which might contribute to the unique elastic and dynamic properties of the vocal folds. Previous studies have shown that type I collagen coexists with type III collagen to form heterotypic fibers, and that this co-existence may be responsible for modulating fibrillogenesis of type I collagen.[53] Collagen is one of the core fibrous proteins responsible for vocal fold tensile elasticity and tissue geometry. Collagen fibers in the vocal fold are stacked top to bottom and cross in the transverse direction, leading to a wavy wicker basket like structure.[54]

Apart from contributing to overall structural and biomechanical backbone of the vocal fold lamina propria, collagens also play an important role in cellular signaling through receptors like integrins and glycoproteins.[55] Signaling by these receptors guides cellular growth, adhesion, proliferation, differentiation, as well as survival of cells, making collagen one of the most important signaling molecules.[56] Collagen therefore, plays an important role in wound healing and tissue repair. Wound healing is characterized by rapid biosynthesis of collagen followed by a cascade of events.[57] Excessive deposition of type I collagen is often used as a marker for fibrosis. Vocal biomechanics can be irreversibly affected by this disruption in collagen organization, and as such, collagen type I has been extensively explored as a potential treatment of scar tissue. Zyderm Collagen Implant I and II, Zyplast, and Phonagel are some examples of bovine soluble collagen injections that have been administered to humans with glottal insufficiency.[50] However, immunologic destruction of the implant and material rejection of these materials has made them less suited for continued use in laryngeal applications. More recently, micronized AlloDerm, a blend of homologus collagen and elastin harvested from cadaveric human skin, has been used as an efficient treatment for patients with incomplete glottal closure. Current advances in the use of collagen and gelatin as tissue engineering scaffolds are discussed below, but first, the significance of HA in the vocal folds, is described.

1.5.2 HA in the Vocal Folds

HA is a naturally occurring glycosaminoglycan consisting of repeating units of D-glucuronic acid and N-acetyl D- glucosamine.[21, 58, 59] (Figure 1-4). It is ubiquitously found in the ECM of all tissues, but is highly concentrated in mechanically active tissues such as the vocal folds, cartilage and dermis. It is synthesized in the inner plasma membrane by a transmembrane protein family called hyaluronan synthases (HAS)[60] and pushed out into the ECM, where it resides for 3-5 days before being degraded by a family of enzymes called hyaluronidases (HYAL).[61] It is the most abundant glycosaminoglycan in the vocal folds, with roughly 6 μg of HA per mg of total protein present at a given time.[13] HA is negatively charged under physiological conditions, and interacts with water to form extensive hydrogen bonds, which allows it to undergo deformation and resist trauma caused to the tissue by expanding up to 1000 times in weight. It thus, acts as a space filler,[22] shock absorber,[23] and tissue damper,[62] which are especially important properties for the vocal folds, since constant vibration results in continuous stresses which need to be absorbed without causing permanent damage. At a physiological pH, the highly polarized HA reacts with ions and is the major modulator of tissue viscosity and osmosis, thus regulating hydration and vocal quality in the vocal folds.[23] Removal of HA from the vocal folds resulted in a 25-40% increase in stiffness of the vocal folds.[59] Alongside, the shear thinning properties of HA reduce vocal tissue stiffness to enable vibration creating optimal conditions for phonation.[59] Additionally, HA is bioactive and has been implicated in cell migration and wound healing responses. Cell surface receptors CD44[63] and receptor for hyaluronan mediated motility (RHAMM)[64] bind to HA and initiate cascades of events such as inflammation, cell motility and cell growth, thus playing an important role in wound healing and aiding the progression to scarring.[21, 65] This bioactivity of HA in promoting wound healing combined with its role in maintaining vocal fold hydration and biomechanics make HA an attractive building block for scaffolds of tissue-engineered vocal folds.

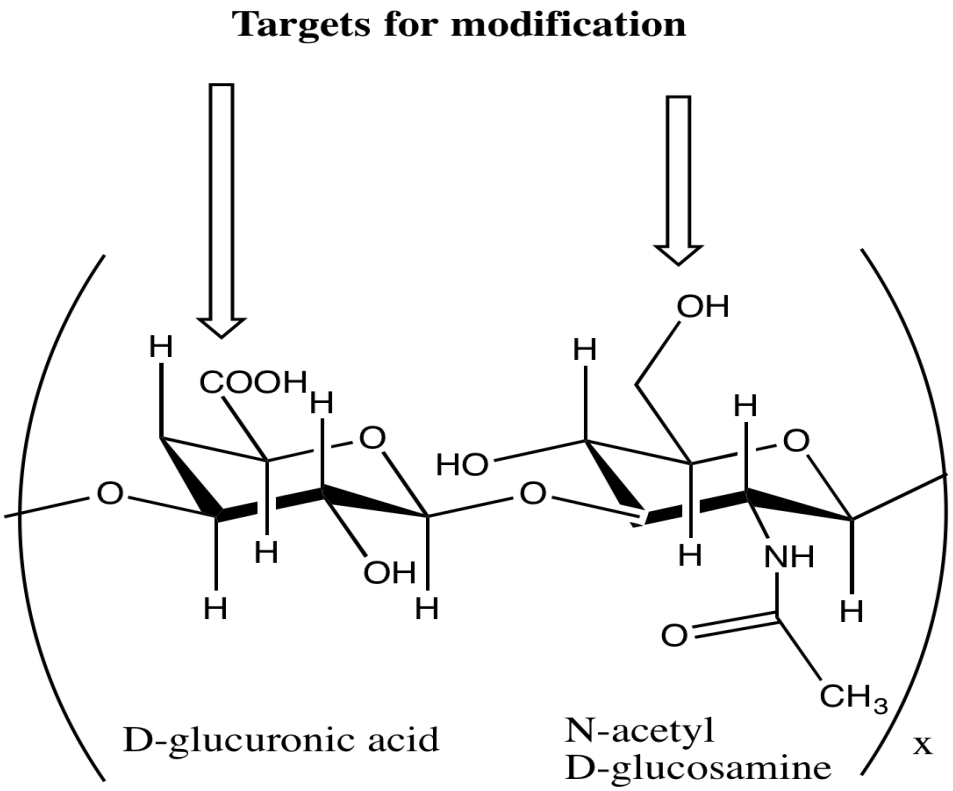

Figure 1-4 Unmodified HA backbone.

Substitutions can be made to the carboxylic (-COOH) or the hydroxyl (-OH) group on the backbone. Adapted from Prestwich et al.[66]

Given the promise of HA for its regenerative capacity, some focus is needed to increase its short half-life. To increase residence time, HA can be functionalized to provide sites for crosslinking, with typical substitutions to the carboxylic group or hydroxyl group on the HA backbone (Figure 1-4). Hylan-B and HYAFF are crosslinked HA gels that have been used for vocal fold augmentation.[67-70] However, these HA based gels used harsher crosslinking chemistries leading to loss of bioactivity. Newer hydrogel combinations have tried to functionalize HA through minimal modifications and milder crosslinking chemistries to preserve its biological activity.

1.5.3 Tissue Engineered Hydrogels using HA and Collagen

Given the importance of HA and collagen in the structural and functional organization of the vocal fold ECM, much research has focused on using these as base materials for 3D scaffolds. Functionalized HA contains crosslinking sites such as thiols, methyacrylates, ahdehyde and dihydrazide groups that can be used to crosslink it to other materials. The following sections talk about the applications of modified HA and collagen hydrogels for vocal fold lamina propria tissue engineering. For ease of distinguishing different HA crosslinking chemistries, sections are divided by the kind of functionalized HA used in the scaffolds.

1.5.3.1 Thiol Functionalized HA hydrogels

In this section, we will review hydrogels that involve modifications to the carboxylic group on the HA backbone (figure 1-4) to provide thiols as sites for crosslinking (Figure 1-5). Crosslinking agents include PEGDA (e.g. Carbylan-SX) and thiolated gelatin (e.g. Carbylan-GSX). Carbylan-SX and Carbylan-GSX can be tuned to have viscoelastic properties within the range of vocal fold tissue[71-73], and slower degradation rates of HA without compromising on biocompatibility by varying parameters such as degree of substitution, concentrations of starting material, ratio of thiols to acrylates, and molecular weights of the HA and PEGDA.[74]

Initial *in vitro* testing of Carbylan-GSX for biocompatibility and non-immunogenicity using both fibroblasts[75] and mesenchymal stem cells showed promising results with lower expression of inflammatory cytokines, and higher expression of ECM proteins. Improved cell adhesion due to Carbylan-GSX caused matrix remodeling guided by cell-ECM interactions.[76] Further, short term and long-term studies using Carbylan-GSX in rabbits have indicated pro-healing responses early during injury, with approach to normal vocal fold viscoelasticity 6 months following treatment.[77-80] This suggests that prophylactic administration of Carbylan-GSX early on during injury can guide improved healing and remodeling processes to restore normal vocal function. Similarly synthesized thiolated HA-Gelatin hydrogels indicate a pro healing response due to ECM remodeling in a rat model.[81]

Alternative strategies have also used thiolated HA to synthesize microgels to harness cell adhesion properties of these gels. Microgels made with thiolated HA-Gelatin (HA-Ge) and reinforced to a composite hydrogel (MRCH) [82] show better adhesion and migration of vocal

fold fibroblasts on these scaffolds in comparison to HA-Gelatin scaffolds without the reinforced microgels. Carbylan-GSX, along with carboxymethylated HA (Extracel), has also been used as a delivery vehicle for combined therapy with bone marrow-mesenchymal stem cells (BM-MSCs) embedded in the hydrogel. Significant improvements in rheological properties and reduction alpha smooth muscle actin expression in rats[83] show that cell-hydrogel combination therapy might work well in reducing myfibroblast differentiation, and thus help restore vocal fold ECM. These promising *in vivo* and supporting *in vitro* studies have paved the way for Extracel to enter planned pre-clinical trial stages.[84]

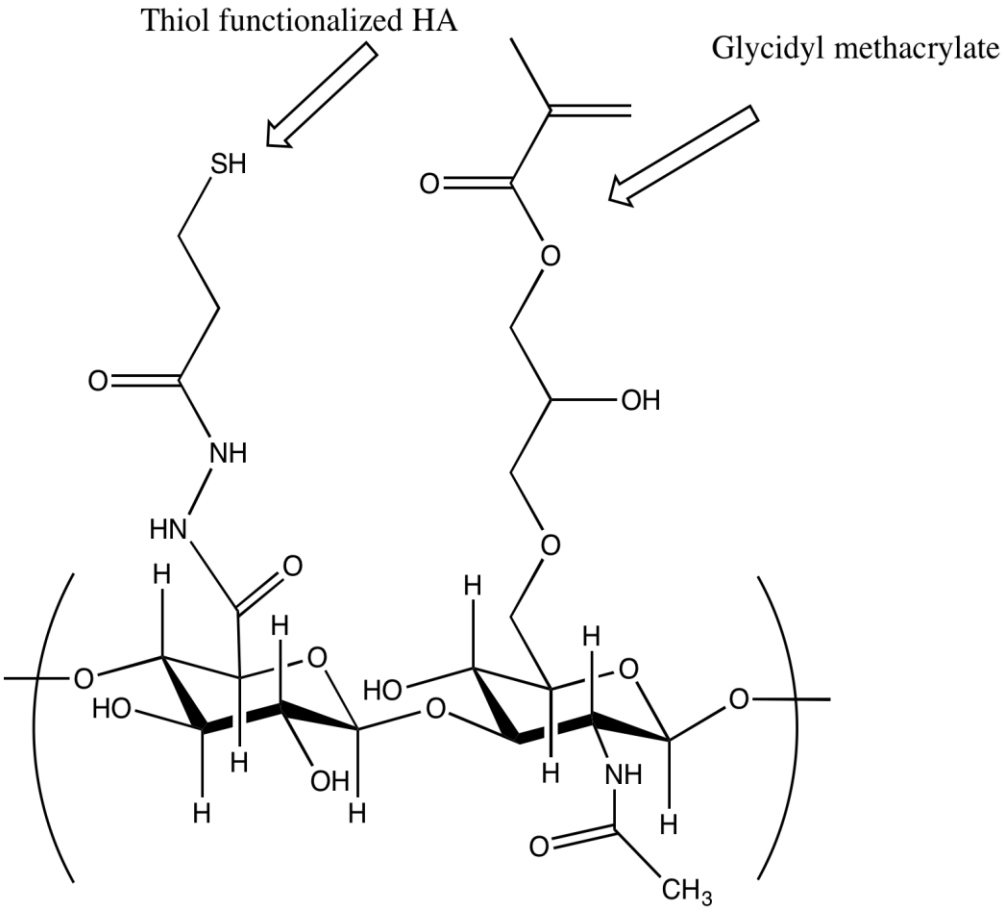

Figure 1-5 Thiol functionalized and methacrylate functionalized HA.
Adapted from Prestwich et al.

1.5.3.2 Methacrylate Functionalized HA hydrogels

In this section, we will review hydrogels that involve modifications to the hydroxyl group on the HA backbone (Figure 1-4) to provide methacrylate groups as sites for crosslinking (Figure 1-5). The advantage of this crosslinking site is that is allows for photopolymerization giving spatial control over gel geometry. HA hydrogels created by reacting photo crosslinkable methacrylate with oxidized HA or oxidized HA with a functional acrylamide[85] resulted in physiologically relevant viscoelastic gels with high degrees of tunability and biocompatibility as shown by their encapsulation of NIH/3T3 cells. HA hydrogels made out of methacrylated HA[86, 87] (Figure 1-5) promote cell spreading and proliferation in 3D networks, showing their ability to support cell adhesion. Further, applying vibration to methacrylated HA which is photopolymerized with PEGDA resulted in a significant decrease in collagen production by human dermal fibroblasts in comparison to static controls. This suggests that vibration can guide ECM changes along with scaffold properties, and hence, restoring native viscoelastic properties may be key to restoring vocal function.

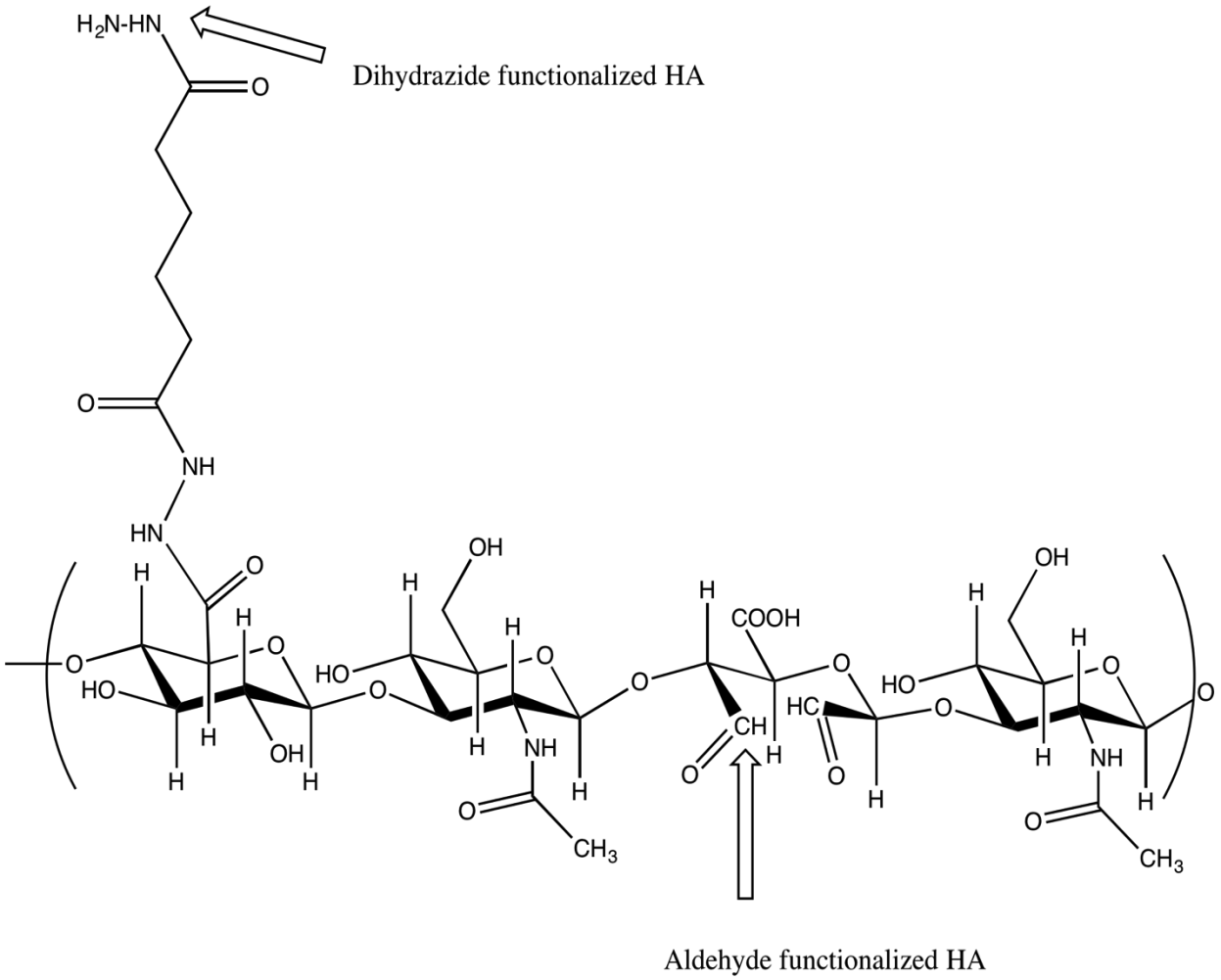

Figure 1-6 Aldehyde and Hydrazide functionalized HA.
Adapted from Prestwich et al.

1.5.3.3 Hydrazide and Aldehyde Functionalized HA hydrogels

In this section, we will review microgels that involve modifications to HA to provide aldehyde and hydrazide functional groups as sites for crosslinking (Figure 1-6). The resultant microgel characteristics allow for controlled degradation profiles, and tunable degrees of functionalization, leading to rapid recovery from mechanical stress. Residual functional groups serve as sites to bind to bulk macromolecules. This is possible because the starting ratios of the aldehyde HA and dihydrazide HA can be independently regulated.[88] These functionalized HA, when used to covalently crosslink with mature or immature collagen fibrils, reduce resorption time of HA significantly. Fibroblasts encapsulated in this gel combination with mature collagen showed proliferation over 28 days and retained their morphology and ability to synthesize ECM.

Histological staining at the end of culture showed much similarity between the scaffolds and native vocal folds, thus showing promise for regeneration.[89] Sahiner et al also these used doubly crosslinked networks consisting of soft HA hydrogel particles modified to contain aldehyde groups in the backbone crosslinked with HAADH,[90] that showed good potential for regeneration due to tailored viscoelastic properties as tested by torsional wave analysis, low gelation time, and high surface area of the networks to improve tissue integration. These hydrazone crosslinked HA gels with dextran when transplanted into ferret vocal folds for 21 days have shown highly tunable crosslinking and viscoelastic properties based on hydrogel compositions, and only mild adverse reactions.[91] Long-term investigations *in vivo* remain to be conducted.

1.5.3.4 Other HA and Collagen Functionalized Gels

Other HA based biocomposite hydrogels include HA-Collagen and Collagen alginate gels investigated by Hahn et al., who reported 50% loss of mass in the collagen HA gels over 28 days; while collagen/alginate gels were stable for at least 42 days *in vitro*, suggesting that alginate/collagen gels are more promising for in vivo implantation.[92] Adipose derived stem cells (ASCs) cultured in cogels[93] of HA or collagen with fibrin showed enhanced potential for differentiation and proliferation in comparison to gels with only fibrin or HA, with elongated cell morphology similar to that of fibroblasts. HA-Alginate hydrogels combined with ASCs[94] implanted into rabbits showed improved macroscopic morphologies in comparison to saline controls showing promise for promoting a healing response. Recently, collagen incorporated into a gelatin sponge has been used as a scaffold system for sustained release of basic fibroblast growth factor.[95]

In summary, biomimetic HA and collagen/gelatin based hydrogels show potential in promoting wound healing and restoring normal vocal function due to their excellent biocompatibility, ability to enhance viscoelastic properties, and regulation of ECM production. Many *in vivo* studies using HA and collagen/gelatin hydrogels have further supplemented the gels with stem cells or growth factors to induce continuous release and restoration. The use of both, HA and collagen has shown potential for recovery from scarring, thus showing that a combination biomaterials approach to healing might be needed for complete regeneration.

1.6 Cell sources

Currently available cell sources for *in vitro* studies mainly include primary fibroblasts obtained from donors, an immortalized vocal fold fibroblast cell line [96], or stem cells differentiated into fibroblasts. Efforts are being made to develop a stratified squamous cell line from human embryonic stem cells, but the long term stability and functionality of these differentiated cells is yet to be validated [97]. The idea of an *in vitro* co-culture as a model system for studying complex tissue response and testing therapeutics is in its nascent stages, with very few experiments being done to this end [71, 97-101]. Due to the lack of an established epithelial cell line, most *in vitro* experiments conducted have been limited to fibroblasts.

For *in vivo* studies, fibroblasts, adipose-derived stem cells (ASCs), bone marrow-derived mesenchymal stem cells (BM-MSCc), adipose derived mesenchymal stem cells (Ad-MSCs) and embryonic stem cells (ESCs) have been used with or without scaffolds in various animal models.

1.6.1 Fibroblasts

Chhetri et al. [102] delivered 3 injections of autologous fibroblasts at weekly intervals directly into the canine lamina propria. After 29 weeks, acoustic performance approached baseline, but an increase in the number of fibroblasts and higher levels of collagen combined with the decrease in levels of elastin indicated incomplete wound healing. Thibeault et al. [103] injected autologous fibroblasts into rabbits with or without a synthetic HA ECM and found that the rabbits with the fibroblasts without the matrix exhibited rheological properties similar to that of control animals. Unfortunately, the potential of this treatment method is limited by the difficulty in harvesting autologous fibroblasts from vocal fold tissue.

1.6.2 Stem Cells

Multiple groups have injected MSCs into the vocal folds of rabbits, with or without scaffolds. Svensson et al. [104] found reduction in viscoelasticity and thickness 10 weeks after MSC injection, but did not find any reduction in collagen I deposition, while Hertegard et al. [105] found improvement in viscoelasticity and reduction in collagen I levels 4 weeks post injection. To increase *in vivo* residence time, Choi et al. [106] embedded MSCs in a collagenous, acellular porcine small intestine submucosa (SIS) scaffold and found improved collagen

distribution and increased HA levels along with still viable MSCs after 8 weeks of treatment. Ohno et al. [107, 108] implanted BM-MSCs with an atelocollagen sponge into canine vocal folds and found similar results. BM-MSCs embedded in an HA matrix known as Extracel were injected in rat scarred vocal folds and shown to increase production of procollagen III and fibronectin, which are essential to wound healing [83]. However, excess amount of myofibroblasts, a marker for pro-fibrosis, were stained in the treated vocal folds, indicating that this treatment method has limited long-term effectiveness.

Adipose derived stem cells have also been shown to be effective at reducing fibrosis and have been shown to synthesize ECM and elongate *in vitro* when seeded in collagen-fibrin or collagen-HA gels [93]. Adipose derived MSCs have shown to increase hepatocyte growth factor (HGF) activity, reduce collagen I disorganization, increase HA and fibronectin levels during acute stages and differentiate into fibroblast type cells after injection into rabbit scarred vocal folds [109, 110].

Long term effects of MSC or ASC injection have not been tested yet, as they possess a risk of malignant transformation *in vivo* especially in a biomechanically active environment. As seen from the above literature, cell based therapies in conjugation with scaffolds result in improved healing and viscoelastic properties. Biomimetic scaffolds are attractive candidates for tissue engineering, as they not only improve the mechanical properties of the tissue, but also present relevant biological cues to cells to support regeneration.

1.7 Preclinical in vitro models currently in use

Few efforts to reconstruct the vocal mucosa *in vitro* in order to better design physiologically relevant models for diagnostic and therapeutic purposes have been undertaken. The lack of a stratified squamous epithelial cell line for the larynx has limited most of these studies conducted to the use of fibroblasts. Recently, some models have tried to address this problem by attempting to reconstruct the mucosa using different types of stem cells induced into a stratified squamous phenotype. While these models show promise, there is no benchmark model made from human primary/immortalized cell origin against which stem cell based models can be evaluated. Advances in the field of tissue engineering have been insufficient due to limited access to disease free epithelial cells and deficient attention to interactions between

different cell types and their ECM. This section will review each of those models and their advantages and limitations.

The first reported *in vitro* model of the vocal fold mucosa was developed by Yamaguchi et al., in 1996 [111]. Porcine fibroblasts were embedded in a collagen I matrix and primary epithelial cells from porcine larynges were extracted, seeded and cultured to confluence on top of this matrix and allowed to grow at an air-liquid interface. Epithelial cells were seeded either on top of cell-free or fibroblasts embedded in a collagen matrix, or in indirect contact with fibroblasts embedded in collagen. The authors found that direct signaling between the fibroblasts and epithelial cells resulted in formation of a better-differentiated stratified squamous epithelium versus when the epithelial cells were cultured on cell-free collagen gels. Interestingly, indirect contact with fibroblasts also resulted in poor stratification and eventual loss of differentiation of epithelial cells. This suggests that direct contacts between fibroblasts and epithelial cells are essential for matrix reorganization and successful differentiation of epithelial cells. The main shortcoming of this model was the lack of reproducibility stemming from the use of highly heterogeneous primary epithelial cells extracted from porcine larynges. While the primary aim was to develop a successful stratified squamous epithelium *in vitro,* further studies to evaluate the integrity of the epithelial barrier and long-term culture conditions were not performed. This limits this system's applicability, as an intact epithelial barrier is essential for a healthy model of the mucosa [112]. While extremely similar to human vocal folds, porcine models have higher levels of collagen and HA levels, resulting in stiffer elastic moduli reported, and thus, do not completely replicate the physiology of human vocal folds and its translation to human health and disease [14, 15, 113]. Therefore a model designed through human origin would provide more relevant information.

Other organotypic models for the vocal folds have attempted using stem cells to circumvent the problem of using primary porcine epithelial cells. Long et al., [114] used adipose-derived stem cells (ASCs) cultured in a fibrin gel in an attempt to reconstruct the vocal mucosa. Transwells were used for culturing the stem cells in fibrin gels reinforced with epidermal growth factor (EGF), fibroblast growth factor (FGF) or no growth factor, and cells were allowed to grow at an air interface. Characterization was done through expression of E-cadherin, an epithelial adherens junction protein [115], and cytokeratin 8, a marker of simple epithelium [116], and vimentin, a mesenchymal cell marker. In an attempt to recreate a bilayer structure including an

epithelium and a lamina propria, they reported that both, physical and biochemical cues using air interface and EGF worked synergistically to result in improved differentiation of ASCs into epithelial cells on the surface and into a mesenchymal phenotype deeper within the fibrin scaffold. While this model has certain advantages, such as a bilayer differentiated successfully into epithelium and mesenchymal cells, it lacks confluency in the epithelial layer and the native ECM organization necessary for an *in vitro* test bed. Further, the study lacked characterization for a myofibroblast phenotype, which is characteristic of profibrosis, and was not optimized for the concentration of EGF or the stiffness of the fibrin gels, both of which might alter behavior of the cells. The use of a growth factor like EGF to drive stem cell differentiation limits the ability of the model to be used as a test bed for screening growth factor therapies.

In a model designed by Imaizumi et al. [101], induced pluripotent stem cells (iPSCs) generated from skin fibroblasts were differentiated into a stratified squamous epithelial phenotype. The iPSCs were cultured in a 3 dimensional HA-PEGDA-Gelatin construct seeded in a Millicell culture well inserts containing membrane filters with either EGF or human vocal fold fibroblasts seeded in the wells the constructs were put into. Differentiation into an epithelial like phenotype was seen in the presence of the hVFFs by 4 weeks of culture based on positive expression of cytokeratin 13 and cytokeratin 14, which are markers of laryngeal epithelial cells. While the use of iPSCs is promising due to their unlimited self-renewal and ease of availability, further characterization is needed to make the model more physiologically relevant. While cytokeratin expression shows the presence of an epithelial phenotype, there is no proof of complete differentiation into an epithelial phenotype only. Future characterization will need to involve probing for a mesenchymal cell type after differentiation, validation of the presence of tight junctions associated with the epithelium, and validation for complete de-differentiation into an epithelial phenotype long term. Though the authors successfully drove differentiation into an epithelial phenotype, use of MilliCell constructs compromised the spaciotemporal organization seen *in vivo* in the vocal folds[9], which limits application of the model to study the effects of direct interactions between fibroblasts and epithelial cells. While it can still provide important information about paracrine signaling, direct contacts have been shown in previous models to enhance stratification, differentiation and proliferation of cells in a heterotypic system [111].

More recently, a breakthrough in developing an *in vitro* mucosa model was reported by Leydon et al. [97], by culturing embryonic stem cells to differentiate into a stratified squamous

epithelium with vocal fold fibroblasts embedded in a collagen matrix. Primary vocal fold fibroblasts were cultured in a type I collagen matrix, simple epithelial cells differentiated from ESCs were grown at confluence on this matrix, and then cultured at an air liquid interface. Media was optimized for the cells, and direct signaling between fibroblasts and epithelial cells was reported to drive differentiation of the simple epithelial cells into a stratified squamous cell type. Expression of cytokeratin 13 and 14, which are markers for stratified squamous epithelium, was demonstrated along with the presence of desmosomes, gap junctions, tight junctions and adherens junctions, all of which are characteristic of the epithelial layer of the mucosa. While these are sizeable advances in the development of an *in vitro* model, certain drawbacks do exist. Staining for the cytokeratins was not uniform among layers of the stratified squamous epithelium, suggesting non-uniform development into a distinctly layered stratified epithelium. Further, the barrier integrity of this epithelium was compromised; making it difficult to use as a model for testing pathological conditions of external challenges and diseases. The potential of ESCs differentiating into malignant cell types due to changes in microenvironment limit the reproducibility of the model and will require precise regulation of the microcellular environment and repeated tests for malignancy. Driving differentiation from simple epithelial cells each time is also tedious and time consuming. Although this model is the closest match to an in vivo stratified squamous epithelium, no efforts were made to characterize the fibroblasts and the matrix environment present below the epithelial cells. It is a relatively well-accepted fact that matrix reorganization and signaling between fibroblasts and epithelial cells lead to regulation of a healthy mucosa *in vivo*. Hence, quantifying changes in the 3D matrix, especially with the use of type I collagen, which is most prone to scarring, need to be conducted.

Most recently, the Welham group described the fabrication of a type I collagen based organotypic model designed by using patient isolated vocal fold fibroblasts and epithelial cells.[117] The resulting engineered biomucosa was not only able to sustain physiologically relevant driving pressures when grafted in canine larynges, but was also successfully able to establish morphologic and proteome level resemblance to the native human mucosa. They also demonstrated the initiation of an immature physiological epithelial barrier function in the model. This well-designed framework offers significant potential for producing a biologically relevant model for vocal fold studies and to date is the closest in vitro mimic of the vocal folds. Nevertheless, although physiological function of the bioengineered mucosa was comparable to

the native vocal folds, it lacked the lamina propria complexity and distribution desired for an in vitro model. The use of relevant scaffold materials that might provide the right microenvironment cues may yield a better biomimetic model. Alongside, primary human donor cells are not easily available for large scale use in vitro, making the model better suited for personalized mucosa replacement rather than use in a laboratory environment.

Two major shortcomings were identified in these models based on this literature survey. First is the lack of a rapid, reproducible, and simple experimental coculture setup with commercially available epithelial cells and fibroblasts. A reproducible coculture based on human cell sources between the two main cell types in the vocal folds is required to study pathophysiology and screen therapeutics efficiently. Second, the scaffolds used to culture cells and develop stratified squamous epithelia in 3D do not mimic the native environment of the vocal folds. The stimuli received by the cells in 3D scaffolds should occur as naturally as possible and mimic the native environment of the vocal folds. The work in this thesis will serve to bridge the gap between these shortcomings as described as follows in the scope of this thesis.

1.8 Scope of this thesis

For the work of this thesis, we focus on engineering a vocal fold lamina propria by strategically combining fibroblasts and epithelial cells into a coculture model and exploring different biomimetic matrices for transferring cells in 3D culture. Chapter 1 focused on the background of vocal fold physiology and the pathophysiology of vocal fold scarring. It then elaborated on the current tissue engineering strategies and cell sources used for vocal fold tissue engineering. This introductory material serves to define the gap this dissertation addresses. Chapter 2 details the design of a scaffold free coculture model between tracheal epithelial cells and vocal fold fibroblasts in an effort to use cell sources that are readily available and are exposed to similar stimuli in vivo as the vocal folds. We focused on developing a model that can mimic healthy and diseased states so it may be useful as a test bed for evaluating therapeutics. Transforming growth factor β1 was chosen to induce diseased state by upregulating the production of α smooth muscle actin, a differentiation marker that is widely implicated in scar tissue formation. The coculture was successfully established when epithelial and mesenchymal phenotypes were maintained in the healthy and disease models. These data were published in the

Laryngoscope. Chapter 3 focuses on evaluating different biomimetic matrices made from natural ECM materials as tissue engineered scaffolds for 3D tissue culture. We hypothesized that the ability to control the viscoelastic and structural characteristics of the scaffold in combination with presenting relevant biological cues to the cells will result in a biomimetic scaffold that can be used as an in vitro platform for testing cellular responses. Since HA and collagen are some of the main constituents of the vocal fold ECM, we chose these natural biomaterials to build novel 3D matrices. We evaluated the structural and biological influence of HA, type I collagen and/or type III collagen scaffolds in a 3D environment in order to evaluate if incorporation of different types of collagens induces differential cell response. Results showed promise in the addition of collagen type III to these scaffolds, which not only improved the mechanical properties of the hydrogels, but also allowed for cell spreading, proliferation, and gene expression pointing towards a healthy tissue microenvironment. Finally, Chapter 4 outlines the proposed next steps of model development and validation and discusses overall conclusions from this thesis.

2. AN IN-VITRO SCAFFOLD-FREE EPITHELIAL-FIBROBLAST COCULTURE MODEL FOR THE LARYNX[118]

2.1 Abstract

2.1.1 Objective

Physiologically relevant, well-characterized *in vitro* vocal fold coculture models are needed to test the effects of various challenges and therapeutics on vocal fold physiology. We characterize a healthy state coculture model, created by using bronchial/tracheal epithelial cells and immortalized vocal fold fibroblasts. We also demonstrate that this model can be induced into a fibroplastic state to overexpress stress fibers using TGFβ1.

2.1.2 Method

Cell metabolic activity of immortalized human vocal fold fibroblasts incubated in different media combinations were confirmed with MTT assay. Fibroblasts were grown to confluence and primary bronchial/tracheal epithelial cells suspended in coculture media were seeded directly over the base layer of the fibroblasts. Cells were treated with TGFβ1 to induce myofibroblast formation. Cell shape and position was confirmed by live cell tracking, fibrosis was confirmed by probing for α smooth muscle actin (α-SMA) and phenotype was confirmed by immunostaining for vimentin and E-cadherin.

2.1.3 Results

Fibroblasts retain metabolic activity in coculture epithelial media. Live cell imaging revealed a layer of epithelial cells atop fibroblasts. α-SMA expression was enhanced in TGFβ1 treated cells, confirming that both cell types maintained a healthy phenotype in coculture, and can be induced into overexpressing stress fibers. Vimentin and E-cadherin immunostaining show that cells retain phenotype in coculture.

2.1.4 Conclusion

These data lay effective groundwork for a functional coculture model that retains the reproducibility necessary to serve as a viable diagnostic and therapeutic screening platform.

2.2 Introduction

In healthy vocal folds, the epithelium serves as a first line of defense, acting as a selective biochemical barrier.[112, 119, 120] Underlying fibroblasts in the lamina propria synthesize most of the extracellular matrix (ECM) in response to autocrine and paracrine signals from the surrounding environment.[121, 122] Homeostasis is thus maintained by complex interactions between various cell types and the ECM.[8, 120, 121, 123] Scarring, the most common cause of vocal deficiencies[5, 35, 39, 48] disrupts homeostasis by causing a cascade of events involving cell signaling, wound healing, and matrix reorganization.[35, 124]

Despite advances in understanding the pathophysiology, effective treatments for scarring remain elusive. While matrix reorganization does take place in the lamina propria, the epithelium is also disrupted upon injury and undergoes restoration.[121] Much research about scarring has focused on lamina propria reorganization using fibroblasts alone[75, 89, 92, 100, 102, 125, 126] or stem cells,[71, 83, 97, 101, 106, 127, 128] and there is emerging evidence on the response of epithelial cells to injury.[97, 123] The lack of an epithelial cell line for the vocal folds, poor proliferative capacity of primary cells, limited viability of ex-vivo tissue, and difficulties associated with handling and cost of animal models have limited investigations into the interactions between the two cell types.

It is widely accepted that cellular and molecular signaling between the epithelial cells and fibroblasts is one of the many factors involved in maintaining homeostasis *in vivo*,[123, 129] but the underlying mechanisms remain largely unexplored. Fibroblasts provide an incomplete picture of wound healing response *in vivo*, since epithelial restoration and signaling events are also likely to play an important role in mediating wound-healing response. While stem cells have advantages such as tunability and increased control of differentiation, there are no models sourced from primary human cells to compare stem cell based approaches to. In order to explore the combination of these epithelial-mesenchymal interactions, our goal was to develop a

reproducible, high throughput, physiologically relevant, *in vitro* bench top model, which takes into account direct interactions between epithelial cells and fibroblasts.

Direct signaling events between multiple cell types have been shown to be crucial in growth, migration, and differentiation of cells.[109, 129-133] Direct contact between cell types can be facilitated in a scaffold-based[89, 97, 101, 114] or scaffold-free[129, 130, 132] platform. Cells respond differently to the material properties of the scaffold.[134] A scaffold-free model enables matrix formation guided by cells themselves based on contact, independent of signaling cues from the scaffold. To investigate whether epithelial-fibroblast interaction, affects cell morphology and phenotype *in vitro*, we established a direct contact, scaffold free cell culture model. We also investigated whether our co-culture model could be induced into an *in vitro* fibroplastic state by the use of TGF-β1. TGF-β1 is a potent cytokine responsible for inducing a wide range of functions such as tissue repair and homeostasis, inflammatory responses, extracellular matrix production and cell proliferation and differentiation.[135] Of particular interest is its ability to induce continuous stress fiber formation and myofibroblast differentiation in fibroblasts, which leads to excess collagen deposition;[122, 126, 136] thus recapitulating an important aspect of fibrotic phenotype *in vitro*. To the best of our knowledge, such an *in vitro* platform to study pathophysiology of TGF-β1 mediated fibrosis and screen for therapeutics does not exist. Based on the assumption that primary cells from the airway are exposed to a similar environment as the larynx and to overcome the shortcoming of limited availability of vocal fold epithelial cells, we chose airway, cuboidal bronchial/tracheal epithelial cells for coculture. This simple coculture model can provide a more physiologically relevant diagnostic and therapeutic platform to carry out more detailed *in vitro* vocal fold research.

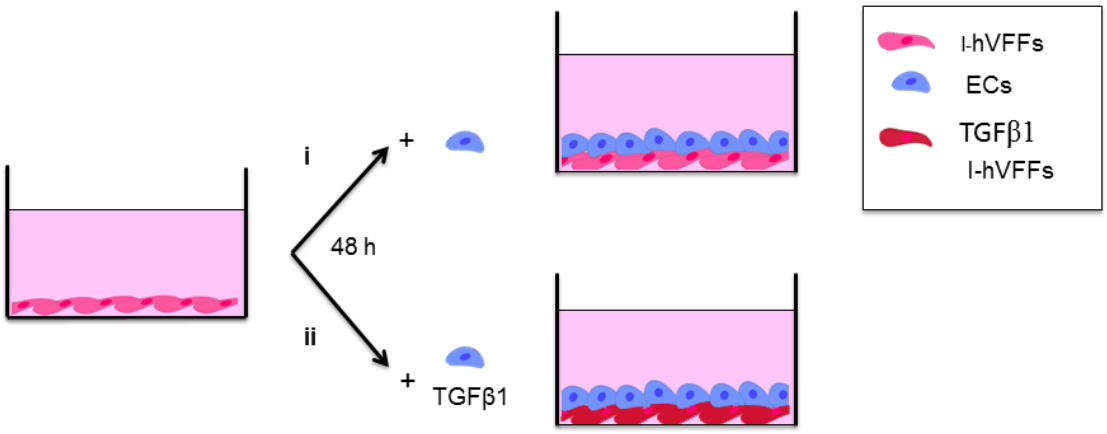

Figure 2-1 Visualization of experimental design.

I-hVFFs were seeded at 3-4 × 10^4 cells/cm^2 and allowed to grow to confluence for 48 hours to enable extracellular matrix formation. After 48 h, ECs were seeded directly on top at a seeding density of 6-7 × 10^4 cells/cm^2, either in (i) complete epithelial media to create a healthy coculture or in (ii) complete epithelial media supplemented with 10 ng/ml TGFβ1 to induce into a fibrotic coculture model

2.3 Materials and Methods

2.3.1 Cell culture

2.3.1.1 Immortalized Vocal Fold Fibroblasts

The immortalized vocal fold fibroblast (I-hVFF) cell line[96] was obtained from Dr. Susan Thibeault at the University of Wisconsin, Madison. The fibroblast culture was maintained in 25 cm^2 tissue-culture (TC)-treated flasks in a 5% CO_2 and 37°C environment in Dulbecco's modified eagle medium (DMEM, Sigma-Aldrich) supplemented with 10% Fetal Bovine Serum (Corning, Corning, NY), 1% Penicillin/Streptomycin (Invitrogen, Carlsbad, CA), 1% MEM non-essential amino acid solution (Sigma-Aldrich, St. Louis, MO) and 200 µg/ml of Geneticin (G418, Teknova, Hollister, CA). Cells from passage 8-12 were used throughout the experiments. All experiments were performed on cell culture treated Ibidi µ-slide Angiogenesis (Ibidi USA Inc., Madison, WI) at an initial seeding density of 3-4 × 10^4 cells/cm^2 unless otherwise mentioned.

2.3.1.2 Primary Bronchial/Tracheal Epithelial Cells (ECs)

Primary bronchial/tracheal epithelial cells were purchased from ATCC (Manassas, VA; Catalog # PCS-300-010) and grown in complete airway epithelial cell serum free basal medium (ATCC-PCS-300-030) supplemented with bronchial/tracheal cell growth kit (ATCC-PCS-300-040) and gentamicin/amphotericin B solution (ATCC-PCS-999-025). The cells were maintained in 25 cm^2 TC-treated flasks in a 5% CO_2 and 37ºC humidified environment. Cells from passage 2-7 were used throughout the experiments at an initial seeding density of $6\text{-}7\times10^4$ cells/cm^2 unless otherwise mentioned.

2.3.2 MTT assay for I-hVFF metabolic activity in coculture media

The effect of different media combinations and cell densities on I-hVFF metabolic activity was tested by using the Vybrant® MTT Cell Proliferation Assay Kit (Molecular Probes, Eugene, OR). The purpose of the assay was to ensure that cells retained metabolic activity at confluence. Cells were seeded in 96 well plates at densities of either 25,000 cells/cm^2 or 37,500 cells/cm^2; and incubated in 4 respective media formulations consisting of: 1) complete fibroblast growth media (control media), 2) complete epithelial growth media, 3) modified media which consisted of complete epithelial growth media with non essential MEM solution and 4) phenol red free complete epithelial growth media. After 48 hours of incubation, 100µL media and MTT solution was added to each well and incubated for 4 hours. 100uL of SDS-HCl solution was then added to each well, mixed thoroughly and incubated for 4 hours to dissolve the formazan formed. Absorbance was read at 570nm on a Spectramax M5 microplate reader (Molecular Devices, Sunnyvale, CA) and was directly co-related with cell viability.

2.3.3 Coculture model:

2.3.3.1 Healthy coculture model

I-hVFFs were seeded and grown for 48 hours to confluence in complete fibroblast growth medium with a media change after 24 hours. ECs were then directly seeded on top of the confluent layer of I-hVFFs, in a suspension of complete epithelial cell media with 2% FBS, which was chosen as the coculture media. After 18-24 hours, the ECs form a layer on top of the I-hVFFs, and are ready to be used as a coculture model (Figure 2-1).

2.3.3.2 TGF-β1 coculture model

TGF--β1 was used to induce stress fiber formation in cells. I-hVFFs were seeded and grown for 48 hours in complete fibroblast growth medium with a media change after 24h. After 48 hours, ECs were seeded directly on top of the I-hVFFs in complete epithelial media containing 10 ng/mL TGFβ1. 18-24 hours after seeding, the ECs formed a layer on top of the I-hVFFs (Figure 2-1).

2.3.4 Live Cell Imaging In Co-Culture

For live cell tracking, I-hVFFs were incubated with 10 μM Cell Tracker™ Orange CMRA (Molecular Probes) for 45mins and washed 3 times with 1X D-PBS. Cells were then trypsinized and seeded at a density of 3×10^4 cells/cm^2. After 48 hours, ECs were labeled with 10 μM Cell Tracker ™ Green CMFDA (Molecular Probes) for 45 minutes, trypsinized and seeded directly on top of the I-hVFFs. Cultures were visualized using a Leica DMI6000 B inverted microscope with an EL6000 external light source (Leica Microsystems, Wetzler, Germany) 24 hours after seeding ECs using a ×10objective. A CooolSNAP HQ^2 camera and Leica application suite (LAS) AF6000 software (Leica Microsystems) were utilized for image acquisition. All images were taken using identical settings for exposure time. Images were edited using ImageJ (National Institutes of Health, Bethesda, MD).

2.3.5 Immunofluorescence studies to assess phenotype

24 hours after seeding ECs in epithelial media containing 2% serum, cultures were fixed in 3% paraformaldehyde for 30 min, permeabilized using 0.5% Triton X-100 (Sigma) in PBS for 30 min, and blocked in 5% milk for 2 hours. Cultures were immunostained for α-smooth muscle actin (αSMA), vimentin and E-cadherin sequentially. To identify stress fibers, cultures were incubated with mouse anti-human αSMA (Sigma; 1:200 dilution) overnight at 4ºC followed by incubation with goat anti-mouse AlexaFluor® 488 (Invitrogen, 1:400 dilution) for 2 hours. To identify I-hVFFs in culture, we used Vimentin, a mesenchymal cell marker. Cultures were incubated overnight at 4ºC with rabbit anti-human vimentin (Cell Signaling Technology, 1:100 dilution), followed by incubation with goat anti-rabbit AlexaFluor® 555 (Cell Signaling Technology, 1:400 dilution) for 2 hours. To identify ECs in culture, we used E-cadherin, an

adherens junction protein. Cultures were incubated overnight at 4^{o}C with rabbit anti-human E-cadherin (Cell Signaling Technology, 1:50 dilution), followed by incubation with goat anti-rabbit AlexaFluor® 555 (Cell Signaling Technology, 1:400 dilution) for 2 hours. Primary antibody was eliminated from the negative control to confirm specificity of secondary antibodies. Samples were washed 3 times to ensure removal of previous antibody. The samples were counterstained with 4', 6 -Diamidino-2-phenylindole (DAPI) for nuclear staining and were visualized using the Leica DMI6000 B inverted microscope at a ×10 objective.

2.3.6 Statistical Analysis

Statistical Analysis was completed using Minitab 17 (State College, PA). The data for the MTT assay are represented as mean with error bars corresponding to standard deviation. Single factor analysis of variance (ANOVA) and Tukey's significant difference post hoc tests were performed to look for differences in both, cell seeding density and different media formulations, and a p value at or below 0.05 was considered statistically significant.

2.4 Results

2.4.1 MTT Assay for I-hVFF Metabolic Activity

Data comparing different I-hVFF cell seeding densities and different media combinations is shown in Figure 2-2. A statistically significant difference in I-hVFF metabolic activity was seen between seeding densities of 37,500 cells/cm^2 and 25,000 cells/cm^2 ($p < 0.05$). To achieve a monolayer of I-hVFFs, cell seeding density of 37,500 cells/cm^2 was selected for all future experiments. I-hVFF viability was highest for control media ($p < 0.05$), but was preserved in epithelial media, which was used as the media for subsequent studies.

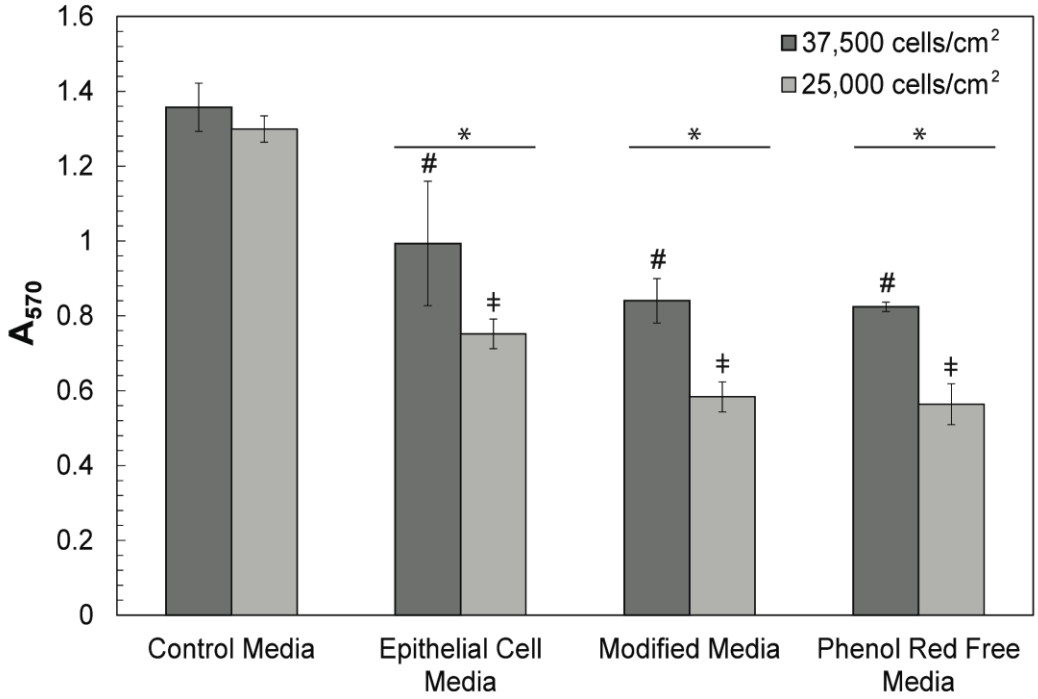

Figure 2-2 MTT assay on I-hVFFs for metabolic activity.
I-hVFFs performed better in epithelial media at a seeding density of 37,500 cells/cm^2 and was hence, chosen for future experiments. As metabolic activity was retained in all medias, epithelial media was chosen as coculture media to ensure that the primary ECs maintain phenotype

2.4.2 Live Cell Coculture Visualization

Fibroblasts and epithelial cells retained viability, as seen from live cell tracker imaging. Fibroblasts displayed an elongated, spindle-shaped morphology and were spread out, and the epithelial cells retained cobblestone-like morphology, and formed a layer on top of the fibroblasts (Figure 2-3).

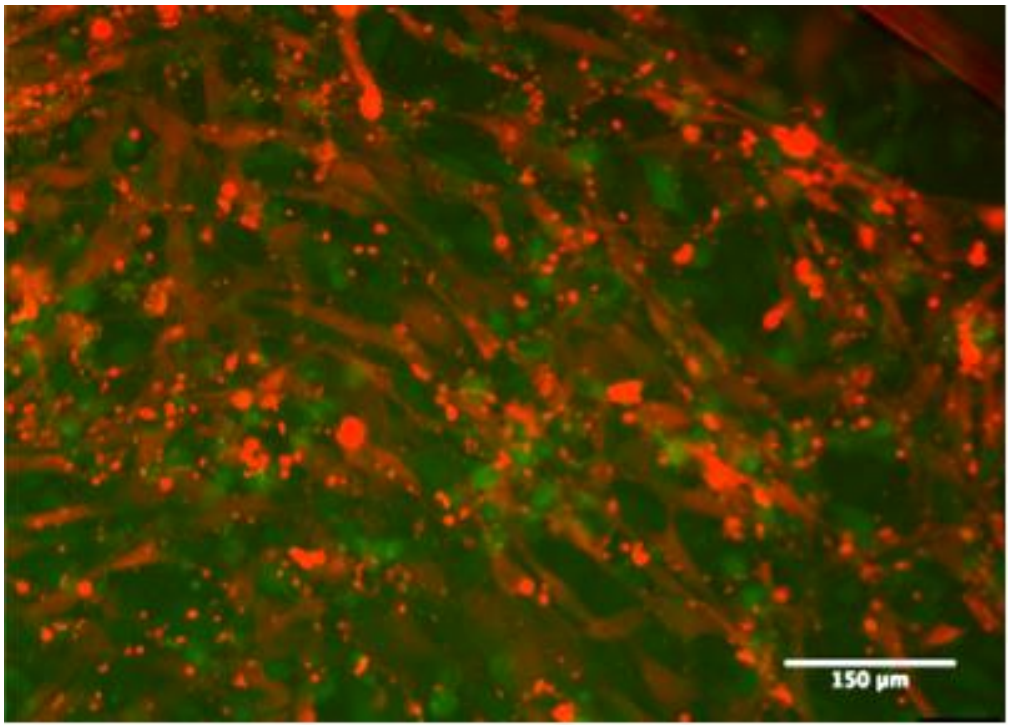

Figure 2-3 Coculture visualization using live Cell Tracker®.
I-hVFFs were tracked with Cell Tracker® Orange CMRA, and ECs were tracked with Cell Tracker® Green CMFDA. Both cells maintain morphology in coculture. Imaged after 24 h of coculture. Scale bar = 150 µm

2.4.3 α-SMA Expression

α-SMA, a well-known marker of myofibroblastic phenotype, was observed in all cells types (Figure 2-4). Induction with TGF-β1 increased stress fiber formation in both, fibroblasts and coculture models, indicating myofibroblast differentiation.

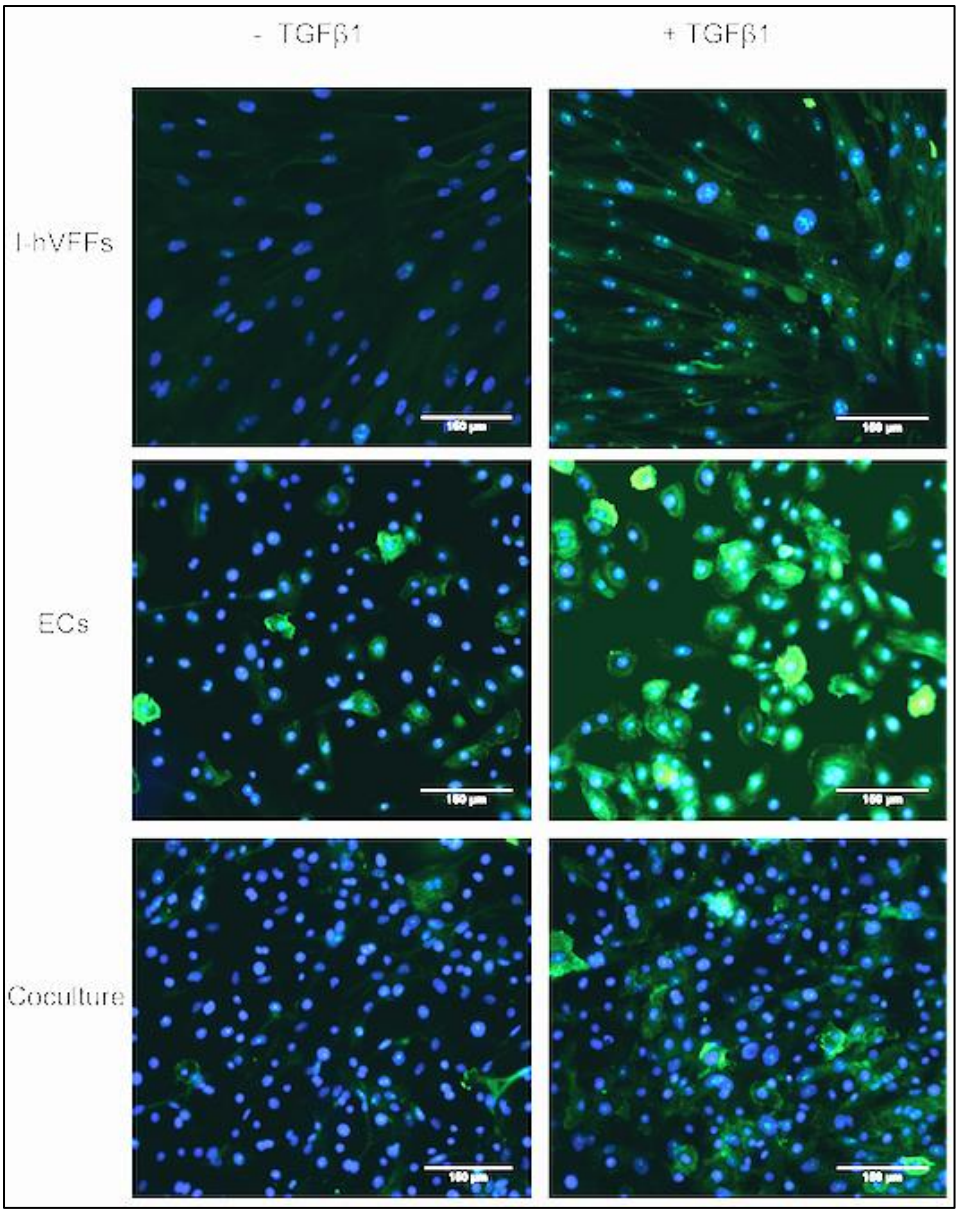

Figure 2-4 Representative images of α-SMA expression in monocultures of I-hVFFs and ECs, and in coculture, with and without addition of TGFβ1.

Increased expression of α-SMA was seen after induction with TGFβ1, suggesting a fibrotic phenotype. Scale bars = 150 μm

2.4.4 E-cadherin Expression

E-cadherin, a common epithelial adherens junction marker, was retained in epithelial cells in monoculture and coculture. E-cadherin expression was maintained after addition of TGF-β1 (Figure 2-5).

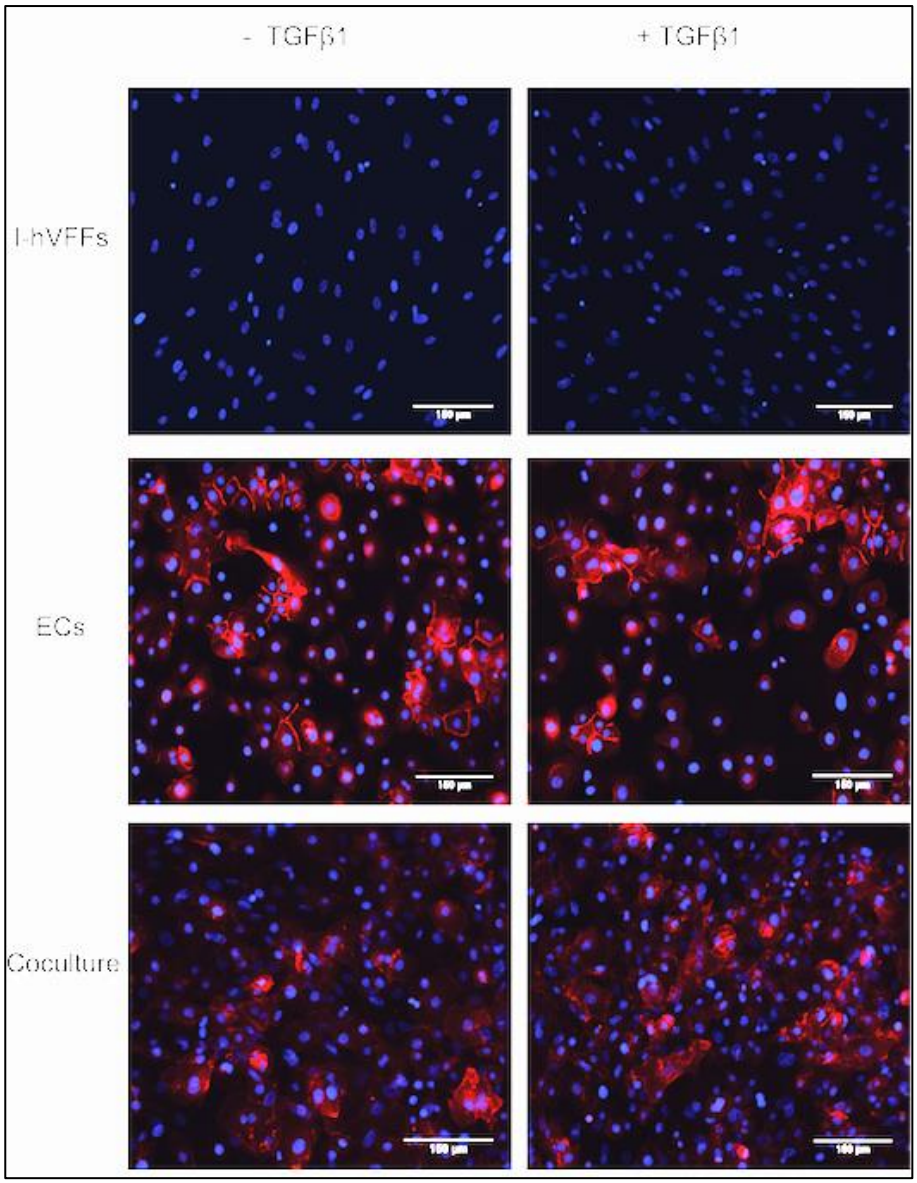

Figure 2-5 Representative images of E-cadherin expression seen in monocultures of ECs and in coculture.
Addition of TGFβ1 did not seem to change expression levels. Scale bars = 150 μm

2.4.5 Vimentin Expression

Vimentin, a common mesenchymal cell marker, was expressed by fibroblasts in monoculture and coculture, with and without the addition of TGF-β1 (Figure 2-6). Mild vimentin staining was observed in epithelial cells.

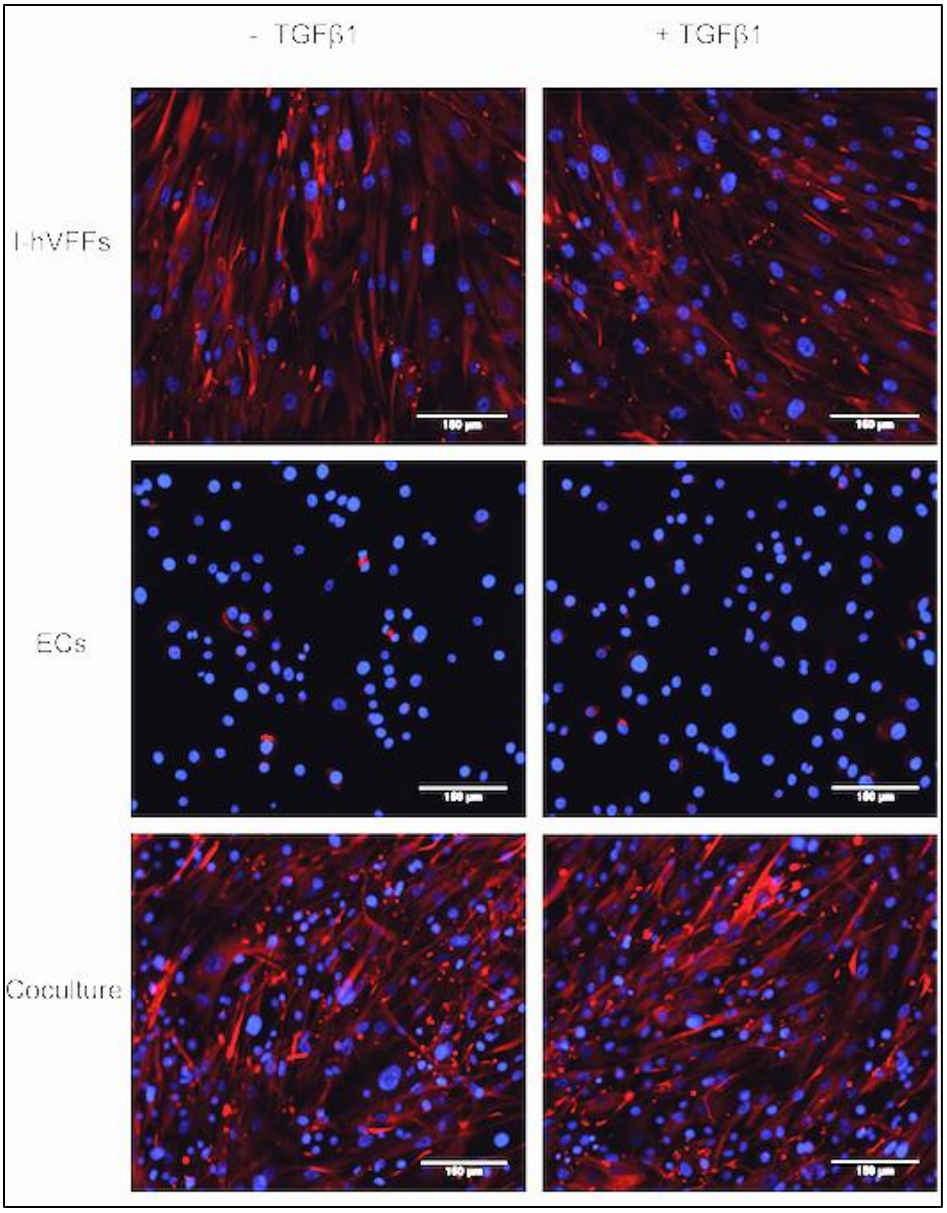

Figure 2-6 Representative images of Vimentin expression seen in monocultures of I-hVFFs and in coculture, with and without addtion of TGFβ1.

Scale bars = 150 μm

2.5 Discussion

Here we characterize a scaffold-free, direct contact epithelial-fibroblast coculture model for the larynx. We demonstrate that both epithelial cells and fibroblasts retain their morphology in coculture, and express cell-specific proteins. We also show that the addition of TGFβ1 induces stress-fiber formation. Activation of myofibroblasts, which express α-SMA, is a characteristic marker of fibrosis.[137] Fibroblasts were grown to confluence for 48 hours to facilitate matrix formation before epithelial cell seeding. This coculture model lays the groundwork for developing a reproducible test bed for high throughput, controlled screening of therapeutics for laryngeal pathologies in the future.

The role of vocal fold epithelium in wound healing response has been gaining increased attention.[123] Vocal fold epithelial cells play a pivotal role as a physical and biochemical barrier.[112, 119, 120] Little is known about the impact of epithelial-fibroblast signaling in the larynx, precluding advances in disease diagnosis and new candidate drug screenings. *In vitro* models provide the advantage of a controlled environment for simulating disease states and screening therapeutics, and are capable of significantly decreasing the cost and amount of time required to screen therapeutics. An *in vitro* direct contact coculture model between primary bronchial/tracheal epithelial cells and vocal fold fibroblasts, two predominant cell types, can enumerate some of the signal transduction and cell-cell interactions *in vivo*.

Current bench top models of the vocal folds use polymeric scaffolds made of collagen, decellularized ECM, hyaluronan or fibrin scaffolds by themselves, or in combination with stem cells and fibroblasts.[97, 101, 114, 138] These models have focused on engineering a functional, multi-layered mucosa but not on establishing a test bed for therapeutics. Our model offers information about cell interactions in fibrotic state while retaining the tunability and reproducibility necessary to serve as a viable diagnostic and therapeutic test platform.

There are some potential limitations to this study. Cell phenotype was maintained in coculture for 24 hours. Future studies will include testing therapeutics in this model. The media for the coculture experiments was epithelial growth media. We chose to use this media because primary epithelial cells are more susceptible to phenotypic changes than immortalized fibroblasts. This might explain why some epithelial cells in monoculture stained for vimentin. Follow-up studies will probe for epithelial-mesenchymal transition using the coculture model. This question is of interest because epithelial-mesenchymal transition, characterized by the reduction in

expression of epithelial adhesion proteins like E-cadherin, and increase in expression of mesenchymal markers such as vimentin and α-SMA, has been associated with multiple diseases such as cancers[139-141] and fibrosis[142, 143] in multiple tissues. The addition of 2% FBS was further shown to preserve epithelial and fibroblast phenotype and hence was used for immunofluorescence studies. Overall, the epithelial cells and fibroblasts survived in coculture and could be induced into a fibrotic model with TGF-β1. While mild α-SMA expression was observed in the control group, significantly higher expression was seen after treating with TGF-β1, suggesting fibrosis. This finding corroborates with published reports.[137] Finally, The use of a non-vocal fold source of epithelial cells is also a limitation. However, cuboidal epithelial cells, which line the airway, are exposed to a similar environment as vocal fold epithelia, and can provide important insights into epithelial-mesenchymal interactions.

In conclusion, we characterized an epithelial-fibroblast coculture. We demonstrated that epithelial cells expressed E-cadherin and that fibroblasts expressed vimentin in coculture at 24 hours. We further showed that the addition of TGF-β1 could induce the model into overexpressing stress fibers. Although, an *in vitro* test bench model has its limitations of being contrived, it provides an important platform for high throughput and targeted screening of a variety of therapeutics before translations into animal models.

2.6 Acknowledgements

The authors thank Dr. Sarah Calve for providing access to her microscope facility. The Purdue Speech Language and Hearing Sciences and Weldon School of Biomedical Engineering supported this work. The study was funded by R01DC011759 (National Institutes of Health/National Institute on Deafness and other Communication Disorders).

3. INCORPORATION OF TYPE I AND III COLLAGENS IN TUNABLE HYALURONAN HYDROGELS FOR VOCAL FOLD TISSUE ENGINEERING

3.1 Introduction

Vocal fold scarring, the resulting complication of nearly all pathological voice disorders, remains one of the most elusive complications to treat medically and with behavioral management.[48] In the case of mechanically active tissues like vocal folds, viscoelastic properties of the tissue govern vibratory mechanics and dictate the cellular and extracellular matrix (ECM) physiology required for phonation.[28] Tissue remodeling during natural wound healing results in excessive collagen deposition and changes in the extracellular matrix organization[33, 35] , which disrupt the viscoelastic properties and cause irreversible fibrosis and depreciation in voice quality.[31] Tissue engineering aims to use biomaterial-based scaffolds, cells and growth factors to intervene during the wound healing process and help sustain regeneration in order to restore native tissue organization.[144] Biomaterial-based scaffolds have the potential to mediate and modulate inflammation as well as proliferation of cells in the tissue, aiming to repair its native architecture.[145] In particular, biological materials from the ECM of the tissue itself are especially attractive, since they can provide the right mechanical and molecular cues for wound healing, along with being highly biocompatible.[146]

In healthy vocal folds, an organized ECM in the lamina propria maintains the viscoelastic properties required for the low amplitude, high frequency vibrations typical in speech.[8] Major components of the ECM include collagen type I and III[15, 147], which provide the tissue with structural support and tensile strength, elastin[148], which provides the tissue with elasticity to sustain vibrations, and hyaluronan (HA)[46], which maintains tissue viscoelastic properties and acts as a shock absorber. Of these, HA is an attractive choice because of its polyanionic nature, bioactivity and ease of tunability.[149] In the vocal folds, HA is known to play a vital role in cell migration, differentiation, and signaling.[62] However, native hyaluronan is difficult to tune and has a low half-life in vivo, where it is degraded by enzymes.[150] Several studies have introduced functional modifications to the HA backbone in order to provide sites for crosslinking.[70, 84, 89, 91] Of these, thiol-modified HA has been shown to be highly

biocompatible for in situ encapsulation of cells.[75] By varying the degree of modification and crosslinker concentrations, HA can be modified to match the mechanical characteristics of most soft tissues.[76] Thiolated HA by itself, however, provides minimal sites for cell attachment and spreading.[151]

An ideal scaffold should provide sites for attachment and spreading of cells, and guide their signaling for regeneration. Many strategies have been developed to improve cell attachment on thiolated HA scaffolds. Several studies have used thiolated HA with crosslinked gelatin to introduce sites for cell attachment through integrin binding and signaling.[75, 79] Gelatin is an unfolded triple helical version of collagen formed by denaturation of collagen type I, and does not mimic the 67nm D-periodicity of fibrillar collagen, resulting in a more disorganized network and different cellular cues in comparison to native collagen.[152] A more optimal approach would include a blend of thiolated HA with collagen, but this blend has not been explored for vocal fold regeneration. Type I collagen by itself or in combination with other modified forms of HA has been used in tissue engineering applications of the vocal folds [89, 92, 95, 107] due to its biocompatibility and role in regulation of cell signaling. Moreover, collagen fibrillogenesis, the spontaneous self-assembly of collagen monomers into fibrils, occurs at physiological conditions[153], making it easy to handle. Collagen type I injections have improved the tensile strength of the tissues and have resulted in better patient outcomes.[154]

Collagen type I and III co-occur in the vocal folds, and make up 43% of its total protein,[15] out of which type III collagen constitutes more then 40%.[51] To date, collagen type III has not been explored as a therapeutic candidate for vocal fold regeneration. Type III collagen is upregulated during development[155] and in wound healing.[156] Furthermore, addition of type III collagen to type I collagen has been shown to regulate its fibril diameter, and results in heterotypic fibers that are more compliant[52, 157]. Therefore a scaffold consisting of both, type I collagen and type III collagen, might lead to a scaffold closely mimicking in vivo tissue environment.

The goal of this study was to create novel hydrogel blends with thiol modified HA, type I collagen, and/or type III collagen blends in order to harness the mechanical stability and tunability of HA and the biological activity of the collagens in cell spreading and signaling. We hypothesized that the incorporation of collagen would make the hydrogel blend more similar to native tissue architecture. Self-assembly of soluble collagen into fibrils depends on pH,

temperature, ionic strength, and surfactants.[158] Electrostatic interactions between HA and collagen are also known to affect collagen fibrillogenesis.[159, 160] Collagen fibril formation is predominantly governed by hydrophobic interactions between non-polar regions of adjacent molecules. In order to form stable interpenetrating collagen fibrils within the highly hydrophilic nonfibrillar HA network, we reduced the net neutral charge on the hydrogel by increasing its pH[161] in order to drive collagen fibrillogenesis at a faster rate. The resulting gel is an interpenetrating fibrillar network of collagen within a nonfibrillar porous matrix formed by HA. The effects of different types of HA - collagen blends on hydrogel microstructure, cell viability and proliferation, and gene expression were evaluated to identify better suited candidates for vocal fold tissue engineering applications.

3.2 Materials and Methods

3.2.1 Hyaluronan modification

Hyaluronan (HA) (MW 100 kDa, Lifecore Biomedical LLC, Chaska, MN) was thiolated according to previous protocols.[76] Briefly, HA was dissolved at 10 mg/mL in degassed Milli-Q water. Dithiobis (propanoic dihydrazide) (DTP, Frontier Scientific, Logan, UT) was added at a ratio of 2 mol DTP: 1 mol HA while the solution was stirring, and the pH was lowered to 4.75 by using 1N HCl. Next, 1-ethyl-3-[3-(dimethylamino)propyl] carbodiimide (EDC, Thermo Scientific, Waltham, MA) was added and the pH was maintained at 4.75 for 15 mins. Adding 1N NaOH to raise the pH to 7.0 stopped the reaction. Dithiothreitol was then added in at least 5-fold molar excess relative to the concentration of DTP to cleave the disulfide bonds and the pH was raised to 8.5 with 1N NAOH. After 24 h, the pH was lowered to 3.5 using 1N HCl and the solution was dialyzed against HCL solution (pH 3.5, 0.3mM) with 100 mM sodium chloride (NaCl) for 2 weeks. Substitution of the glucuronate carboxyl groups by thiol groups was determined using an Ellmans assay to quantify free sulfhydryl groups. Final percent substitution of the HA was determined to be 12% and was used for all further experiments.

3.2.2 Hydrogel Preparation

Poly(ethylene) glycol diacrylate (PEGDA, MW 3400, Alfa Aesar, Tewksbury, MA) was used as a bifunctional electrophilic crosslinker that reacts with the substituted thiol groups on

hyaluronan via Michael-type addition. The hydrogel was formed by mixing HA, PEGDA, and different formulations of collagens to form HA, HA-Col-I, HA-Col-III and HA-Col-I-Col-III hydrogels. Stock concentrations of HA and PEGDA were prepared at 3.75% and 7.18% (w/v) in PBS respectively by solubilizing them and adjusting the pH to 7.8 using 1N NaOH. The solutions were filtered through a 0.2 u Syringe filter (Supor). Stock concentrations of rat-tail collagen type I (BD Biosciences, Franklin Lakes, NJ), and bovine collagen type III (MilliporeSigma, St. Louis, MO) were prepared on ice at 10 mg/mL in sterile 20 mM acetic acid. The pH of the collagen solutions was adjusted to 7.4 on ice using sterile 10× phosphate buffered saline (PBS), 1N NaOH and 1× PBS. The neutralized, ice-cold solutions of HA, PEGDA and collagen were mixed to form gels at a final concentration of 1.5% (w/v) HA, 0.718% (w/v) PEGDA, and 4 mg/mL type I collagen and/or 4mg/ml type III collagen.

3.2.3 Rheological Characterization

The viscoelastic mechanical properties of the gels were tested on an ARG2 rheometer (TA instruments, New Castle, DE) using a 20 mm parallel plate geometry and a gap of 250-400 um. The gels were prepared on Teflon coated slides (Tekdon) and allowed to polymerize for 3 h before running frequency sweeps. The linear range of viscoelastic response was measured in triplicate with a frequency sweep from 0.1 to 100 rad/s at a controlled stress of 1 Pa.

3.2.4 Cryoscanning Electron Microscopy (CryoSEM) for Hydrogel Microstructure

CryoSEM was performed at the Purdue Electron Microscopy Facility to analyze the microstructure of the HA-collagen gels. Hydrogels were prepared on SEM stage holders and incubated for 2 h at 37 ^{o}C to allow polymerization. The sample holders were then moved to a cryo holder, flash frozen by immersing in liquid nitrogen and moved to a Gatan Alto 2500 prepchamber under vacuum to be fractured. Once fractured with a scalpel, the samples were sublimated at a temperature -90 ^{o}C for 10-15 mins and sputter coated with platinum. Images were taken on the FEI NOVA nanoSEM at a microscope temperature of – 140 ^{o}C using the Everhart-Thornley (ET) detector at 5kV with a spot size of 3. All samples were tested in triplicate.

3.2.5 Hydrogel Swelling Ratio

Hydrogels were placed in 1X PBS at 37 ^{o}C for 48 Hours. Swelling ratio (Q) was calculated as the ratio of the weight of the swollen gel to the weight of the dry gel. Swollen gels were weighed and washed 5× with distilled water and then dried under vacuum for 3 days to determine the weight of dry gels.

3.2.6 Degradation of HA in hydrogels

The biocompatibility of the modified HA in the HA collagen blend gels was measured using a modified carbazole assay according to previous methods.[162] HA, HA-Col I, HA-Col III and HA-Col I-Col III gels were evaluated in this study. Hydrogel blends were polymerized in four chamber slides (Nunc Lab-TekII, VWR Scientific). The slides were left at 4 ^{o}C overnight for curing. For each hydrogel blend, three replicate gels were incubated with hyaluronidase (50 units ml^{-1} in PBS) at 37 °C. At selected time points of 0, 2, 4, 6, 8, and 10 h, 750 µl of hyaluronidase enzyme solution was removed and replaced with an equal amount of fresh enzyme solution. Amount of thiolated HA degradation was measured by the release of glucuronic acid into the supernatant using a modified carbazole assay in a 96-well plate format. The absorbance of the collected solutions was measured on the M5 microplate reader at a wavelength of 550 nm. Percent HA degradation was calculated across all time points for the gels.

3.2.7 Cell Encapsulation in hydrogel blends

Immortalized human vocal fold fibroblasts (I-hVFFs) obtained from Madison, WI[96] were trypsinized, counted and pelleted to a final concentration of 1×10^{6} cells/mL and resuspended in gel solution for embedding. 10 uL aliquots of the cell-gel suspension were placed onto ibidi u-slide angiogenesis (Ibidi inc). The slides were placed in an incubator (37 ^{o}C and 5% CO_2) for 3 h to allow complete gelation, after which complete I-hVFF medium [Dulbecco's Modified Eagles Medium (DMEM, Sigma) with 10% FBS, 1% Pen/Strep, 1% minimal essential medium (MEM) non-essential amino acid solution (Sigma), and 10 mg/mL geneticin (Teknova)] was added to the wells.

3.2.8 Cell Viability and Cytoskeleton Organization

To visualize cell viability, the cell gel constructs were stained using the live/dead cytotoxicity kit (Invitrogen). Constructs were harvested at days 1, 7, 14, and 21 and stained with 4uM calcein AM and 6 uM ethidium homodimer-1 in PBS for 30 mins. Adding ethanol to one of the constructs for 45 mins was used a dead cell control. To observe actin staining, the constructs were fixed in 4% paraformaldehyde (PFA) for 30 mins, permeabilized with 0.1% Triton X-100 for 30 mins, blocked with 5% milk for 2 h, and stained with Alexa Fluor 633 Phalloidin (Invitrogen) and DAPI for 1 h. The stained constructs were imaged using a Ziess 720 confocal microscope.

3.2.9 Assessment of new DNA synthesis in encapsulated cells

The EdU proliferation assay was used to quantify cell proliferation in gels according to previous methods.[163] EdU was added to each well at a final concentration of 1 uM for 10 h for days 1, 7, 14 and 21. The gels were then fixed with 4% PFA for 30 min, rinsed 3X with DPBS, permeabilized with 0.5% Triton-X 100 for 30 min, rinsed, blocked using 5% milk for 2 h, and incubated with Alexa Fluor 488 conjugated azide (Invitrogen) diluted in 1M Tris (pH 8.5), 25 mM copper (II) sulfate and 0.25 M ascorbic acid.

3.2.10 Gene Expression for ECM constituents

Quantitative reverse transcription-polymerase chain reaction (qRT-PCR) was used to analyze expression of ECM related genes for I-hVFFs embedded in the different hydrogel blends. Once harvested, the constructs were digested in hyaluronidase (7500 U/mL) for 45 min, centrifuged and lysed. RNA was extracted from the constructs using QIAshredders and RNeasy mini kit (Qiagen, Frederick, MD) using the manufacturers protocol. The purified RNA concentration was measured using a NanoDrop 2000 spectrophotometer. The RNA was then reverse transcribed into cDNA using the high-capacity cDNA reverse transcription kit (Applied Biosystems) following manufacturers instructions. qPCR was performed for 40 cycles using the TaqMan gene expression mastermix (Life Technologies, Waltham, MA), TaqMan probes for COL1A1, COL3A1 Decorin, Fibronectin, and MMP1, and an Applied Biosystems 7500 real-time PCR machine. The cycling conditions were: 50 ^{o}C for 2 min, 95 ^{o}C for 10 min, and 40 cycles of 95 ^{o}C

for 15 sec, and 60 ^{o}C for 1 min. Data was normalized to B-actin, which was used as an endogenous control. Each individual sample was tested in triplicate. Data was analyzed using the comparative Ct method to show fold difference in gene expression compared to control (HA gels).

3.2.11 Statistical Analysis

Data are represented as means, with error bars corresponding to standard deviation. Single factor equal variance ANOVA and Tukey's post hoc tests were performed using Minitab for analysis of rheology, swelling ratio, degradation, proliferation and gene expression. A probability value of 95% ($P < 0.05$) was used to determine statistical significance.

3.3 Results

3.3.1 Gel Preparation

Preliminary experiments to incorporate collagen in the thiolated HA scaffolds by raising the pH of the gels between 7.2-7.4 were unsuccessful because the collagen precipitated out in solution once the gels were swollen. Stable incorporation of collagen in the HA-PEGDA gels was achieved by increasing the rate of collagen fibrillogenesis by neutralizing its pH to 7.8, which is close to collagen's isoelectric point.[161] Four types of hydrogel blends were evaluated in this study: HA alone, HA with type I collagen (HA-Col I), HA with type III collagen (HA-Col III), and HA with type I collagen and type III collagen (HA-Col I-Col III).

3.3.2 Rheological Characterization

Rheological tests were performed to examine the mechanical properties of the different gel blends. Frequency sweeps run between 0.1 - 100 rad/s showed that the hydrogels containing collagen have a higher storage modulus (G') and loss modulus (G'') in comparison to HA alone ($P<0.05$) (Figure 3-1). Overall, the HA hydrogel was the weakest, with a G' value of 188.5 ± 24 and a G'' value of 1.2 ± 0.86 at 1 rad/s. The addition of collagen enhanced the mechanical properties of the gel by increasing the linear viscoelastic range, as well as increasing the elastic response of the gels, with G' values ranging from 954.9± 74.5, 881.7 ± 70.9, and 812.4 ± 175.3 at 1 rad/s for the HA-Col I, HA-Col III and HA-Col I-Col III gels, respectively. At 1 rad/s, all

hydrogel blends containing collagen were significantly different in comparison to the HA alone gel ($P<0.05$). The addition of collagen increased the viscous response of the gels, with G'' values ranging from 26.5 ± 8.59, 17 ± 3.39, and 18.1 ± 16.96 at 1 rad/s for the HA-Col I, HA-Col III and HA-Col I-Col III gels, respectively.

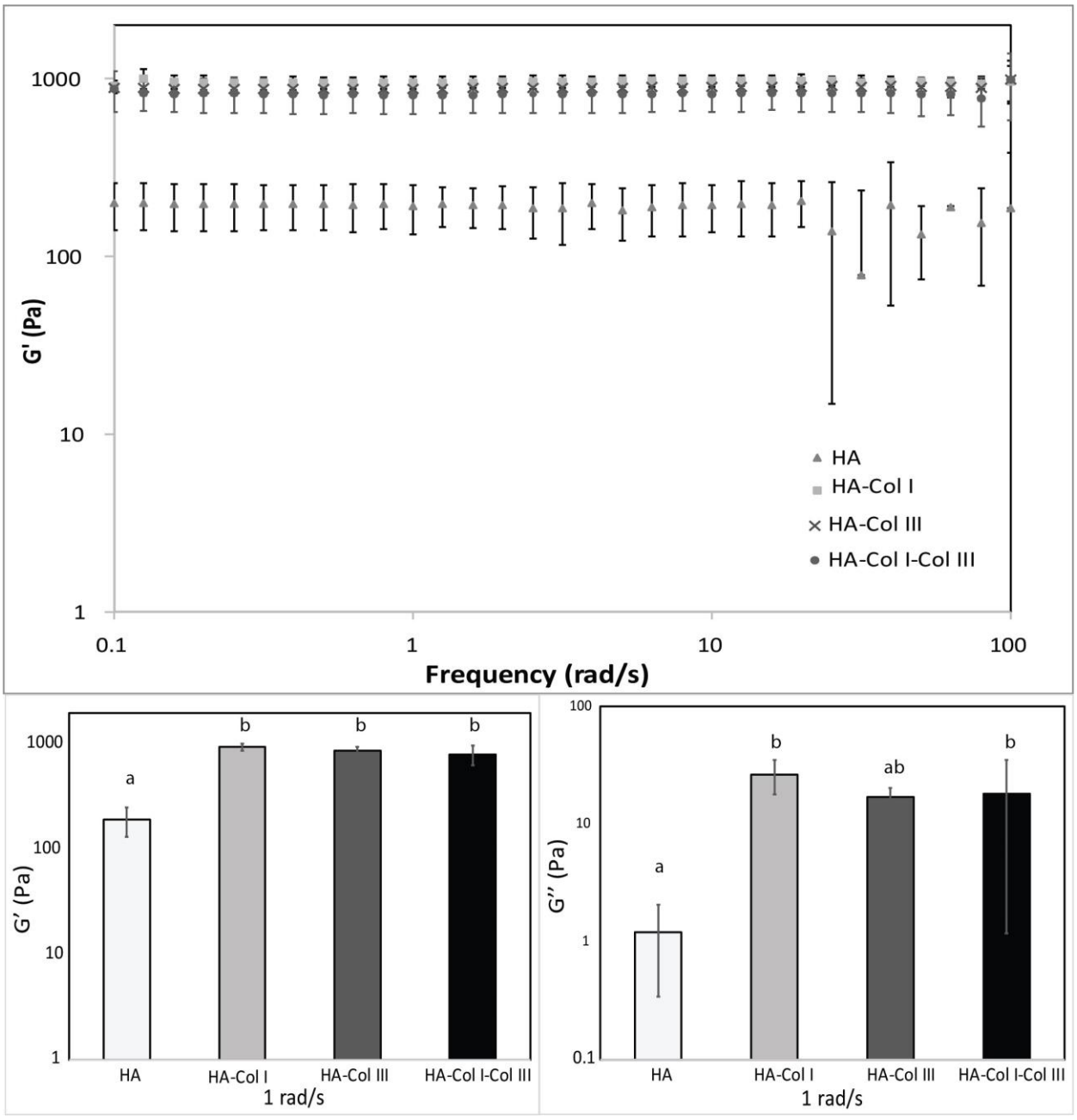

Figure 3-1 Rheological Characterization of Hydrogel Blends.

At 1 rad/s, storage modulus (G') and loss modulus (G'') values of HA alone hydrogels were significantly different in comparison to HA-Col blended hydrogels ($P < 0.05$). Error bars show standard deviation. The addition of collagen improved the mechanical properties of the hydrogels, with an increase in the linear viscoelastic range as well as G' and G'' values.

3.3.3 Hydrogel Microstructure using Cryo-SEM

Cryo-SEM was performed to evaluate the network structure of the hydrogel blends. (Figure 3-2). For the HA alone gels, the large non fibrillar porous structures appeared circular. Collagen within the HA can be seen as interdigitated fibrillar networks within varying pore sizes for all HA gels with collagen. A closer inspection of the images points to subtle qualitative differences between the HA-Col I, HA-Col III and HA-Col I-Col III gels. The fibrillar elements in the HA-Col III gels appeared smaller in comparison to the ones in HA-Col I or HA-Col I-Col III gels. HA-Col I-Col III gels appear to have long interpenetrating fibrils in comparison to the short fibrils seen in HA-Col I and HA-Col III gels.

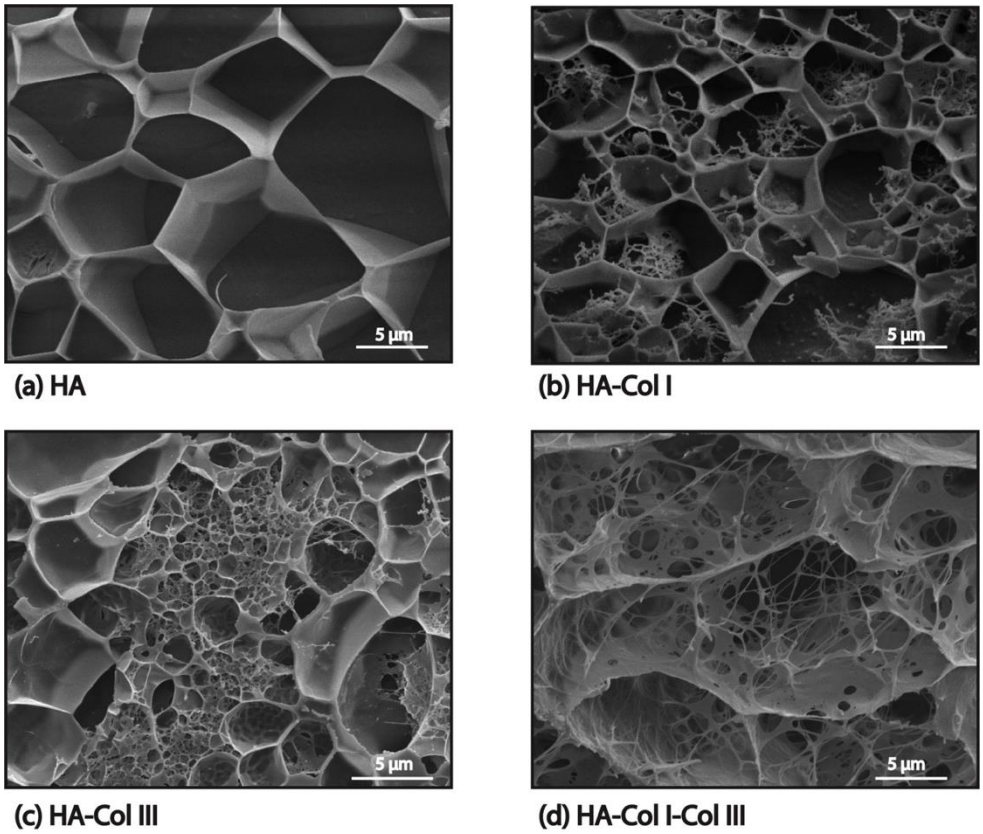

Figure 3-2 Representative Cryo-SEM Images of Hydrogel Blends

Incorporation of collagen can be seen by the interpenetrating fibrillar structures in the honeycomb like non fibrillar HA. Scale bar = 5 µm.

3.3.4 Hydrogel Swelling Ratio

To quantify the swelling ratio of the hydrogels, gels were swollen to equilibrium for 48 hours in 1X DPBS, weighed, then dried using a lyophilizer and weighed again to get their dry weight. HA hydrogels are known to swell to a large extent without dissolution of the gel. This is evident by the high swelling ratio of = 34.6 ± 3.82 for HA-only gels. (Figure 3-3). Addition of collagen to the HA hydrogels significantly reduced the swelling ratio of the hydrogels ($P < 0.05$). This is not surprising, as fibrillar collagen hydrogels are known to not swell.[164] Despite this reduction, all hydrogels have a relatively high swelling ratio, making them highly permeable, which could facilitate the exchange of oxygen, nutrients, and other water soluble metabolites.

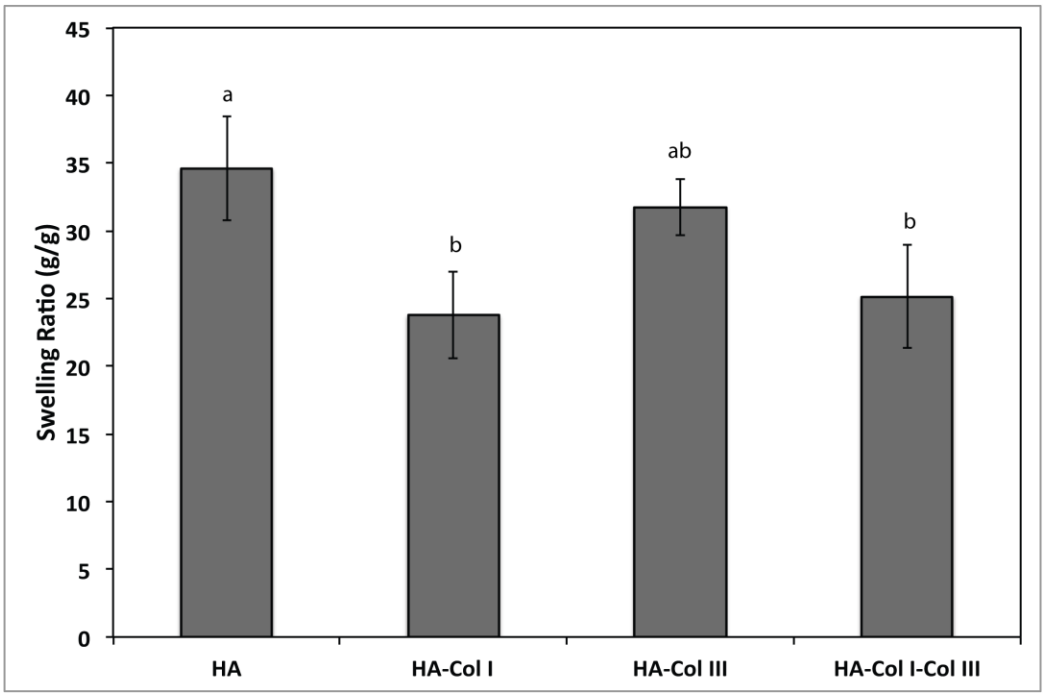

Figure 3-3 Swelling Ratios for Hydrogel Blends.

Means that do not share a letter are statistically significant ($P < 0.05$). Addition of collagen decreased the swelling ratios of the HA hydrogels.

3.3.5 Degradation of HA in hydrogels

Enzymatic degradation of the hydrogels was monitored to mimic in vivo conditions by incubating the gels in hyaluronidase solution. Hyaluronidase cleaves β-N-acetyl-hexosamine-(1 → 4) glycosidic bonds in HA, releasing glucuronic acid residues, which can be measured through the carbazole assay. At 10h, more than 90% of the HA in the HA gels had degraded, but only more than 60% of HA-Col I, HA-Col III, and HA-Col I-Col III gels had degraded in the presence of enzyme (Figure 3-4). In sum, addition of both type I collagen and type III collagen, reduced the amount of HA degradation after hyaluronidase by atleast 10%.

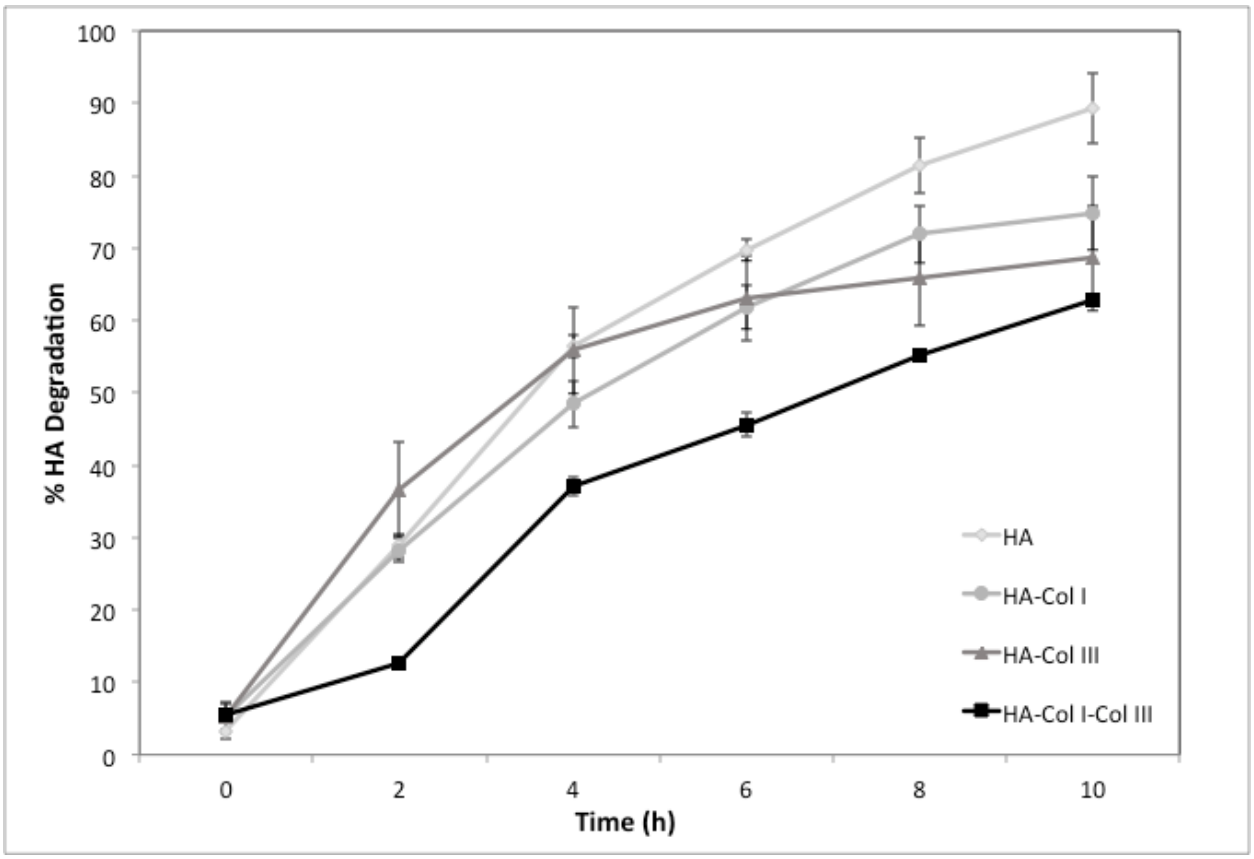

Figure 3-4 Hyaluronidase Degradation of Thiolated HA in Hydrogels Blends.

Reduced degradation of HA was seen with the addition of collagen, correlating with the reduced swelling ratios of the hydrogels containing HA and collagen. Error bars depict standard deviation.

3.3.6 Cell Encapsulation, Viability and Cytoskeletal Reorganization

Encapsulation of cells in the hydrogels was achieved by mixing the cells with HA, PEGDA and collagen type I and/or type III followed by a two hour incubation at 37 ^{o}C. Majority of cells remained viable at day 1 in all hydrogels as seen by the live/dead assay, showing that the in situ encapsulation process was biocompatible (Figure 3-5). The cells appeared to be live and densely populated at 21 days, showing viability in 3D culture in the HA-Col blend gels throughout time of culture. However, the majority of the cells in the HA alone scaffold had migrated away from the scaffold due to lack of adhesion to the HA.

To assess cell morphology and cytoskeletal organization, the cells were stained with phalloidin, which binds to the actin network in the cells. At day 1, the cells showed a rounded morphology in all the gels (Figure 3-6). By day 7, the cells in all HA-Col hydrogels appeared to be distinctly elongated and more spindle shaped, showing organized cytoskeletal networks. The cells maintained this elongated morphology in the HA-Col hydrogels until the end of culture at day 21, pointing towards the role of collagen in providing a matrix for cellular attachment and signaling. The cell morphology and distribution appeared similar across all the different HA-Col hydrogels. Cells in the HA alone gels, however, failed to attach and spread like the ones in HA-Col gels, owing to the lack of polar adhesion forces and proteins required for cell spreading.

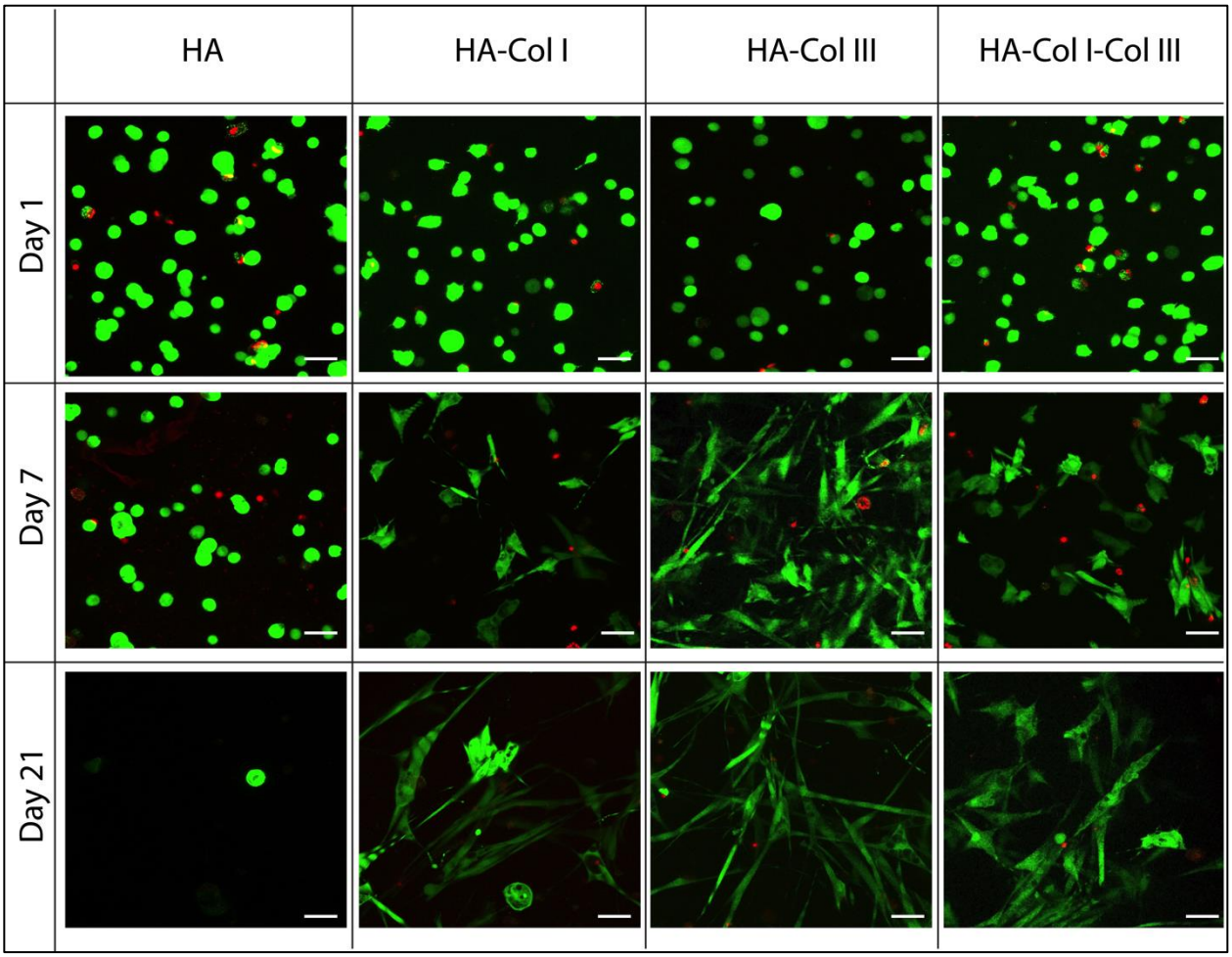

Figure 3-5 Live Dead Viability Assay on Fibroblasts Encapsulated in Hydrogel Blends Over 21 Days.

Calcein AM in green stains live cells and ethidium homodimer in red stains dead cells. Majority of the cells in the HA-Col blend hydrogels remained viable even at the end of 21 days of culture. Scale bar = 50 μm.

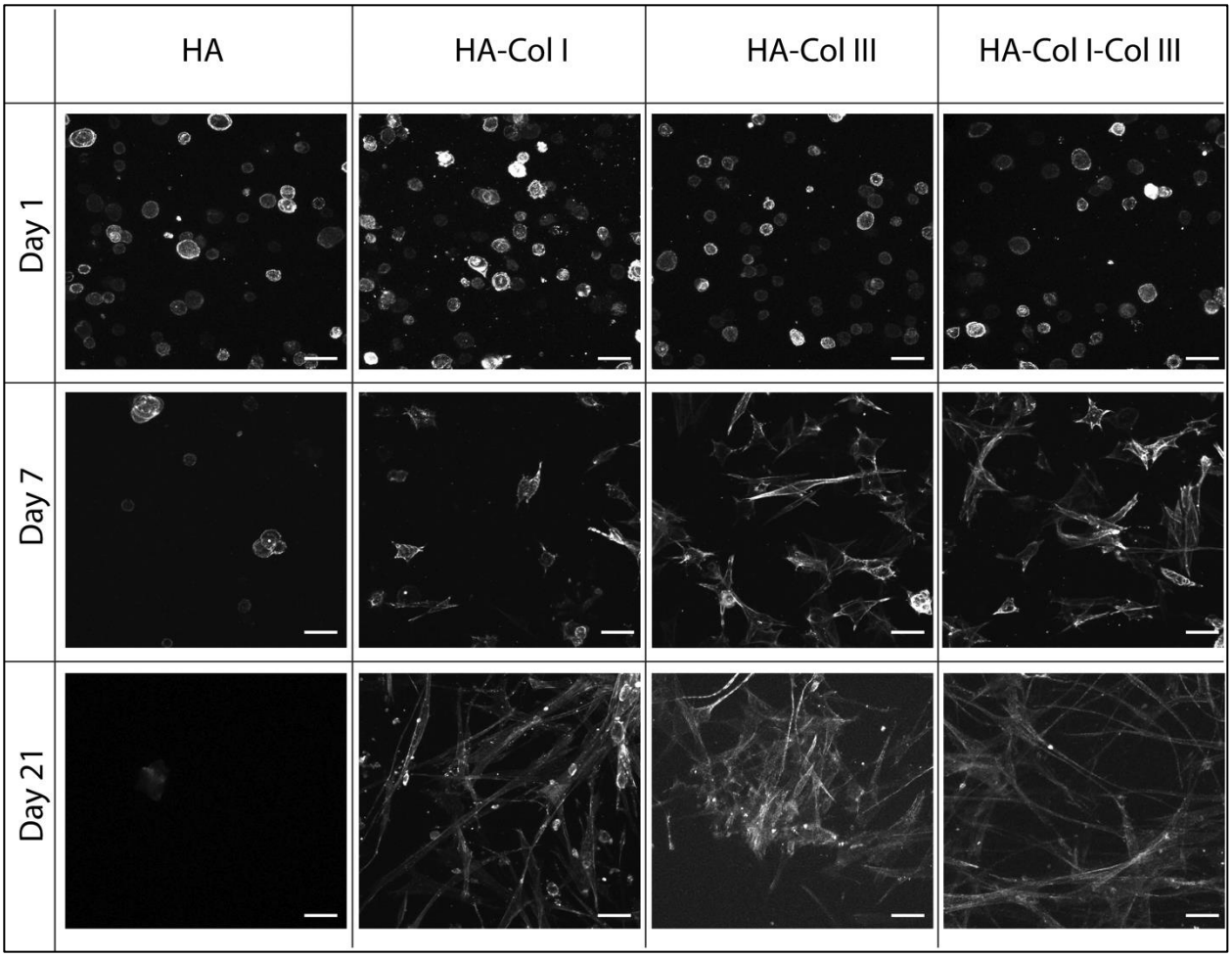

Figure 3-6 F-actin Staining in Hydrogel Blends.

Phalloidin was used to stain the actin cytoskeleton of fibroblasts encapsulated in the different hydrogel blends. At 21 days, cells develop extensive cytoskeletal networks as seen by their spreading in the HA-Col blend hydrogels. Scale bar = 50 μm.

3.3.7 New DNA synthesis in encapsulated cells

Cells maintained their ability to proliferate in the HA-Col blend gels over 21 days, as seen by the increase in cell number over time and the detection of EdU in the cells at 21 days (Figure 3-7). No proliferative cells were seen in the HA alone gels after 14 days, suggesting that the addition of collagen provided signaling cues for cell adhesion and proliferation.

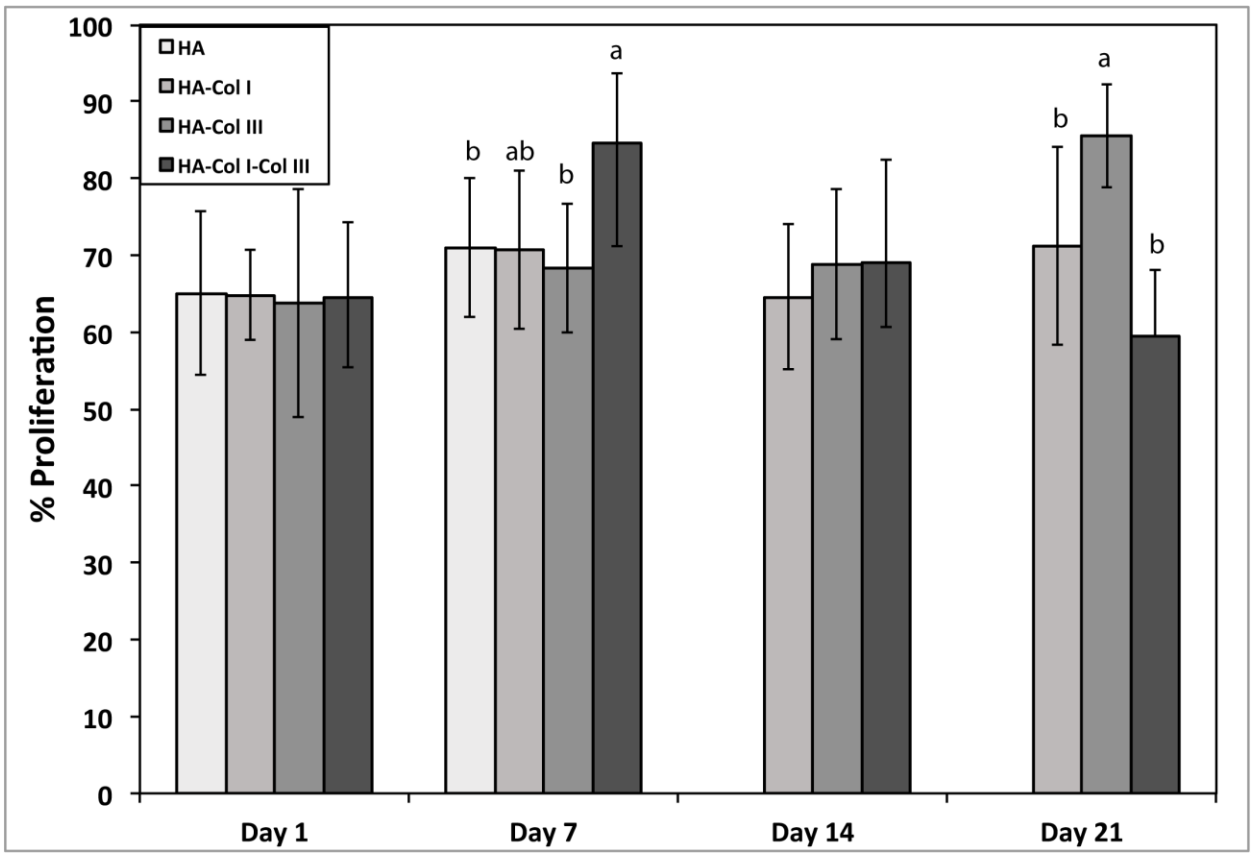

Figure 3-7 Percent Proliferation of Fibroblasts Encapsulated in Hydrogel Blends.

Fibroblasts remain in a proliferative state at the end of 21 days of culture in HA-Col blend hydrogels as seen by the incorporation of EdU into the newly synthesized DNA. Error bars depict standard deviation. Means that do not share a letter are significantly different ($P < 0.05$).

3.3.8 Gene expression

In order to evaluate changes in fibroblast gene expression as a function of different scaffold microenvironments, gene expression for various ECM constituents was analyzed after seven days of culture. ΔCt was calclulated by using β-actin as housekeeping gene, and fold changes in gene expression were normalized to HA only gels (Figure 3-8). Col1A1 and Col3A1 gene expression levels in HA-Col I gels were significantly lower than those in HA gels ($P < 0.05$). MMP1 gene expression was significantly downregulated in all the gels containing collagen ($P < 0.05$). Decorin gene expression was upregulated in HA-Col I gels, and downregulated in both, HA-Col III and HA-Col I-Col III gels. There were no significant differences for fibronectin gene expression between different hydrogels.

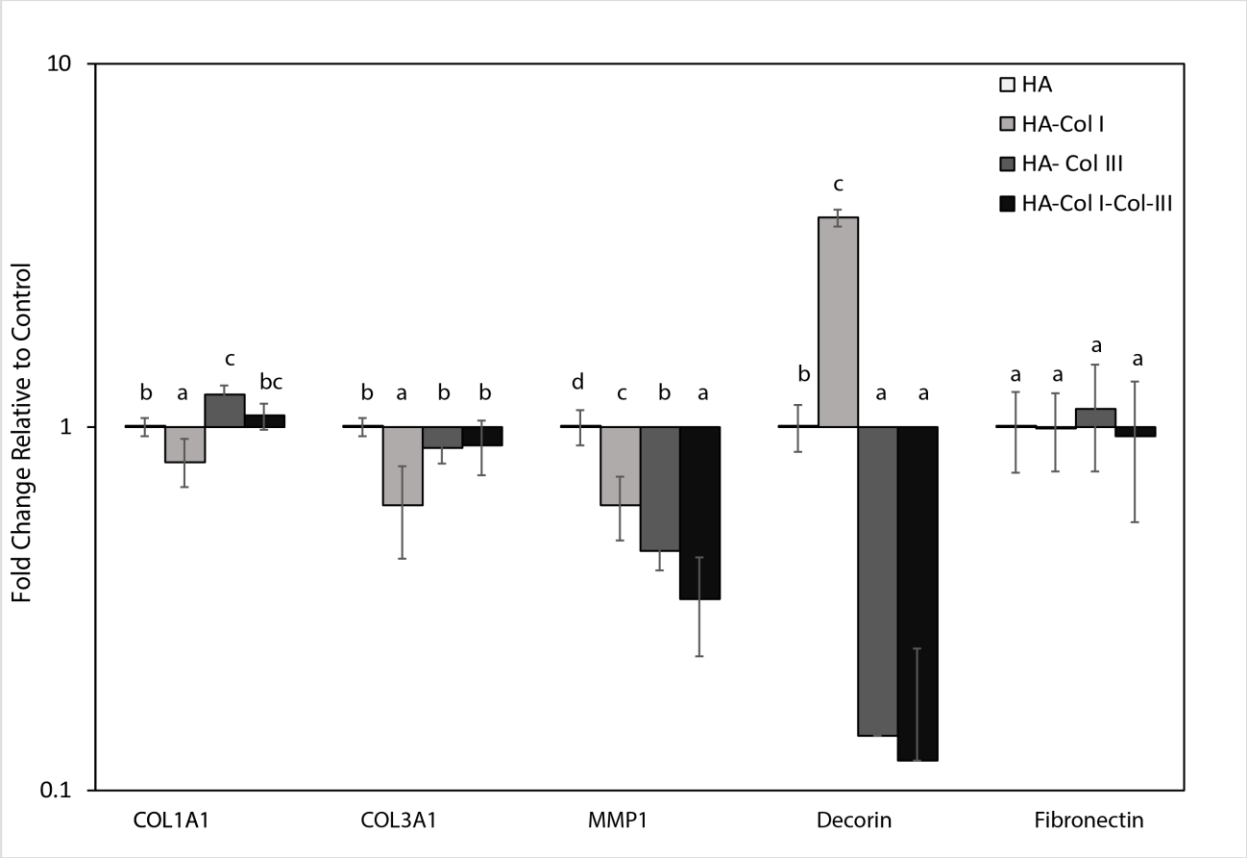

Figure 3-8 Gene Expression of Fibroblasts Encapsulated in Different Hydrogel Blends.

Fold changes in fibroblast ECM related genes when compared to HA alone gels show that cells respond differently to their microenvironments. Error bars represent standard deviation. Means that do not share a letter are significantly different ($P < 0.05$).

3.4 Discussion

In this study, the response of vocal fold fibroblasts to different engineered matrices containing HA and collagen blends was tested under static conditions. In an effort to recapitulate the native ECM environment of the vocal folds, we chose to use three of the most abundant ECM molecules in the vocal fold lamina propria, namely collagen type I, collagen type III and HA. As naturally occurring, highly biocompatible biomaterials, they have the potential to modulate cell responses to injury and improve wound healing to reduce vocal fold scarring. Thiol-modified HA has been used for various tissue engineering applications and is known to be compatible with in situ encapsulation of cells. However, it has been widely used in combination with crosslinked gelatin instead of fibrillar collagen, which more closely replicates the composition in vivo.[75,

79] In this study, we demonstrate for the first time that the major types of fibrillar collagens found in the vocal folds, namely type I collagen and type III collagen, can be co-polymerized with thiolated HA gels. This was achieved by increasing the rate of collagen fibrillogenesis by neutralizing the pH to 7.8, which is collagen's isoelectric point.[161] This is hypothesized to drive fibrillogenesis of collagen faster than the Michael type crosslinking between HA and PEGDA, with the ultimate result being an interpenetrating hydrogel network. The incorporation of collagen into modified hyaluronic acid hydrogels not only enhances the mechanical integrity of the gels, but also provides cues for attachment and proliferation of cells.

Four different types of hydrogels were evaluated in the study, HA crosslinked with PEGDA alone, HA-PEGDA with interpenetrating collagen type I fibrils, HA-PEGDA with interpenetrating collagen type III fibrils and HA-PEGDA with a blend of collagen type I and collagen type III. The effects of these hydrogels on mechanical properties, hydrogel microstructure, swelling and degradation, as well as cell behavior was evaluated.

The elastic storage modulus of vocal folds lies between 100 - 1000 Pa.[28, 30] For a biologically active tissue like the vocal folds, if the scaffold is to be implanted at the site of scarring, it is important that the hydrogel characteristics closely match the in vivo tissue viscoelastic environment, as cellular responses are known to vary based on stiffnesses of the local physical environment.[165] Collagen hydrogels by themselves show relatively poor mechanical properties for tissue engineering purposes.[166] Using thiol modified HA, the rheological properties can be tuned by varying the polymer weight and crosslinking density. We chose a molecular weight of 100 kDa, since a higher molecular weight would result in a stiffer gel due to the added chain entanglement, and the addition of collagen already added sufficiently to the stiffness of the hydrogels (Figure 3-1). All the hydrogels are within the physiologically relevant range for mechanical characteristics, and can be used as scaffolds for tissue engineering. Storage moduli increased with the addition of collagen, indicating that the addition of collagen improved the elastic properties of the hydrogels. HA-Col I hydrogels showed a trend towards higher G' values, which can be attributed to the shorter and thicker fibrils formed by type I collagen. Loss moduli (G'') values also increased with the addition of collagen in comparison to HA alone gels, indicating that the gels became more viscoelastic.

Cryo SEM was used to observe the microstructure of the different gels and support the data obtained from the rheological properties of the gels. HA alone gels can be seen as a porous

network formed by the covalent crosslinks within the hydrogel. Qualitatively, the pores appear to form a non-fibrillar network with interconnected channels. The addition of collagen appears to change this porous microstructure by the interpenetrating fibrillar structures present in the HA-Col blends. Various glycosaminoglycans (GAGs), including HA, are known to alter collagen fibrillogenesis.[167] Additionally, collagen fibril assembly is also dependent on the structure, assembly and concentration of GAGs.[168] The subtle differences in the hydrogel microstructure due to the different types of collagens can be attributed to the chemical assembly of the HA-Col blend gels. The competing Michael type crosslinking between thiols and acrylates increases the solution viscosity dramatically, inhibiting collagen mobility and rate of fibrillogenesis within the matrix. Increasing the pH during gelation supported more rapid collagen assembly, in part overcoming the rapid increase in viscosity due to crosslinking. The resulting matrix appears to have short, interdigitated fibrils of collagen. Fibrils formed by type I collagen appear thicker than the fibrils formed by collagen type III. This is consistent with the data in the literature showing that type I collagen fibrils have a diameter of 150-300nm and type III collagen fibrils have a diameter of 25-100nm.[52]

Equilibrium swelling ratios demonstrate that the hydrogels have a high degree of swelling, and thus, can provide access to oxygen, nutrients and metabolites required by the cells in order to sustain long term culture. The addition of collagen reduces the swelling ratio of the gels. This observation is consistent with the literature, which demonstrates the non-swelling nature of collagen hydrogels.[164] Mehra and coworkers[168] have shown that the addition of thiolated HA to type I collagen hydrogels inhibits commonly seen collagen contraction in pure type I collagen gels, making the hydrogels more biocompatible due to inhibition of contraction. This behavior is important for long-term culturing of cells, since fibroblast mediated contraction of collagen can provide altered signaling cues to the cells.[169] No visible contraction of gels was seen even after 21 days in culture (data not shown), despite the distinct spindle shaped elongated cytoskeletal processes seen in the HA-Col blend gels.

Another advantage of using biodegradable HA is that the degradation products of HA have been shown to be non-toxic in tissues.[170] Previous studies in our lab have shown that higher degrees of substitution (44%) reduce the biological activity of the HA.[162] While the hydrogel degradation data due to hyaluronidases cannot be explained by simple enzyme kinetics, this study demonstrated that the HA hydrogels remain bioactive despite the 12% modification on the

backbone, since the enzyme can still recognize the glycosidic linkages for cleavage. Reduced degradation in the gels containing collagen correlates with the cryo-SEM and swelling data, as it is likely that the addition of collagen fibrils within the HA pores may decrease hyaluronidase diffusion through the gels and reduce access to cleavage sites on the HA due to the reduced swelling ratio as well as the additional volume conferred by the presence of the collagen fibrils. Overall, these results demonstrate that, even with thiol substitution of the HA, the enzyme can still recognize the glycosidic linkages for cleavage, and the HA maintains its bioactivity.

To determine the biocompatibility of the matrices, encapsulated fibroblasts were tested for viability until the end of culture using a live/dead assay kit. At day 1, despite the rounded morphology, most cells appeared viable, confirming that the in situ encapsulation method was biocompatible. Prolonged culture of vocal fold fibroblasts in the encapsulated gels showed that collagen is essential for viability, adhesion, and retention of cells in the matrices. Cells appeared to have migrated out of the scaffold in HA alone gels by day 14. Studies have shown that cells migrate faster on softer gels,[171] and that HA is a key player in cell migration,[21] which can explain this observation. On the HA-Col blend hydrogels, however, cells remained viable even at 21 days, with distinctly visible spindle shaped morphology, confirming the biomimetic nature of the blend hydrogels. There is evidence in the literature that cell spreading on fibrillar collagen is mediated through α2β1 and α11β1 integrins,[172, 173] but this interaction is much weaker on gelatin, possibly due to a reduction in poly-proline-II content of gelatin.[152] Binding the gelatin is dependent on a different set of integrins (αvβ3 and α5β1)[174], which have implications on cell signaling in vivo. Crosslinking with gelatin also affects cell adhesion, with increasing non-specific non-integrin based adhesion seen due to increased gelatin crosslinking density.[152] Overall, since these studies point to reduced bioavailability of important native integrin ligands on collagen in the use of gelatin, we hypothesized that fibrillar collagens will provide superior characteristics to the hydrogels and mimic the native ECM environment better. In this study, viability did not seem to be affected during the 21 days of culture, and the cells formed long cytoskeletal projections to interact with other cells and the ECM.

The interpenetrating fibrillar network created by collagen not only supported cell viability and adhesion, but also facilitated cell proliferation, as seen by the incorporation of EdU in proliferating cells. Differences in the proliferation rates of the cells in the different hydrogels at various time points indicate that the matrix environment affects cell proliferation. However, there

is no clear trend, implying that cell proliferation is not a function of the type of collagen in the gel alone; instead, many other factors, including the overall microstructure, and the viscoelasticity of the matrix, play an important role in proliferation.

Gene expression of ECM constituents showed that the cells responded differently to the incorporation of type I collagen versus type III collagen in the HA hydrogels. MMP1 is a fibroblast collagenase known to breakdown interstitial collagen type I, II and III and is overexpressed during fibrosis and tissue repair.[43, 175] Significant downregulation of MMP1 in gels containing collagen was seen in comparison to HA alone gels. HA is known to be one of the major ECM components upregulated during wound healing,[176] in order to promote migration of cells into the site of injury.[177] Reduced degradation of HA in the presence of collagen, combined with the decreased MMP1 expression in gels containing collagen suggest that collagen protection of HA might be promoting a healthy tissue environment with less matrix turnover by the cells. Decorin gene expression was significantly upregulated in HA-Col I hydrogels and significantly downregulated in HA-Col III and HA-Col I-Col III hydrogels in comparison to HA gels. Decorin binds to type I collagen and reduces its fibril diameter, thus modulating collagen fibrillogenesis.[42] Decorin expression during fibrosis is highly differential.[178] Certain reports suggest that decorin administration prevents fibrosis progression,[179, 180] while others suggest physiological induction of decorin expression mediated by TGFβ1, suggesting that an upregulation of this proteoglycan can be detrimental in fibrosing tissue.[181-183] Downregulation of decorin has been implicated in scarless wound healing in early gestation fetal fibroblasts and fetal skin fibroblasts.[184] This effect suggests that an upregulation in decorin as seen in the HA-Col I gels might be detrimental to healthy tissue composition, as a delay in collagen fibrillogenesis might result in matrix irregularities. Overall, the addition of type III collagen to the scaffolds appears to correlate to a state that supports healthier tissue formation and regeneration. As we hypothesized, the elevated expression of type III collagen in developmental tissues and elastic soft tissues like the vocal folds may play an important role in maintaining a physiologically relevant matrix environment.

3.5 Conclusion

In this study, we evaluated the biocompatibility and functionality of HA and collagen blended 3D scaffolds for *in vitro* static culture of vocal fold fibroblasts. Four types of hydrogels were studied, with thiolated HA as the base scaffold material. By driving the rate of collagen fibrillogenesis faster, stable incorporation of fibrillar type I collagen and type III collagen in the nonfibrillar HA network was achieved. HA, HA-Col I, HA-Col III and HA-Col I-Col III hydrogels were evaluated for their mechanical properties, bioavailability and biocompatibility and their influence on vocal fold fibroblast cell behavior. All four hydrogels allowed for *in situ* I-hVFF encapsulation. The incorporation of collagen not only improved the mechanical properties of the hydrogels, but also provided for better cell attachment and adhesion in the scaffolds. The incorporation of fibrillar collagen types I and III within the widely characterized and biocompatible thiolated HA hydrogels is an attractive candidate for tissue engineering due to its functional biomimetic nature. Cells responded differently to scaffolds containing type I collagen and type III collagen as seen by the differences in gene expression, suggesting that addition of type III collagen provides a healthier tissue microenvironment. Future work will involve testing the regenerative and wound healing abilities of the scaffolds in vivo, as well as incorporating in physiologically relevant mechanical stimulations to create in vitro functional testing models.

4. CONCLUSIONS AND FUTURE DIRECTIONS

The overarching question driving this work was whether we could engineer an in vitro vocal fold model of physiological relevance by using commercially available epithelial cells and fibroblasts and exploring different scaffold based 3D microenvironments including HA, type I collagen and type III collagen. Overall, this work represents the initial stages of model development for a novel 3D vocal fold tissue engineering model with potential for screening therapeutics, mechanistic study and experiments on disease progression.

Within this context, Chapter 1 introduced the current tissue engineering based preclinical models used for the vocal folds and identified the advantages and disadvantages of these models. Two key shortcomings were identified - 1) the lack of an epithelial cell line for establishing vocal fold cocultures, and 2) the absence of a biomimetic 3D tissue microenvironment in current models. To bridge this gap, the proposed in vitro model in this dissertation focused on the use of a commercially available epithelial cell line from tracheal epithelial cells for establishing a coculture in chapter 2, and the development of a biologically relevant scaffold environment for transferring the culture in 3D in chapter 3.

Chapter 2 more specifically focused on the design of a scaffold free healthy and diseased state coculture model for the vocal folds by using tracheal epithelial cells and vocal fold fibroblasts. Currently, efforts are being made to develop an epithelial vocal fold cell line derived from stem cells,[97] but there is no benchmark model of primary human cell origin to test the stem cell model against. While the use of primary tracheal epithelial cells in place of vocal fold epithelial cells has certain drawbacks such as being harvested from a different tissue and not being of stratified squamous nature, it is a close match to the ambient environment that the vocal folds are exposed to in the airway. In the absence of a stratified squamous cell line that does not need to be differentiated from stem cells, it is an appealing alternative, and can provide valuable information on the effect of epithelial - mesenchymal interactions in vocal fold signaling and disease. We demonstrated that both, fibroblasts and epithelial cells, maintain their phenotype in coculture at 24 hours. Further, we established a disease state model by inducing the healthy coculture to produce αSMA with the use of TGFβ1. Our model offers information about cell interactions in healthy and fibrotic states while retaining the tunability and reproducibility

necessary to serve as a viable diagnostic and therapeutic test platform. By using cells from human sources and by creating an almost confluent layer of cells, we hypothesize that this model will provide more accurate information about disease states as well as significantly reduce the cost of screening new therapeutics in patients. In the future, this model can be used as is for screening anti-fibrotic therapeutics, or can be transferred into 3D culture in the scaffolds described in chapter 3.

Chapter 3 focused on evaluating different biomimetic 3D scaffolds for tissue engineering of the vocal folds. To mimic the natural ECM microenvironment of the vocal folds as closely as possible, HA, type I collagen, and type III collagen were chosen as natural starting materials for scaffold design. To increase the half life of the HA in the scaffolds and to provide the scaffolds with tunability, hyaluronan was modified to contain thiol groups on its backbone that could then be crosslinked with acrylate groups on the biologically neutral PEGDA. The resulting HA-PEGDA hydrogel could be controlled for viscoelastic properties without loss of bioactivity of the HA. The addition of fibrillar type I collagen and type III collagen provided the scaffold with functional sites for cell adhesion and spreading, as well as reinforced the viscoelastic properties of the scaffolds. Type I collagen and gelatin have been used extensively in vocal fold tissue engineering research and model development, but to date, no study has evaluated the use of type III collagen as a potential scaffold for cell growth. It is known that type III collagen comprises of more than 40% of the total vocal fold collagen[51] and plays an important role in soft tissues to make them more compliant and elastic.[52] We therefore chose to examine the effect of the addition of type I collagen and type III collagen to thiolated HA scaffolds and hypothesized that the addition of both types of collagen might result in a scaffold better suited to mimic healthy vocal fold tissue.

Using these three components, HA, type I collagen, and type III collagen, we first characterized four kinds of hydrogel blends – HA only, HA-Col I, HA-Col III, and HA-Col I-Col III by examining their mechanical stiffness, microstructural architecture, and swelling and degradation properties. The incorporation of collagen reinforced the HA scaffolds and improved their mechanical properties, and made the gels more viscoelastic in comparison to HA alone gels. Addition of collagen changed the architecture of the porous HA hydrogels, which corroborated with a reduction in swelling ratios and degradation with the addition of collagen. To further characterize response of vocal fold fibroblasts embedded in each of these hydrogels, we

conducted assays on cell viability, proliferation, cytoskeletal organization and gene expression. Incorporation of collagen was required for adhesion and proliferation of cells, as cells in the HA alone constructs migrated out of the scaffolds by day 14. Long – term 21- day culture showed that cells remained viable and proliferative in all the HA-Col gel blends during the in situ encapsulation and through the time of culture. Finally, we hypothesized that cells would respond differently to the microenvironments that they are subjected to, and found that the gene expression of cells in HA-Col I scaffolds was different to that of cells in HA-Col III and HA-Col I-Col III scaffolds. Addition of type III collagen to the scaffolds lead to a decrease in MMP1 and decorin gene expression, pointing towards a healthy tissue microenvironment. Overall, the HA-Col I-Col III scaffolds showed most promise as a relevant regenerative scaffold for the vocal folds. To make this scaffold more clinically relevant, future studies could involve translational studies to test the regenerative and wound healing capacities of this scaffold in vivo in rat, rabbit, or porcine models.

The results from this work have made it clear that the ECM composition and microenvironment are important factors to consider in the development of a 3D in vitro model. While this scaffold does not recreate the exact intricate tissue microenvironment found in vivo, the ability to engineer natural materials found in vivo to mimic tissue biochemical and structural cues brings us one step closer to developing an in vitro model with physiological relevance. Proposed next steps for expanding on the work done in this thesis would include the reintroduction of tracheal epithelial cells back into the 3D HA-Col I-Col III scaffolds encapsulated with vocal fold fibroblasts to create a functional coculture model in 3D. For future purposes, instead of tracheal epithelial cells, stratified squamous epithelial cells from the cornea could be used as well.

Key aspects of designing the 3D coculture would be the culture of the epithelial cells at air-liquid interface to make the model more physiologically relevant, as well as the development of a basement membrane in order to simulate the different layers of the vocal folds. A key function of the epithelium in the vocal folds is to act as a barrier between the external environment and underlying tissue.[112, 123] Therefore, in addition to phenotype testing of the epithelial cells in the model, efforts will need to be taken towards characterizing the barrier function of the epithelial layer. This can be done by several ways, including testing for intercellular epithelial junctions like gap junctions, tight junctions, and adherens junctions, as well as tracking the

penetration of a tracer molecule such as lanthanum nitrate.[97] To probe for the generation of a basement membrane, transmission electron microscopy (TEM) could be conducted or the constructs could be stained for laminin and type IV collagen.[185]

To validate that the 3D coculture model accurately represents the important aspects of vocal folds, histological and immunohistochemical comparisons between human vocal folds and the 3D constructs could be performed. Another step towards validating the model is to confirm that the protein expression and distribution within the in-vitro model correlates with what is known about the vocal folds in vivo. Protein level studies can be conducted in line with the Welham group's method of conducting proteomic analysis between the native vocal fold mucosa and the engineered mucosa by using liquid chromatography–tandem mass spectrometry (LC-MS/MS).[117] Alternatively, the model could be induced into a fibrotic state and the effect of growth factors on stimulating fibrosis in humans could be studied in a controlled environment using this model. Finally, mechanistic studies by simulating vibrations at physiologically relevant frequencies in bioreactors could be conducted to complete the physiological relevance of the model and understand the impact of biomechanics on vocal fold cell behavior.[186]

Altogether, this model would provide a high level of tunability, clinical relevance, and user control, and could offer great potential to serve as a tool for probing into the mechanisms of vocal fold disease, as well as developing and screening new therapeutics. Ulitmately, utilizing models that closely mimic the native tissue environment such as the one developed in this dissertation could lead to a higher number of effective anti-fibrotic drugs in clinical trials at a faster rate, leading to better patient outcomes.

APPENDIX

PROTOCOLS

IMMUNOSTAINING FOR αSMA, VIMENTIN, AND E-CADHERIN

Source: mouse anti-human αSMA – Sigma; rabbit anti-human Vimentin and E-cadherin, and goat anti-rabbit AlexaFluor® 555 – Cell Signaling Technology; goat anti-mouse AlexaFluor® 488– Invitrogen

Notes: Always add a secondary only control, with 5% milk in place of primary antibody to check specificity of secondary antibody. Add more washes if needed.

Method:

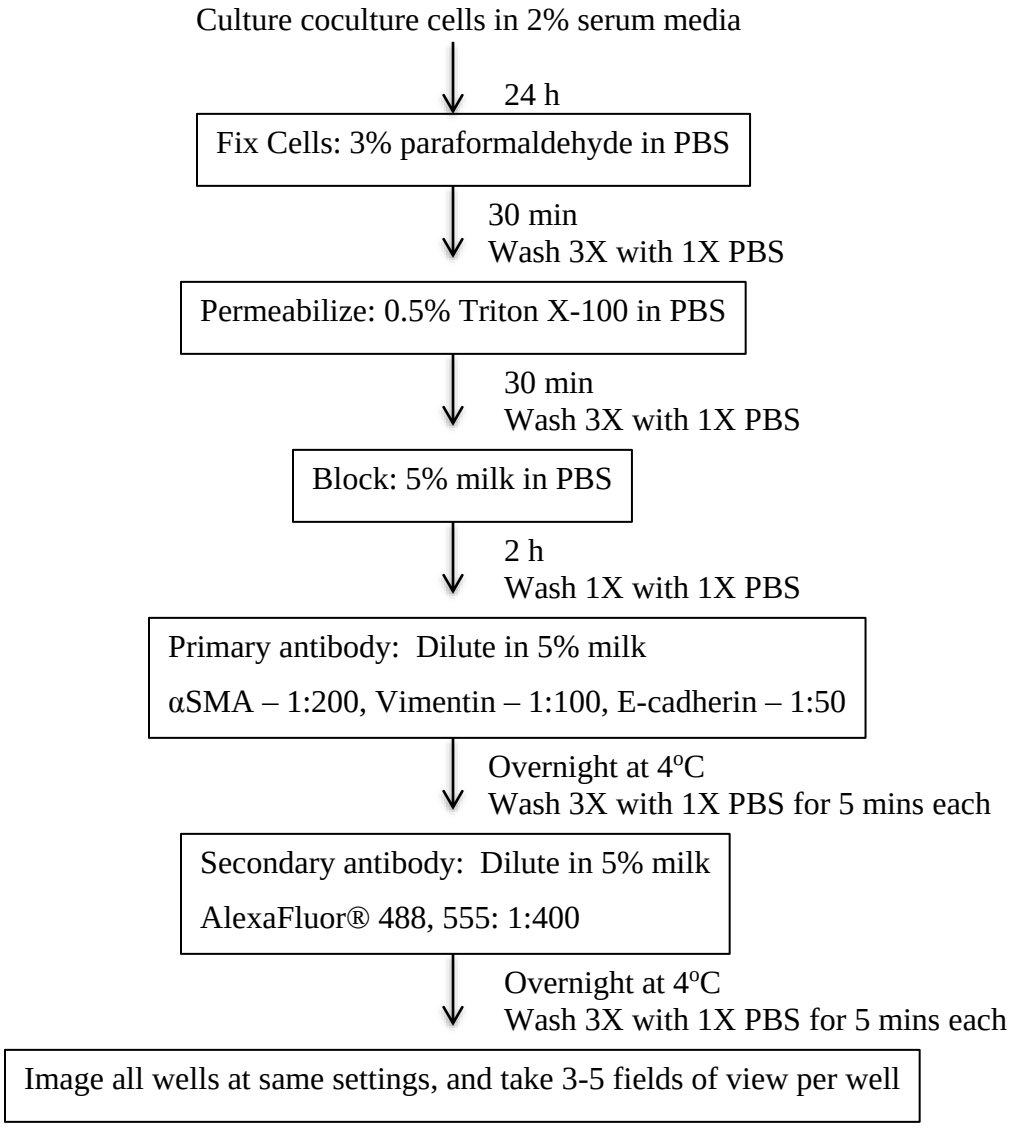

SYNTHESIS OF THIOLATED HA

Source: HA - Lifecore Biomedical LLC*; DTP – Frontier Scientific; EDC – Thermo Fischer

*Note: Use molecular weight of ~100KDa. Higher molecular weights harder to work with and more viscous.

Abbreviations:

EDC: N-(3-dimethylaminopropyl)-N'-ethylcarbodiimide

DTT: Dithiothreitol

DTP: dithiobis(propanoic dihydrazide)

Methods:

1. Dissolve hyaluronan at **10mg/ml** in degassed Milli-Q water. (500 mg in 50mL). To obtain degassed Milli-Q, keep it under vacuum for 30 mins.
2. Add DTP at a concentration of 2 mol DTP : 1 mol HA (627 mg) while the solution is stirring.
3. Add EDC to the solution at a ratio of 0.5 mol EDC : 1 mol HA (126.3 mg) once DTP has dissolved. Lower pH to 4.75 by adding 1N HCL. This begins the reaction. (Viscosity will increase and gel will likely form)
4. Maintain pH at 4.75 (add 10 uL) every 2 mins, and react for 15 mins to get 12% substituted HA.
5. Stop reaction by increasing pH to 7.0 using 1N NaOH.
6. Add DTT in at least 5-fold molar excess relative to DTP and raise and maintain pH to 8.5 with 1N NaOH. (If gel forms, will dissolve at this stage)
7. Stir for 24 hours
8. Lower pH to 3.5 with 1N HCL.
9. Dialyze against pH 3.5, 0.3mM HCL solution with 100mM NaCL for 2 weeks.
10. Dialyze against pH 3.5, 0.3mM HCL solution to remove salt for 1 week.
11. Centrifuge and lyophilize supernatant.
12. Keep lyophilized HA under nitrogen to prevent from cross-linking with self and store at -20^{o}C.

Reaction Scheme:

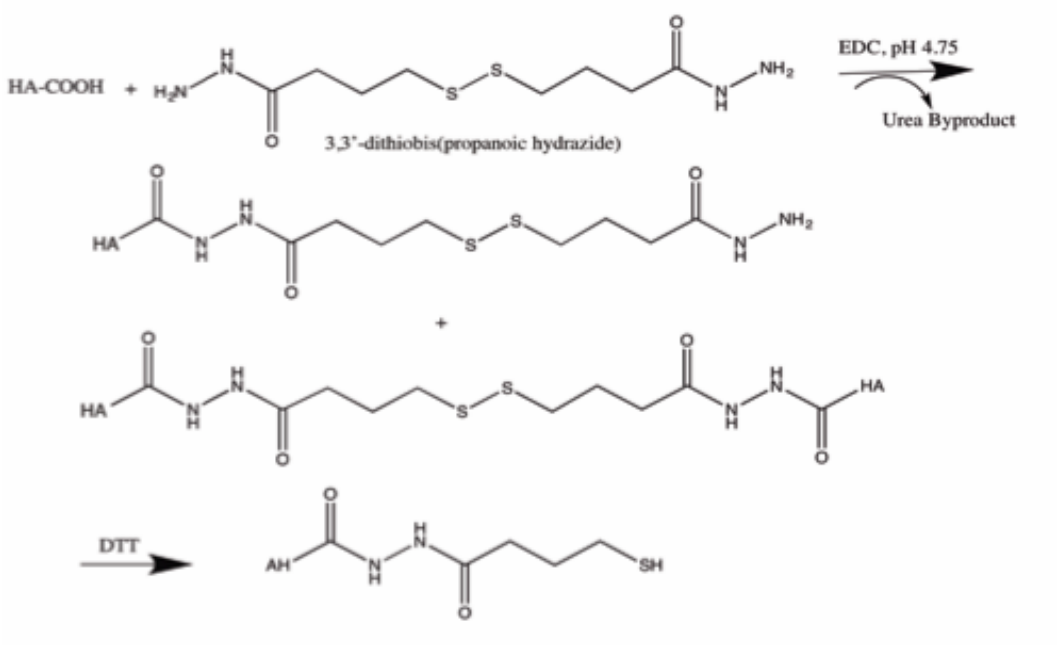

ELLMAN'S ASSAY FOR PERCENT SUBSTITUTION OF HA

Source: Ellman's Reagent, Cysteine Hydrochloride Monohydrate - Thermo Scientific

Methods:

1. Prepare reaction buffer: 0.1 M sodium phosphate, pH 8, containing 1mM EDTA. (pH 1st then add the EDTA so it's easier to dissolve)
2. Prepare Ellman's reagent solution: 4 mg/mL Ellman's reagent in reaction buffer
3. Prepare cysteine standards in reaction buffer as follows:

Standard	Volume of Reaction Buffer (ml)	Amount of Cysteine	Final Concentration (mM)
A	10	2.634 mg	1.5
B	0.5	2.5 mL of A	1.25
C	1	2 mL of A	1
D	1.5	1.5 mL of A	0.75
E	2	1 mL of A	0.5
F	2.5	0.5 mL of A	0.25
G	3	0	0

4. Prepare thiolated HA samples at 2 mg/mL and 1 mg/mL
5. Prepare test tubes, each containing 50 μL of Ellman's reagent solution and 2.5 mL of reaction buffer
6. Add 250 μL of each standard or unknown prepared in steps 3 and 4 to test tubes
7. Mix and incubate at room temperature for 15 mins
8. Transfer 200 μL of sample to a 96 well plate
9. Read absorbance at 412 nm
10. Plot values obtained from the standard to generate a standard curve
11. Calculate molar concentrations of the thiolated HA from the standard curve, making sure the absorbance values for the HA are within the linear range of the standard curve
12. Percent thiolation is calculated as total mols of thiols/ total mols of HA
13. Example standard curve:

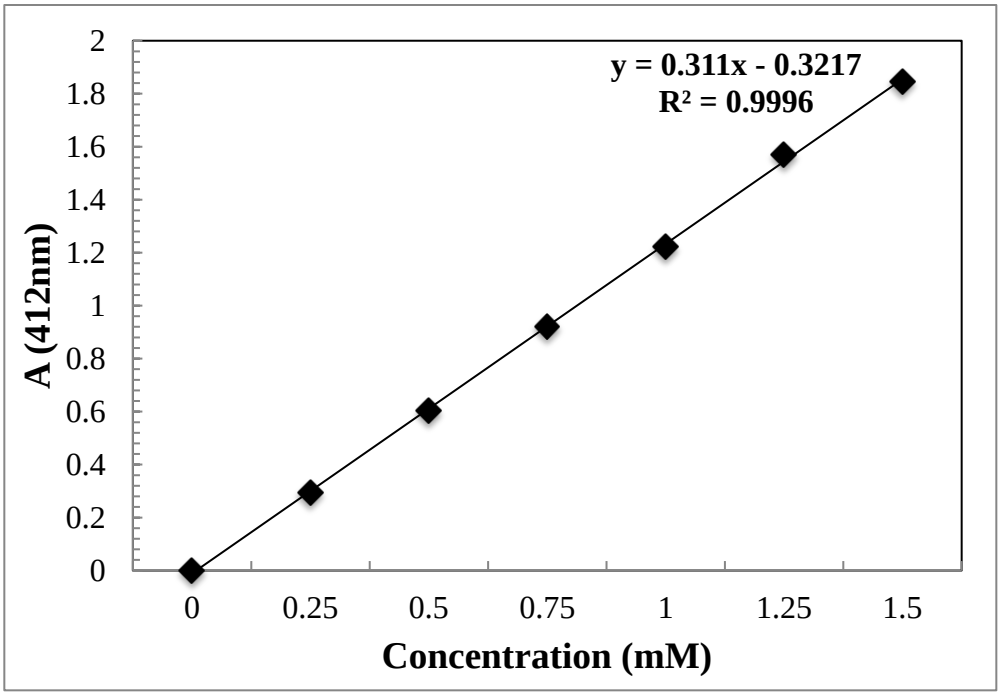
y = 0.311x - 0.3217
R² = 0.9996
A (412nm)
Concentration (mM)
0
0.2
0.4
0.6
0.8
1
1.2
1.4
1.6
1.8
2
0
0.25
0.5
0.75
1
1.25
1.5

GEL PREPARATION AND CELL ENCAPSULATION

Source: PEGDA – MW 3400, Alfa Aesar; rat tail collagen type I – BD Biosciences; bovine type III collagen – Millipore Sigma

Methods:

1. Before starting, dissolve type III collagen at 12 mg/mL in 20 mM acetic acid by shaking overnight at 4 ^{o}C. Sterile filter dissolved collagen solution and run BSA assay to find out concentration of filtered solution. Dilute collagen stock to 10 mg/mL and store at 4 ^{o}C until use.
2. Dissolve HA and PEGDA in DMEM supplemented with 1% penicillin/streptomycin, 1% MEM non-essential amino acid solution, and 10 mg/mL Geneticin at stock concentrations of 37.5 mg/mL and 71.8 mg/mL, respectively
3. pH solutions on ice to 7.8 using 1N NaOH
4. Trypsinize and count vocal fold fibroblasts (atleast 3 confluent T75 flasks)
5. Add 150000 cells to 0.5 mL eppendorf tubes, centrifuge at 200 rcf for 5 mins to get pellet, and carefully pipette out all the remaining media without disrupting pellet
6. On ice, aliquot 150 μL of 10.61 mg/mL stock type I collagen in the biosafety cabinet and add the following sterile neutralizing solutions to the collagen – 25.875 μL sterile filtered 10X PBS, 3.2 μL of sterile filtered 1N NaOH, 22.765 μL sterile 1X PBS
7. On ice, aliquot 150 μL of 10 mg/mL sterile type III collagen in the biosafety cabinet and add the following sterile neutralizing solutions to the collagen – 18.75 μL sterile filtered 10X PBS, 3.4 μL of sterile filtered 1N NaOH, 15.35 μL sterile 1X PBS

*Note: DO NOT sterile filter this neutralized collagen, as it results in the loss of a significant amount of collagen in the filter and poor fibril formation. These neutralizing concentrations are based on the average amount (n =3) of NaOH required to neutralize 150 μL collagen solution.

8. Add the following amounts of HA, PEGDA, type I collagen, and type III collagen to break the cell pellet

Gel	Amount of HA (µL)	Amount of Type I Collagen (µL)	Amount of Type III Collagen (µL)	Amount of PEGDA (µL)	Total Hydrogel Volume (µL)
HA	60 + 15µL DMEM	0	0	15 + 60 µL DMEM	150
HA-Col I	60	75	0	15	150
HA-Col III	60	0	75	15	150
HA-Col I-Col III	60	37.5	37.5	15	150

9. This results in a gel of the following final concentrations: 1.5% (15 mg/mL) HA, 4 mg/mL Col I + Col III, and 1:1 ratio of HA (thiol) to PEGDA (acrylate)
10. You have about 5 mins before the collagen starts gelling even on ice, so work fast and use positive displacement pipettes to pipette everything
11. Add 10 µL of cell-gel solution to ibidi µ-slide angiogenesis wells, and allow complete polymerization for 2h
12. Add 50 µL of media on top of the gels, and change media every 24 hours for time of culture

RHEOLOGY ON HYDROGELS

Design: To compare G' and G'' of HA, HA-Col I, HA-Col III, and HA-Col I-Col III hydrogels

Methods:

1. Dissolve HA and PEGDA at 37.5 mg/mL and 71.8 mg/mL respectively in 1X PBS
2. pH to 7.8 using 1N NaOH
3. Sterile filter both solutions and keep on ice
4. Neutralize type I collagen and type III collagen as mentioned in gel preparation and cell encapsulation
5. Mix the neutralized HA, PEGDA, type I collagen and type III collagen as follows

Gel	**Amount of HA (µL)**	**Amount of Type I Collagen (µL)**	**Amount of Type III Collagen (µL)**	**Amount of PEGDA (µL)**	**Total Hydrogel Volume (µL)**
HA	60 + 15µL PBS	0	0	15 + 60 µL PBS	150
HA-Col I	60	75	0	15	150
HA-Col III	60	0	75	15	150
HA-Col I-Col III	60	37.5	37.5	15	150

6. Add 100 µL of hydrogel solution on Tekdon rheology slides and allow polymerization for 3 hours at 37 ^{o}C.
7. Make an n=3 of each type of hydrogel according to table. Use different stock solutions for each n, so they may be considered biological replicates
8. Run stress and frequency sweeps on the TA instruments ARG2 rheometer
9. Stress sweep: 0.1 – 100 rad/s, frequency = 1 rad/s, log scale, 21 ^{o}C
10. Frequency sweep: 0.1 – 100 rad/s, oscillatory stress = 1 Pa, log scale, 21 ^{o}C

CRYO SEM ON HYDROGELS

Methods:

1. 75 μL gels were allowed to polymerize directly on the cryoSEM stage holders, so they wouldn't be damaged while handling
2. After polymerization for 3 hours at 37 ^{o}C, the samples were moved to cryo holders and cryoSEM was performed
1. Turn on nitrogen switch on the wall to circulate nitrogen through pipes
2. Vent the stage and replace it with the cryostage
3. Use a funnel to pour liquid nitrogen into the prep chamber, anticontaminator and microscope.
4. Wait for prep chamber temperature to read -180^{o}C and microscope temperature to read -140^{o}C.
5. Put liquid nitrogen under vacuum where its temperature goes down to -210^{o}C where it freezes and forms slush
6. Load sample onto cryoholder and snap freeze sample using the liquid nitrogen slush
7. After a minute, the sample is frozen. Start vacuum in prep chamber
8. Transfer sample to prep chamber and fracture with one clean cut to expose the sample
9. Transfer sample to microscope stage and set microscope temperature to -90^{o}C.
10. Start sublimating the sample by starting high voltage beam
11. After about 10 mins, you can see walls of porosity to reveal sample microstructure
12. Once sublimated enough, transfer sample to prep chamber and sputter coat with platinum for 120 s. *Current is conducted into the prep chamber through argon, and the argon is ionized. Ionized argon hits the platinum, and the platinum falls on the sample to coat it.
13. While sample is being coated, decrease temperature of the microscope to -140^{o}C.
14. After coating, transfer the sample back to the microscope, and turn on high voltage to start imaging
15. For imaging, we use the Everhart-Thornley detector at 5kV voltage and a spot size of 3. Take images at 10000X.

MODIFIED CARBAZOLE ASSAY FOR URONIC ACID DETECTION

Methods: Hyaluronidase digestion of HA gels

1. Prepare n=3 with separate stock solutions for each n.
2. Make 100 μL gels of each kind – HA alone, HA-Col I, HA-Col III, and HA-Col I-Col III in the wells of 4 chamber slides (Nalge Nunc)
3. Allow polymerization at 37 ^{o}C for 2 hours, then place in 4 ^{o}C fridge to allow gels to cure overnight
4. At t=0 the next day, add 1 mL of 50 U/mL Hyaluronidase in 1X PBS to each hydrogel well
5. Immediately remove 750 μL of solution and store at -80 ^{o}C until further analysis
6. Restore the 750 μL with fresh hyaluronidase solution, to make volume up to 1 mL
7. Place gel on rocker at 37 ^{o}C in a humidified environment
8. Remove 750 μL solution from wells at t= 0, 2, 4, 6, 8, 10 hours and replace with equal amount of fresh hyaluronidase solution
9. Run carbazole assay on all timepoints as follows:

Methods: Modified cabazole assay

1. Prepare standards for generating a standard curve by using thiolated HA as explained in steps 2-4
2. Prepare stock solution of 1 mg/mL thiolated HA in 50U/mL HAase in **sterile** PBS
3. Serially dilute down to 0.5 mg/mL, 0.25 mg/mL and so on in 50 U/mL HAase in sterile PBS
4. Add 40 μl of each standard concentration to get the following mass (μg) in a 96 well plate: 40 μg, 20 μg, 10μg, 5 μg, 2.5 μg, 1.25 μg, 0 μg
5. Add 40 μl of unknown solution from each timepoint to the 96 well plate
6. To each well, add 200 μL of 25 mM sodium tetraborate in concentrated sulfuric acid
7. Heat plate at 100 ^{o}C in an oven
8. Cool plate to RT for 15 mins
9. Add 50 μL of 0.125% carbazole in absolute ethanol to each well
10. Incubate at 100 ^{o}C in an oven
11. Cool plate to RT for 15 mins
12. Read absorbance at 550 nm

13. To get % degradation of HA, find out mass (μg) of HA in solution from standard curve, multiply by volume (in this case, 750 μL), and convert that into percent of original HA concentration (for 1.5% HA gels, 1.5 mg in 100 μL starting HA) in the gel.
14. Example standard curve:

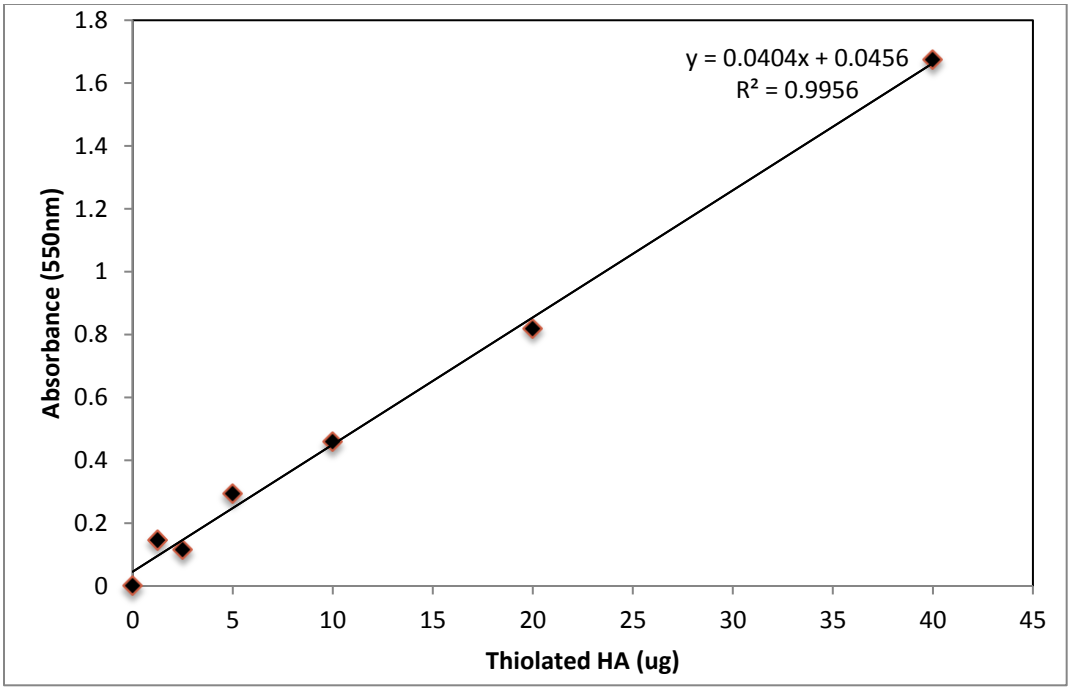

IMMUNOSTAINING FOR F-ACTIN

Source: AlexaFluor® 633 Phalloidin – Invitrogen

Notes: Always add a secondary only control, with 5% milk in place of primary antibody to check specificity of secondary antibody. Add more washes if needed.

Method:

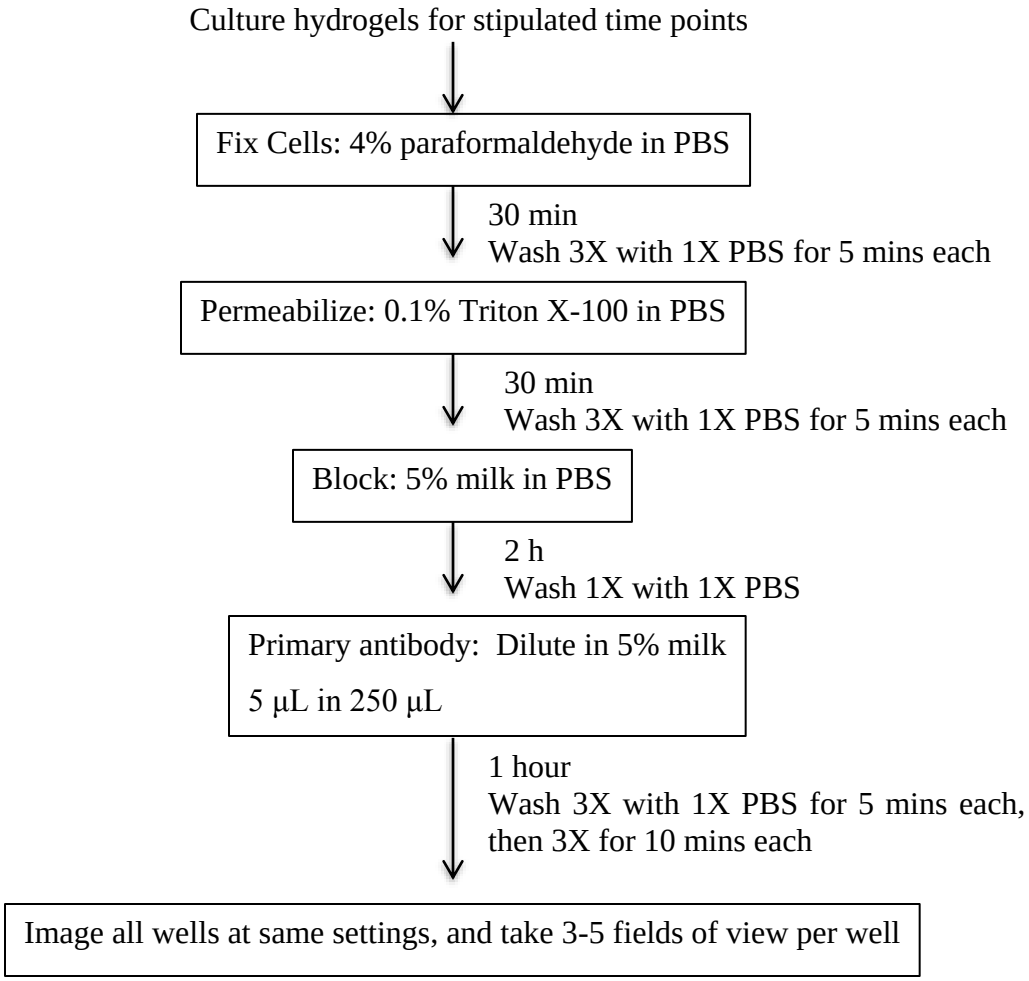

qPCR FOR CELLS EXTRACTED FROM HYDROGELS

Methods: Gel Setup and RNA Purification

1. Make 9 50 μL gels with 1×10^6 cells/ml of fibroblasts
2. Culture cells in cell gel constructs for 7 days
3. For extracting cells, carefully use tweezers to scoop gels out in a 2 mL eppendorf tube
4. Combine all 9 gels to make 1 sample
5. Add 500 μL of 7500 U/mL hyaluronidase in PBS to the tubes, and shake gently at 37 ºC. I used a thermocycler to keep temperature stable during this time.
6. After 45 mins, centrifuge the cells at 200 rcf for 10 mins
7. Carefully pipette out supernatant and discard it
8. Add 350 μL lysis buffer that comes with the Qiagen or Clonetech kit with 3.5 μL β-mercaptoethanol to the pellet and disrupt any remaining gel by pipetting up and down.
9. Pass the lysis solution through QIAshredders and centrifuge at 10000 g for 1 min
10. Follow RNA purification protocol as mentioned in kit and elute in 30 μL nuclease free water

Methods: Reverse Transcription

1. Quantify the amount of RNA in each purified sample on the Nanodrop atleast 2 times.
2. Follow the protocol in the High Capacity Reverse Transcription (RT) Kit by Applied Biosystems to make 2X complete RT buffer
3. Add 10 μL of total eluted RNA and 10μL of the 2X complete RT buffer to PCR tubes for a final reaction volume of 20 μL.

***Note:** If you eluted RNA in 30 μL of nuclease free water, this should give you 2-3 reactions per sample

4. Centrifuge the tubes down for 2 mins to remove any air bubbles created
5. Run RT to get cDNA in the thermo cycler at the following conditions:
    a. Step 1 = 25 ºC, 10 min
    b. Step 2 = 37 ºC, 120 min
    c. Step 3 = 85 ºC, 5 min
    d. Step 4 = 4 ºC, infinity
6. Once RT is complete, store samples at -80ºC until you run the quantitative real time PCR.

Methods: qPCR

1. Thaw the TaqMan probes and cDNA on ice
2. Your cDNA concentration is half the concentration of your starting total RNA, since you diluted it 1:1 with the RT buffer
3. Calculate the amount of nuclease free water required to dilute the cDNA in all your samples to a concentration of 1 ng/mL
4. Prepare the TaqMan Gene Expression Master Mix plus appropriate TaqMan probes for each gene as listed on the Applied Biosystems TaqMan catalog.
5. Aliquot out 45 μL of TaqMan Master Mix + probe of appropriate gene in a 96 well PCR plate
6. Run each gene of each sample at least in triplicate
7. Combine cDNA from each RT reaction for each sample separately so you have one cDNA stock for each sample
8. Dilute all cDNA samples to 1 ng/mL
9. Add 5 μL of each sample to the corresponding well with Master Mix + probe mix well
10. Once all the samples have been added to the wells, cap the wells with 8-strip optical caps, and centrifuge at 200 rcf for 2 min to get rid of any air bubbles
11. Run the qPCR reaction on the Applied Biosystems 7500 as follows:
    a. Step 1 = 50 ^{o}C, 2 min, UDG incubation
    b. Step 2 = 95 ^{o}C, 10 min, Hold, AmpliTaq Gold, UP Enzyme Activation
    c. Cycle = 40 cycles : 95^{o}C, 15 s (denature), 60 ^{o}C, 1 min (anneal/extend)
    d. Select standard mode, not fast
    e. Reaction volume = 50 μL
12. Analyze the data using the ΔΔCt method and normalize data to β-actin as housekeeping gene
13. Follow the Applied Biosystems PCR analysis guide for conducting ΔΔCt calculations

REFERENCES

[1] N. Roy, R.M. Merrill, S.D. Gray, E.M. Smith, Voice disorders in the general population: prevalence, risk factors, and occupational impact, Laryngoscope 115(11) (2005) 1988-95.

[2] S.M. Cohen, J. Kim, N. Roy, C. Asche, M. Courey, Prevalence and causes of dysphonia in a large treatment-seeking population, Laryngoscope 122(2) (2012) 343-8.

[3] S.M. Cohen, J. Kim, N. Roy, C. Asche, M. Courey, Direct health care costs of laryngeal diseases and disorders, The Laryngoscope 122(7) (2012) 1582-1588.

[4] J.A. DiMasi, H.G. Grabowski, R.W. Hansen, Innovation in the pharmaceutical industry: New estimates of R&D costs, Journal of Health Economics 47 (2016) 20-33.

[5] J.K. Kutty, K. Webb, Tissue engineering therapies for the vocal fold lamina propria, Tissue engineering. Part B, Reviews 15(3) (2009) 249-62.

[6] E.J. Hunter, J.G. Švec, I.R. Titze, Comparison of the Produced and Perceived Voice Range Profiles in Untrained and Trained Classical Singers, Journal of Voice 20(4) (2006) 513-526.

[7] M. Hirano, Morphological Structure of the Vocal Cord as a Vibrator and its Variations, Folia phoniatrica et logopaedica 26(2) (1974) 89-94.

[8] S.D. Gray, Cellular physiology of the vocal folds, Otolaryngologic clinics of North America 33(4) (2000) 679-98.

[9] M. Hirano, Structure of the vocal fold in normal and disease states. Anatomical and physical study., ASHA Rep 11 (1981).

[10] A.K. Miri, Mechanical Characterization of Vocal Fold Tissue: A Review Study, Journal of Voice 28(6) (2014) 657-667.

[11] I.R. Titze, Principles of voice production, Iowa City, Ia : National Center for Voice and Speech, Iowa City, Ia, 2000.

[12] T. Tateya, I. Tateya, D.M. Bless, Collagen Subtypes in Human Vocal Folds, Annals of Otology, Rhinology & Laryngology 115(6) (2006) 469-476.

[13] M.S. Hahn, C.Y. Jao, W. Faquin, K.J. Grande-Allen, Glycosaminoglycan Composition of the Vocal Fold Lamina Propria in Relation to Function, Annals of Otology, Rhinology & Laryngology 117(5) (2008) 371-381.

[14] M.S. Hahn, J.B. Kobler, B.C. Starcher, S.M. Zeitels, R. Langer, Quantitative and comparative studies of the vocal fold extracellular matrix. I: Elastic fibers and hyaluronic acid, The Annals of otology, rhinology, and laryngology 115(2) (2006) 156-64.

[15] M.S. Hahn, J.B. Kobler, S.M. Zeitels, R. Langer, Quantitative and Comparative Studies of the Vocal Fold Extracellular Matrix II: Collagen, Annals of Otology, Rhinology & Laryngology 115(3) (2006) 225-232.

[16] K. Ishii, W.G. Zhai, M. Akita, H. Hirose, Ultrastructure of the Lamina Propria of the Human Vocal Fold, Acta Oto-laryngologica 116(5) (1996) 778-782.

[17] T.H. Hammond, S.D. Gray, J.E. Butler, Age- and Gender-Related Collagen Distribution in Human Vocal Folds, Annals of Otology, Rhinology & Laryngology 109(10) (2000) 913-920.

[18] T.H. Hammond, R. Zhou, E.H. Hammond, A. Pawlak, S.D. Gray, The intermediate layer: A morphologic study of the elastin and hyaluronic acid constituents of normal human vocal folds, Journal of Voice 11(1) (1997) 59-66.

[19] A.S. Pawlak, T. Hammond, E. Hammond, S.D. Gray, Immunocytochemical study of proteoglycans in vocal folds, The Annals of otology, rhinology, and laryngology 105(1) (1996) 6-11.

[20] T.H. Hammond, R. Zhou, E.H. Hammond, A. Pawlak, S.D. Gray, The intermediate layer: a morphologic study of the elastin and hyaluronic acid constituents of normal human vocal folds, Journal of voice : official journal of the Voice Foundation 11(1) (1997) 59-66.

[21] K.T. Dicker, L.A. Gurski, S. Pradhan-Bhatt, R.L. Witt, M.C. Farach-Carson, X. Jia, Hyaluronan: a simple polysaccharide with diverse biological functions, Acta biomaterialia 10(4) (2014) 1558-70.

[22] S.D. Gray, I.R. Titze, R. Chan, T.H. Hammond, Vocal fold proteoglycans and their influence on biomechanics, The Laryngoscope 109(6) (1999) 845-854.

[23] A.S. Pawlak, E. Hammond, T. Hammond, S.D. Gray, Immunocytochemical Study of Proteoglycans in Vocal Folds, Annals of Otology, Rhinology & Laryngology 105(1) (1996) 6-11.

[24] J.E. Butler, T.H. Hammond, S.D. Gray, Gender-Related Differences of Hyaluronic Acid Distribution in the Human Vocal Fold, The Laryngoscope 111(5) (2001) 907-911.

[25] M. Catten, S.D. Gray, T.H. Hammond, R. Zhou, E. Hammond, Analysis of cellular location and concentration in vocal fold lamina propria, Otolaryngology--head and neck surgery : official journal of American Academy of Otolaryngology-Head and Neck Surgery 118(5) (1998) 663-7.

[26] R.W. Chan, I.R. Titze, Dependence of phonation threshold pressure on vocal tract acoustics and vocal fold tissue mechanics, J Acoust Soc Am 119(4) (2006) 2351-62.

[27] R.W. Chan, I.R. Titze, Viscoelastic shear properties of human vocal fold mucosa: Measurement methodology and empirical results, The Journal of the Acoustical Society of America 106(4) (1999) 2008-2021.

[28] R.W. Chan, Measurements of vocal fold tissue viscoelasticity: approaching the male phonatory frequency range, J Acoust Soc Am 115(6) (2004) 3161-70.

[29] R.W. Chan, M.L. Rodriguez, A simple-shear rheometer for linear viscoelastic characterization of vocal fold tissues at phonatory frequencies, The Journal of the Acoustical Society of America 124(2) (2008) 1207-1219.

[30] S.S. Teller, A.J. Farran, L. Xiao, T. Jiao, R.L. Duncan, R.J. Clifton, X. Jia, High-frequency viscoelastic shear properties of vocal fold tissues: implications for vocal fold tissue engineering, Tissue Engineering. Part A 18(19-20) (2012) 2008-19.

[31] N. Bhattacharyya, The prevalence of voice problems among adults in the United States, Laryngoscope 124(10) (2014) 2359-62.

[32] M.S. Benninger, D. Alessi, S. Archer, R. Bastian, C. Ford, J. Koufman, R.T. Sataloff, J.R. Spiegel, P. Woo, Vocal fold scarring: current concepts and management, Otolaryngology--head and neck surgery : official journal of American Academy of Otolaryngology-Head and Neck Surgery 115(5) (1996) 474-82.

[33] J.K. Hansen, S.L. Thibeault, Current Understanding and Review of the Literature: Vocal Fold Scarring, Journal of Voice 20(1) (2006) 110-120.

[34] B. Rousseau, S. Hirano, R.W. Chan, N.V. Welham, S.L. Thibeault, C.N. Ford, D.M. Bless, Characterization of chronic vocal fold scarring in a rabbit model, Journal of Voice 18(1) (2004) 116-124.

[35] S. Hirano, S. Minamiguchi, M. Yamashita, T. Ohno, S.-i. Kanemaru, M. Kitamura, Histologic Characterization of Human Scarred Vocal Folds, Journal of Voice 23(4) (2009) 399-407.

[36] B. Rousseau, S. Hirano, T.D. Scheidt, N.V. Welham, S.L. Thibeault, R.W. Chan, D.M. Bless, Characterization of Vocal Fold Scarring in a Canine Model, Laryngoscope 113(4) (2003) 620-627.

[37] S.L. Thibeault, S.D. Gray, D.M. Bless, R.W. Chan, C.N. Ford, Histologic and Rheologic Characterization of Vocal Fold Scarring, Journal of Voice 16(1) (2002) 96-104.

[38] S. Hirano, D.M. Bless, B. Rousseau, N. Welham, T. Scheidt, C.N. Ford, Fibronectin and Adhesion Molecules on Canine Scarred Vocal Folds, Laryngoscope 113(6) (2003) 966-972.

[39] H.K. Heris, A.K. Miri, N.R. Ghattamaneni, N.Y.K. Li, S.L. Thibeault, P.W. Wiseman, L. Mongeau, Microstructural and mechanical characterization of scarred vocal folds, Journal of biomechanics 48(4) (2015) 708-711.

[40] T. Tateya, I. Tateya, J.H. Sohn, D.M. Bless, Histologic characterization of rat vocal fold scarring, The Annals of otology, rhinology, and laryngology 114(3) (2005) 183.

[41] M. Yamashita, D.M. Bless, N.V. Welham, Morphological and Extracellular Matrix Changes following Vocal Fold Injury in Mice, Cells Tissues Organs 192(4) (2010) 262-271.

[42] S.L. Thibeault, D.M. Bless, S.D. Gray, Interstitial protein alterations in rabbit vocal fold with scar, Journal of Voice 17(3) (2003) 377-383.

[43] B. Rousseau, P.J. Ge, T. Ohno, L.C. French, S.L. Thibeault, Extracellular Matrix Gene Expression after Vocal Fold Injury in a Rabbit Model, Annals of Otology, Rhinology & Laryngology 117(8) (2008) 598-603.

[44] S.L. Thibeault, B. Rousseau, N.V. Welham, S. Hirano, D.M. Bless, Hyaluronan Levels in Acute Vocal Fold Scar, Laryngoscope 114(4) (2004) 760-764.

[45] B. Rousseau, J. Sohn, I. Tateya, D.W. Montequin, D.M. Bless, Functional Outcomes of Reduced Hyaluronan in Acute Vocal Fold Scar, Annals of Otology, Rhinology & Laryngology 113(10) (2004) 767-776.

[46] I. Tateya, T. Tateya, M. Watanuki, D.M. Bless, Homeostasis of hyaluronic acid in normal and scarred vocal folds, Journal of voice : official journal of the Voice Foundation 29(2) (2015) 133-9.

[47] B. Palsson, Tissue Engineering, Hoboken : Taylor and Francis, Hoboken, 2010.

[48] G. Friedrich, F.G. Dikkers, C. Arens, M. Remacle, M. Hess, A. Giovanni, S. Duflo, A. Hantzakos, V. Bachy, M. Gugatschka, Vocal fold scars: current concepts and future directions. Consensus report of the phonosurgery committee of the European laryngological society, Eur Arch Otorhinolaryngol 270(9) (2013) 2491-2507.

[49] S. Hirano, Current treatment of vocal fold scarring, Current opinion in otolaryngology & head and neck surgery 13(3) (2005) 143.

[50] S.S. Tang, V. Mohad, M. Gowda, S.L. Thibeault, Insights Into the Role of Collagen in Vocal Fold Health and Disease, Journal of Voice 31(5) (2017) 520-527.

[51] D. Munoz-Pinto, P. Whittaker, M.S. Hahn, Lamina propria cellularity and collagen composition: an integrated assessment of structure in humans, The Annals of otology, rhinology, and laryngology 118(4) (2009) 299-306.

[52] M. Asgari, N. Latifi, H.K. Heris, H. Vali, L. Mongeau, In vitro fibrillogenesis of tropocollagen type III in collagen type I affects its relative fibrillar topology and mechanics, Sci Rep 7(1) (2017) 1392.

[53] T. Tateya, I. Tateya, D.M. Bless, Immuno-scanning electron microscopy of collagen types I and III in human vocal fold lamina propria, The Annals of otology, rhinology, and laryngology 116(2) (2007) 156-9.

[54] M. Sivasankar, A. Ivanisevic, Atomic force microscopy investigation of vocal fold collagen, Laryngoscope 117(10) (2007) 1876-81.

[55] K. Gelse, E. Pöschl, T. Aigner, Collagens—structure, function, and biosynthesis, Advanced Drug Delivery Reviews 55(12) (2003) 1531-1546.

[56] D.S. Harburger, D.A. Calderwood, Integrin signalling at a glance, Journal of Cell Science 122(2) (2009) 159-163.

[57] A.C.d.O. Gonzalez, T.F. Costa, Z.d.A. Andrade, A.R.A.P. Medrado, Wound healing - A literature review, Anais Brasileiros de Dermatologia 91(5) (2016) 614-620.

[58] P.D. Ward, S.L. Thibeault, S.D. Gray, Hyaluronic Acid: Its Role in Voice, Journal of Voice 16(3) (2002) 303-309.

[59] R.W. Chan, S.D. Gray, I.R. Titze, The importance of hyaluronic acid in vocal fold biomechanics, Otolaryngology--head and neck surgery : official journal of American Academy of Otolaryngology-Head and Neck Surgery 124(6) (2001) 607-14.

[60] D. Vigetti, E. Karousou, M. Viola, S. Deleonibus, G. De Luca, A. Passi, Hyaluronan: biosynthesis and signaling, Biochimica et biophysica acta 1840(8) (2014) 2452-9.

[61] B. Smedsrød, Cellular events in the uptake and degradation of hyaluronan, Advanced Drug Delivery Reviews 7(2) (1991) 265-278.

[62] P.D. Ward, S.L. Thibeault, S.D. Gray, Hyaluronic acid: its role in voice, Journal of voice : official journal of the Voice Foundation 16(3) (2002) 303-9.

[63] E.A. Turley, Hyaluronan-binding proteins and receptors, Advanced Drug Delivery Reviews 7(2) (1991) 257-264.

[64] R. Krasinski, H. Tchorzewski, [Hyaluronan-mediated regulation of inflammation], Postepy higieny i medycyny doswiadczalnej (Online) 61 (2007) 683-9.

[65] D. Jiang, J. Liang, P.W. Noble, Hyaluronan in tissue injury and repair, Annual review of cell and developmental biology 23 (2007) 435-61.

[66] X.Z. Shu, Y. Liu, Y. Luo, M.C. Roberts, G.D. Prestwich, Disulfide Cross-Linked Hyaluronan Hydrogels, Biomacromolecules 3(6) (2002) 1304-1311.

[67] S. Hertegård, L. Hallén, C. Laurent, E. Lindström, K. Olofsson, P. Testad, Å. Dahlqvist, Cross-Linked Hyaluronan Used as Augmentation Substance for Treatment of Glottal Insufficiency: Safety Aspects and Vocal Fold Function, The Laryngoscope 112(12) (2002) 2211-2219.

[68] S. Hertegard, L. Hallen, C. Laurent, E. Lindstrom, K. Olofsson, P. Testad, A. Dahlqvist, Cross-linked hyaluronan versus collagen for injection treatment of glottal insufficiency: 2-year follow-up, Acta Otolaryngol 124(10) (2004) 1208-14.

[69] D. Campoccia, P. Doherty, M. Radice, P. Brun, G. Abatangelo, D.F. Williams, Semisynthetic resorbable materials from hyaluronan esterification, Biomaterials 19(23) (1998) 2101-27.

[70] C.L. Finck, B. Harmegnies, A. Remacle, P. Lefebvre, Implantation of esterified hyaluronic acid in microdissected Reinke's space after vocal fold microsurgery: short- and long-term results, Journal of voice : official journal of the Voice Foundation 24(5) (2010) 626-35.

[71] X. Chen, S.L. Thibeault, Cell-cell interaction between vocal fold fibroblasts and bone marrow mesenchymal stromal cells in three-dimensional hyaluronan hydrogel, J Tissue Eng Regen Med (2013).

[72] T. Caton, S.L. Thibeault, S. Klemuk, M.E. Smith, Viscoelasticity of Hyaluronan and Nonhyaluronan Based Vocal Fold Injectables: Implications for Mucosal Versus Muscle Use, The Laryngoscope 117(3) (2007) 516-521.

[73] S. Kazemirad, H.K. Heris, L. Mongeau, Viscoelasticity of hyaluronic acid-gelatin hydrogels for vocal fold tissue engineering, Journal of Biomedical Materials Research Part B: Applied Biomaterials 104(2) (2016) 283-290.

[74] K.P. Vercruysse, D.M. Marecak, J.F. Marecek, G.D. Prestwich, Synthesis and in vitro degradation of new polyvalent hydrazide cross-linked hydrogels of hyaluronic acid, Bioconjugate chemistry 8(5) (1997) 686-94.

[75] X. Chen, S.L. Thibeault, Biocompatibility of a synthetic extracellular matrix on immortalized vocal fold fibroblasts in 3-D culture, Acta biomaterialia 6(8) (2010) 2940-8.

[76] X.Z. Shu, Y. Liu, F. Palumbo, G.D. Prestwich, Disulfide-crosslinked hyaluronan-gelatin hydrogel films: a covalent mimic of the extracellular matrix for in vitro cell growth, Biomaterials 24(21) (2003) 3825-34.

[77] S.L. Thibeault, S.A. Klemuk, X. Chen, B.H. Quinchia Johnson, In Vivo engineering of the vocal fold ECM with injectable HA hydrogels-late effects on tissue repair and biomechanics in a rabbit model, Journal of voice : official journal of the Voice Foundation 25(2) (2011) 249-53.

[78] S. Duflo, S.L. Thibeault, W. Li, X.Z. Shu, G. Prestwich, Effect of a synthetic extracellular matrix on vocal fold lamina propria gene expression in early wound healing, Tissue engineering 12(11) (2006) 3201-7.

[79] S. Duflo, S.L. Thibeault, W. Li, X.Z. Shu, G.D. Prestwich, Vocal fold tissue repair in vivo using a synthetic extracellular matrix, Tissue engineering 12(8) (2006) 2171-80.

[80] S.L. Thibeault, S. Duflo, Inflammatory cytokine responses to synthetic extracellular matrix injection to the vocal fold lamina propria, The Annals of otology, rhinology, and laryngology 117(3) (2008) 221-6.

[81] J.M.S. Coppoolse, T.G. Van Kooten, H.K. Heris, L. Mongeau, N.Y.K. Li, S.L. Thibeault, J. Pitaro, O. Akinpelu, S.J. Daniel, An In Vivo Study of Composite Microgels Based on Hyaluronic Acid and Gelatin for the Reconstruction of Surgically Injured Rat Vocal Folds, Journal of Speech, Language, and Hearing Research 57(2) (2014).

[82] H.K. Heris, J. Daoud, S. Sheibani, H. Vali, M. Tabrizian, L. Mongeau, Investigation of the Viability, Adhesion, and Migration of Human Fibroblasts in a Hyaluronic Acid/Gelatin Microgel-Reinforced Composite Hydrogel for Vocal Fold Tissue Regeneration, Advanced healthcare materials 5(2) (2016) 255-65.

[83] B.Q. Johnson, R. Fox, X. Chen, S. Thibeault, Tissue regeneration of the vocal fold using bone marrow mesenchymal stem cells and synthetic extracellular matrix injections in rats, Laryngoscope 120(3) (2010) 537-45.

[84] J. Gaston, S.L. Thibeault, Hyaluronic acid hydrogels for vocal fold wound healing, Biomatter 3(1) (2013) e23799.

[85] X. Jia, J.A. Burdick, J. Kobler, R.J. Clifton, J.J. Rosowski, S.M. Zeitels, R. Langer, Synthesis and Characterization of in Situ Cross-Linkable Hyaluronic Acid-Based Hydrogels with Potential Application for Vocal Fold Regeneration, Macromolecules 37(9) (2004) 3239-3248.

[86] J.K. Kutty, K. Webb, Vibration Stimulates Vocal Mucosa-like Matrix Expression by Hydrogel-encapsulated Fibroblasts, Journal of tissue engineering and regenerative medicine 4(1) (2010) 62-72.

[87] J.K. Kutty, K. Webb, Mechanomimetic hydrogels for vocal fold lamina propria regeneration, Journal of biomaterials science. Polymer edition 20(5-6) (2009) 737-56.

[88] X. Jia, Y. Yeo, R.J. Clifton, T. Jiao, D.S. Kohane, J.B. Kobler, S.M. Zeitels, R. Langer, Hyaluronic acid-based microgels and microgel networks for vocal fold regeneration, Biomacromolecules 7(12) (2006) 3336-44.

[89] A.J. Farran, S.S. Teller, A.K. Jha, T. Jiao, R.A. Hule, R.J. Clifton, D.P. Pochan, R.L. Duncan, X. Jia, Effects of matrix composition, microstructure, and viscoelasticity on the behaviors of vocal fold fibroblasts cultured in three-dimensional hydrogel networks, Tissue Engineering. Part A 16(4) (2010) 1247-61.

[90] N. Sahiner, A.K. Jha, D. Nguyen, X. Jia, Fabrication and characterization of cross-linkable hydrogel particles based on hyaluronic acid: potential application in vocal fold regeneration, Journal of biomaterials science. Polymer edition 19(2) (2008) 223-43.

[91] Y. Luo, J.B. Kobler, J.T. Heaton, X. Jia, S.M. Zeitels, R. Langer, Injectable hyaluronic acid-dextran hydrogels and effects of implantation in ferret vocal fold, Journal of biomedical materials research. Part B, Applied biomaterials 93(2) (2010) 386-93.

[92] M.S. Hahn, B.A. Teply, M.M. Stevens, S.M. Zeitels, R. Langer, Collagen composite hydrogels for vocal fold lamina propria restoration, Biomaterials 27(7) (2006) 1104-9.

[93] H. Park, S. Karajanagi, K. Wolak, J. Aanestad, L. Daheron, J.B. Kobler, G. Lopez-Guerra, J.T. Heaton, R.S. Langer, S.M. Zeitels, Three-dimensional hydrogel model using adipose-derived stem cells for vocal fold augmentation, Tissue Engineering. Part A 16(2) (2010) 535-43.

[94] Y.m. Kim, S.H. Oh, J.s. Choi, S. Lee, J.C. Ra, J.H. Lee, J.y. Lim, Adipose‐derived stem cell‐containing hyaluronic acid/alginate hydrogel improves vocal fold wound healing, Laryngoscope 124(3) (2014) E64-E72.

[95] N. Hiwatashi, S. Hirano, M. Mizuta, T. Kobayashi, Y. Kawai, S.I. Kanemaru, T. Nakamura, J. Ito, K. Kawai, S. Suzuki, The efficacy of a novel collagen-gelatin scaffold with basic fibroblast growth factor for the treatment of vocal fold scar, J Tissue Eng Regen Med (2015).

[96] X. Chen, S.L. Thibeault, Novel isolation and biochemical characterization of immortalized fibroblasts for tissue engineering vocal fold lamina propria, Tissue engineering. Part C, Methods 15(2) (2009) 201-12.

[97] C. Leydon, J.A. Selekman, S. Palecek, S.L. Thibeault, Human Embryonic Stem Cell-Derived Epithelial Cells in a Novel In Vitro Model of Vocal Mucosa, Tissue Engineering Part A (2013) 130626063917000.

[98] S.N. King, S.E. Hanson, X. Chen, J. Kim, P. Hematti, S.L. Thibeault, In vitro characterization of macrophage interaction with mesenchymal stromal cell-hyaluronan hydrogel constructs, Journal of biomedical materials research. Part A 102(3) (2014) 890-902.

[99] Y. Kumai, J.B. Kobler, H. Park, M. Galindo, V.L.M. Herrera, S.M. Zeitels, Modulation of vocal fold scar fibroblasts by adipose-derived stem/stromal cells, The Laryngoscope 120(2) (2010) 330-337.

[100] S.N. King, F. Chen, M.E. Jette, S.L. Thibeault, Vocal fold fibroblasts immunoregulate activated macrophage phenotype, Cytokine 61(1) (2013) 228-36.

[101] M. Imaizumi, Y. Sato, D.T. Yang, S.L. Thibeault, In vitro epithelial differentiation of human induced pluripotent stem cells for vocal fold tissue engineering, The Annals of otology, rhinology, and laryngology 122(12) (2013) 737-47.

[102] D.K. Chhetri, C. Head, E. Revazova, S. Hart, S. Bhuta, G.S. Berke, Lamina propria replacement therapy with cultured autologous fibroblasts for vocal fold scars, Otolaryngology--head and neck surgery : official journal of American Academy of Otolaryngology-Head and Neck Surgery 131(6) (2004) 864-70.

[103] S.L. Thibeault, S.A. Klemuk, M.E. Smith, C. Leugers, G. Prestwich, In vivo comparison of biomimetic approaches for tissue regeneration of the scarred vocal fold.(Report), Tissue Engineering, Part A: Tissue Engineering 15(7) (2009) 1481.

[104] B. Svensson, S.R. Nagubothu, J. Cedervall, R.W. Chan, K. Le Blanc, M. Kimura, L. Ahrlund-Richter, A. Tolf, S. Hertegard, Injection of human mesenchymal stem cells improves healing of vocal folds after scar excision--a xenograft analysis, Laryngoscope 121(10) (2011) 2185-90.

[105] S. Hertegard, J. Cedervall, B. Svensson, K. Forsberg, F.H. Maurer, D. Vidovska, P. Olivius, L. Ahrlund-Richter, K. Le Blanc, Viscoelastic and histologic properties in scarred rabbit vocal folds after mesenchymal stem cell injection, Laryngoscope 116(7) (2006) 1248-54.

[106] J.W. Choi, J.K. Park, J.W. Chang, Y. Kim da, M.S. Kim, Y.S. Shin, C.H. Kim, Small intestine submucosa and mesenchymal stem cells composite gel for scarless vocal fold regeneration, Biomaterials 35(18) (2014) 4911-8.

[107] S. Ohno, S. Hirano, S. Kanemaru, Y. Kitani, T. Kojima, I. Tateya, T. Nakamura, J. Ito, Implantation of an atelocollagen sponge with autologous bone marrow-derived mesenchymal stromal cells for treatment of vocal fold scarring in a canine model, The Annals of otology, rhinology, and laryngology 120(6) (2011) 401-8.

[108] S. Ohno, S. Hirano, I. Tateya, S. Kanemaru, H. Umeda, A. Suehiro, Y. Kitani, Y. Kishimoto, T. Kojima, T. Nakamura, J. Ito, Atelocollagen sponge as a stem cell implantation scaffold for the treatment of scarred vocal folds, The Annals of otology, rhinology, and laryngology 118(11) (2009) 805-10.

[109] W. Xu, R. Hu, E. Fan, D. Han, Adipose-Derived Mesenchymal Stem Cells in Collagen—Hyaluronic Acid Gel Composite Scaffolds for Vocal Fold Regeneration, Annals of Otology, Rhinology & Laryngology 120(2) (2011) 123-130.

[110] Y.M. Kim, S.H. Oh, J.S. Choi, S. Lee, J.C. Ra, J.H. Lee, J.Y. Lim, Adipose-derived stem cell-containing hyaluronic acid/alginate hydrogel improves vocal fold wound healing, Laryngoscope 124(3) (2014) E64-72.

[111] T. Yamaguchi, T. Shin, H. Sugihara, Reconstruction of the laryngeal mucosa: a three-dimensional collagen gel matrix culture, Archives of Otolaryngology–Head & Neck Surgery 122(6) (1996) 649-654.

[112] M. Sivasankar, E. Erickson, M. Rosenblatt, R.C. Branski, Hypertonic challenge to porcine vocal folds: effects on epithelial barrier function, Otolaryngology--head and neck surgery : official journal of American Academy of Otolaryngology-Head and Neck Surgery 142(1) (2010) 79-84.

[113] S.S. Teller, A.J.E. Farran, L. Xiao, T. Jiao, R.L. Duncan, R.J. Clifton, X. Jia, High-frequency viscoelastic shear properties of vocal fold tissues: implications for vocal fold tissue engineering, Tissue Engineering. Part A 18(19-20) (2012) 2008.

[114] J.L. Long, P. Zuk, G.S. Berke, D.K. Chhetri, Epithelial differentiation of adipose‐derived stem cells for laryngeal tissue engineering, Laryngoscope 120(1) (2010) 125-131.

[115] G.A. Gill, A. Buda, M. Moorghen, P.W. Dettmar, M. Pignatelli, Characterisation of adherens and tight junctional molecules in normal animal larynx; determining a suitable model for studying molecular abnormalities in human laryngopharyngeal reflux, Journal of Clinical Pathology 58(12) (2005) 1265-1270.

[116] H.H. Bragulla, D.G. Homberger, Structure and functions of keratin proteins in simple, stratified, keratinized and cornified epithelia, Journal of Anatomy 214(4) (2009) 516-559.

[117] C. Ling, Q. Li, M.E. Brown, Y. Kishimoto, Y. Toya, E.E. Devine, K.-O. Choi, K. Nishimoto, I.G. Norman, T. Tsegyal, J.J. Jiang, W.J. Burlingham, S. Gunasekaran, L.M. Smith, B.L. Frey, N.V. Welham, Bioengineered vocal fold mucosa for voice restoration, Science Translational Medicine 7(314) (2015) 314ra187-314ra187.

[118] T. Walimbe, A. Panitch, M.P. Sivasankar, An in vitro scaffold-free epithelial–fibroblast coculture model for the larynx, The Laryngoscope 127(6) (2017) E185-E192.

[119] E.E. Levendoski, C. Leydon, S.L. Thibeault, Vocal Fold Epithelial Barrier in Health and Injury A Research Review, Journal of speech, language, and hearing research : JSLHR 57(5) (2014) 1679-1691.

[120] E. Erickson-Levendoski, M.P. Sivasankar, Role for Ion Transport in Porcine Vocal Fold Epithelial Defense to Acid Challenge, Otolaryngology -- Head and Neck Surgery 146(2) (2012) 272-278.

[121] L. Palencia, A. Das, S.P. Palecek, S.L. Thibeault, C. Leydon, Epidermal growth factor mediated healing in stem cell-derived vocal fold mucosa, The Journal of surgical research 197(1) (2015) 32-8.

[122] N. Hiwatashi, R. Bing, I. Kraja, R.C. Branski, Mesenchymal stem cells have antifibrotic effects on transforming growth factor‐β1‐stimulated vocal fold fibroblasts, The Laryngoscope (2016).

[123] C. Leydon, M. Imaizumi, R.S. Bartlett, S.F. Wang, S.L. Thibeault, Epithelial cells are active participants in vocal fold wound healing: an in vivo animal model of injury, PloS one 9(12) (2014) e115389.

[124] X. Lim, I. Tateya, T. Tateya, A. Muñoz-Del-Río, D.M. Bless, Immediate Inflammatory Response and Scar Formation in Wounded Vocal Folds, Annals of Otology, Rhinology & Laryngology 115(12) (2006) 921-929.

[125] N. Hiwatashi, S. Hirano, M. Mizuta, I. Tateya, S. Kanemaru, T. Nakamura, J. Ito, K. Kawai, S. Suzuki, Biocompatibility and efficacy of collagen/gelatin sponge scaffold with sustained release of basic fibroblast growth factor on vocal fold fibroblasts in 3-dimensional culture, The Annals of otology, rhinology, and laryngology 124(2) (2015) 116-25.

[126] X. Chen, S.L. Thibeault, Response of Fibroblasts to Transforming Growth Factor-β1 on Two-Dimensional and in Three-Dimensional Hyaluronan Hydrogels, Tissue Engineering. Part A 18(23-24) (2012) 2528-38.

[127] A.J.E. Farran, S.S. Teller, F. Jia, J.C. Rodney, R.L. Duncan, X. Jia, Design and Characterization of a Dynamic Vibrational Culture System, Journal of tissue engineering and regenerative medicine 7(3) (2013) 213-225.

[128] J.M. Fishman, J. Long, M. Gugatschka, P. De Coppi, S. Hirano, S. Hertegard, S.L. Thibeault, M.A. Birchall, Stem cell approaches for vocal fold regeneration, The Laryngoscope (2016) n/a-n/a.

[129] S. Suzuki, M. Sato, H. Senoo, K. Ishikawa, Direct cell-cell interaction enhances pro-MMP-2 production and activation in co-culture of laryngeal cancer cells and fibroblasts: involvement of EMMPRIN and MT1-MMP, Experimental cell research 293(2) (2004) 259-66.

[130] R.A. Scott, A.K. Ramaswamy, K. Park, A. Panitch, Decorin mimic promotes endothelial cell health in endothelial monolayers and endothelial–smooth muscle co-cultures, Journal of Tissue Engineering and Regenerative Medicine (2015) n/a-n/a.

[131] T.B. Lombardo Bedran, D. Palomari Spolidorio, D. Grenier, Green tea polyphenol epigallocatechin-3-gallate and cranberry proanthocyanidins act in synergy with cathelicidin (LL-37) to reduce the LPS-induced inflammatory response in a three-dimensional co-culture model of gingival epithelial cells and fibroblasts, Archives of Oral Biology 60(6) (2015) 845-853.

[132] S. Chaterji, K. Park, A. Panitch, Scaffold-free in vitro arterial mimetics: the importance of smooth muscle-endothelium contact, Tissue Engineering. Part A 16(6) (2010) 1901-12.

[133] D. Papazian, V.R. Wagtmann, S. Hansen, P.A. Wurtzen, Direct contact between dendritic cells and bronchial epithelial cells inhibits T cell recall responses towards mite and pollen allergen extracts in vitro, Clinical and experimental immunology (2015).

[134] H. Liao, D. Munoz-Pinto, X. Qu, Y. Hou, M.A. Grunlan, M.S. Hahn, Influence of hydrogel mechanical properties and mesh size on vocal fold fibroblast extracellular matrix production and phenotype, Acta biomaterialia 4(5) (2008) 1161-71.

[135] A. Biernacka, M. Dobaczewski, N.G. Frangogiannis, TGF-β signaling in fibrosis, Growth factors (Chur, Switzerland) 29(5) (2011) 196-202.

[136] B. Vyas, K. Ishikawa, S. Duflo, X. Chen, S.L. Thibeault, Inhibitory effects of hepatocyte growth factor and interleukin-6 on transforming growth factor-beta1 mediated vocal fold fibroblast-myofibroblast differentiation, The Annals of otology, rhinology, and laryngology 119(5) (2010) 350-7.

[137] A. Branco, S.M. Bartley, S.N. King, M.E. Jette, S.L. Thibeault, Vocal fold myofibroblast profile of scarring, Laryngoscope 126(3) (2016) E110-7.

[138] J.S. Choi, S. Lee, Y. Kim da, Y.M. Kim, M.S. Kim, J.Y. Lim, Functional remodeling after vocal fold injury by small intestinal submucosa gel containing hepatocyte growth factor, Biomaterials 40 (2015) 98-106.

[139] T. Vu, L. Jin, P.K. Datta, Effect of Cigarette Smoking on Epithelial to Mesenchymal Transition (EMT) in Lung Cancer, Journal of clinical medicine 5(4) (2016).

[140] F.M. Davis, T.A. Stewart, E.W. Thompson, G.R. Monteith, Targeting EMT in cancer: opportunities for pharmacological intervention, Trends in pharmacological sciences 35(9) (2014) 479-88.

[141] K.R. Ginnebaugh, A. Ahmad, F.H. Sarkar, The therapeutic potential of targeting the epithelial-mesenchymal transition in cancer, Expert opinion on therapeutic targets 18(7) (2014) 731-45.

[142] T. Chen, H. Nie, X. Gao, J. Yang, J. Pu, Z. Chen, X. Cui, Y. Wang, H. Wang, G. Jia, Epithelial-mesenchymal transition involved in pulmonary fibrosis induced by multi-walled carbon nanotubes via TGF-beta/Smad signaling pathway, Toxicology letters 226(2) (2014) 150-62.

[143] M. Li, F. Luan, Y. Zhao, H. Hao, Y. Zhou, W. Han, X. Fu, Epithelial-mesenchymal transition: An emerging target in tissue fibrosis, Experimental biology and medicine (Maywood, N.J.) 241(1) (2016) 1-13.

[144] C.A.v. Blitterswijk, Tissue engineering, 2nd edition.. ed., Amsterdam : Academic Press2015.

[145] Z. Tong, X. Jia, Biomaterials-Based Strategies for the Engineering of Mechanically Active Soft Tissues, MRS communications 2(2) (2012) 31-39.

[146] S.F. Badylak, The extracellular matrix as a biologic scaffold material, Biomaterials 28(25) (2007) 3587-93.

[147] T. Tateya, I. Tateya, D.M. Bless, Collagen subtypes in human vocal folds, The Annals of otology, rhinology, and laryngology 115(6) (2006) 469-76.

[148] M.S. Hahn, J.B. Kobler, B.C. Starcher, S.M. Zeitels, R. Langer, Quantitative and Comparative Studies of the Vocal Fold Extracellular Matrix I: Elastic Fibers and Hyaluronic Acid, Annals of Otology, Rhinology & Laryngology 115(2) (2006) 156-164.

[149] T. Walimbe, A. Panitch, P.M. Sivasankar, A Review of Hyaluronic Acid and Hyaluronic Acid-based Hydrogels for Vocal Fold Tissue Engineering, Journal of Voice 31(4) (2017) 416-423.

[150] L. Lebel, Clearance of hyaluronan from the circulation, Advanced Drug Delivery Reviews 7(2) (1991) 221-235.

[151] S. Ouasti, R. Donno, F. Cellesi, M.J. Sherratt, G. Terenghi, N. Tirelli, Network connectivity, mechanical properties and cell adhesion for hyaluronic acid/PEG hydrogels, Biomaterials 32(27) (2011) 6456-70.

[152] N. Davidenko, C.F. Schuster, D.V. Bax, R.W. Farndale, S. Hamaia, S.M. Best, R.E. Cameron, Evaluation of cell binding to collagen and gelatin: a study of the effect of 2D and 3D architecture and surface chemistry, Journal of materials science. Materials in medicine 27(10) (2016) 148.

[153] K.E. Kadler, A. Hill, E.G. Canty-Laird, Collagen fibrillogenesis: fibronectin, integrins, and minor collagens as organizers and nucleators, Current Opinion in Cell Biology 20(5-24) (2008) 495-501.

[154] P.S. Mallur, C.A. Rosen, Vocal Fold Injection: Review of Indications, Techniques, and Materials for Augmentation, Clinical and Experimental Otorhinolaryngology 3(4) (2010) 177-182.

[155] L. Cuttle, M. Nataatmadja, J.F. Fraser, M. Kempf, R.M. Kimble, M.T. Hayes, Collagen in the scarless fetal skin wound: detection with picrosirius-polarization, Wound repair and regeneration : official publication of the Wound Healing Society [and] the European Tissue Repair Society 13(2) (2005) 198-204.

[156] P. Betz, A. Nerlich, J. Wilske, J. Tubel, R. Penning, W. Eisenmenger, Analysis of the immunohistochemical localization of collagen type III and V for the time-estimation of human skin wounds, International journal of legal medicine 105(6) (1993) 329-32.

[157] K. Stuart, A. Panitch, Characterization of Gels Composed of Blends of Collagen I, Collagen III, and Chondroitin Sulfate, Biomacromolecules 10(1) (2009) 25-31.

[158] J. Bella, Collagen structure: new tricks from a very old dog, The Biochemical journal 473(8) (2016) 1001-25.

[159] X. Xin, A. Borzacchiello, P.A. Netti, L. Ambrosio, L. Nicolais, Hyaluronic-acid-based semi-interpenetrating materials, Journal of Biomaterials Science, Polymer Edition 15(9) (2004) 1223-1236.

[160] Y.-l. Yang, L.J. Kaufman, Rheology and Confocal Reflectance Microscopy as Probes of Mechanical Properties and Structure during Collagen and Collagen/Hyaluronan Self-Assembly, Biophysical Journal 96(4) (2009) 1566-1585.

[161] J.H. Highberger, The Isoelectric Point of Collagen, Journal of the American Chemical Society 61(9) (1939) 2302-2303.

[162] D. Eng, M. Caplan, M. Preul, A. Panitch, Hyaluronan scaffolds: A balance between backbone functionalization and bioactivity, Acta biomaterialia 6(7) (2010) 2407-2414.

[163] S. Calve, S.J. Odelberg, H.-G. Simon, A Transitional Extracellular Matrix Instructs Cell Behavior During Muscle Regeneration, Developmental biology 344(1) (2010) 259-271.

[164] V.K. Lai, D.S. Nedrelow, S.P. Lake, B. Kim, E.M. Weiss, R.T. Tranquillo, V.H. Barocas, Swelling of Collagen-Hyaluronic Acid Co-Gels: An In Vitro Residual Stress Model, Annals of biomedical engineering 44(10) (2016) 2984-2993.

[165] T. Yeung, P.C. Georges, L.A. Flanagan, B. Marg, M. Ortiz, M. Funaki, N. Zahir, W. Ming, V. Weaver, P.A. Janmey, Effects of substrate stiffness on cell morphology, cytoskeletal structure, and adhesion, Cell motility and the cytoskeleton 60(1) (2005) 24-34.

[166] N.N. Vazquez-Portalati, C.E. Kilmer, A. Panitch, J.C. Liu, Characterization of Collagen Type I and II Blended Hydrogels for Articular Cartilage Tissue Engineering, Biomacromolecules 17(10) (2016) 3145-3152.

[167] Y.L. Yang, L.J. Kaufman, Rheology and confocal reflectance microscopy as probes of mechanical properties and structure during collagen and collagen/hyaluronan self-assembly, Biophysical journal 96(4) (2009) 1566-85.

[168] T.D. Mehra, K. Ghosh, X.Z. Shu, G.D. Prestwich, R.A. Clark, Molecular stenting with a crosslinked hyaluronan derivative inhibits collagen gel contraction, The Journal of investigative dermatology 126(10) (2006) 2202-9.

[169] Z. Feng, Y. Wagatsuma, M. Kikuchi, T. Kosawada, T. Nakamura, D. Sato, N. Shirasawa, T. Kitajima, M. Umezu, The mechanisms of fibroblast-mediated compaction of collagen gels and the mechanical niche around individual fibroblasts, Biomaterials 35(28) (2014) 8078-91.

[170] X. Zheng Shu, Y. Liu, F.S. Palumbo, Y. Luo, G.D. Prestwich, In situ crosslinkable hyaluronan hydrogels for tissue engineering, Biomaterials 25(7-8) (2004) 1339-48.

[171] K. Ghosh, Z. Pan, E. Guan, S. Ge, Y. Liu, T. Nakamura, X.-D. Ren, M. Rafailovich, R.A.F. Clark, Cell adaptation to a physiologically relevant ECM mimic with different viscoelastic properties, Biomaterials 28(4) (2007) 671-679.

[172] M. Barczyk, S. Carracedo, D. Gullberg, Integrins, Cell and tissue research 339(1) (2010) 269-80.

[173] J. Heino, The collagen family members as cell adhesion proteins, BioEssays : news and reviews in molecular, cellular and developmental biology 29(10) (2007) 1001-10.

[174] P.L. Jones, J. Crack, M. Rabinovitch, Regulation of tenascin-C, a vascular smooth muscle cell survival factor that interacts with the alpha v beta 3 integrin to promote epidermal growth factor receptor phosphorylation and growth, The Journal of cell biology 139(1) (1997) 279-93.

[175] I.O. Rosas, T.J. Richards, K. Konishi, Y. Zhang, K. Gibson, A.E. Lokshin, K.O. Lindell, J. Cisneros, S.D. MacDonald, A. Pardo, F. Sciurba, J. Dauber, M. Selman, B.R. Gochuico, N. Kaminski, MMP1 and MMP7 as Potential Peripheral Blood Biomarkers in Idiopathic Pulmonary Fibrosis, PLOS Medicine 5(4) (2008) e93.

[176] S. Calve, J. Isaac, J.P. Gumucio, C.L. Mendias, Hyaluronic acid, HAS1, and HAS2 are significantly upregulated during muscle hypertrophy, American Journal of Physiology - Cell Physiology 303(5) (2012) C577-C588.

[177] D. Vigetti, A. Genasetti, E. Karousou, M. Viola, P. Moretto, M. Clerici, S. Deleonibus, G. De Luca, V.C. Hascall, A. Passi, Proinflammatory Cytokines Induce Hyaluronan Synthesis and Monocyte Adhesion in Human Endothelial Cells through Hyaluronan Synthase 2 (HAS2) and the Nuclear Factor-κB (NF-κB) Pathway, Journal of Biological Chemistry 285(32) (2010) 24639-24645.

[178] S. Zanotti, T. Negri, C. Cappelletti, P. Bernasconi, E. Canioni, C. Di Blasi, E. Pegoraro, C. Angelini, P. Ciscato, A. Prelle, R. Mantegazza, L. Morandi, M. Mora, Decorin and biglycan expression is differentially altered in several muscular dystrophies, Brain : a journal of neurology 128(Pt 11) (2005) 2546-55.

[179] R. Ma, S. He, X. Liang, H. Yu, Y. Liang, X. Cai, Decorin prevents the development of CCl(4)-induced liver fibrosis in mice, Chinese medical journal 127(6) (2014) 1100-4.

[180] K. Chaudhary, H. Moore, A. Tandon, S. Gupta, R. Khanna, R.R. Mohan, Nanotechnology and adeno-associated virus-based decorin gene therapy ameliorates peritoneal fibrosis, American journal of physiology. Renal physiology 307(7) (2014) F777-82.

[181] T. Gambichler, A. Kreuter, M. Skrygan, B. Burkert, P. Altmeyer, G. Schieren, Decorin is significantly overexpressed in nephrogenic systemic fibrosis, American journal of clinical pathology 132(1) (2009) 139-43.

[182] J. Hao, H. Ju, S. Zhao, A. Junaid, T. Scammell-La Fleur, I.M.C. Dixon, Elevation of Expression of Smads 2, 3, and 4, Decorin and TGF-βin the Chronic Phase of Myocardial Infarct Scar Healing, Journal of Molecular and Cellular Cardiology 31(3) (1999) 667-678.

[183] K. Kuroda, H. Shinkai, Gene expression of types I and III collagen, decorin, matrix metalloproteinases and tissue inhibitors of metalloproteinases in skin fibroblasts from patients with systemic sclerosis, Archives of dermatological research 289(10) (1997) 567-72.

[184] S.R. Beanes, C. Dang, C. Soo, Y. Wang, M. Urata, K. Ting, E.W. Fonkalsrud, P. Benhaim, M.H. Hedrick, J.B. Atkinson, H.P. Lorenz, Down-regulation of decorin, a transforming growth factor–beta modulator, is associated with scarless fetal wound healing, Journal of Pediatric Surgery 36(11) (2001) 1666-1671.

[185] S.D. Gray, S.S.N. Pignatari, P. Harding, Morphologic ultrastructure of anchoring fibers in normal vocal fold basement membrane zone, Journal of Voice 8(1) (1994) 48-52.

[186] N.Y.K. Li, H.K. Heris, L. Mongeau, Current Understanding and Future Directions for Vocal Fold Mechanobiology, Journal of cytology & molecular biology 1(1) (2013) 001.

VITA

EDUCATION

PhD., Biomedical Engineering, Purdue University *Sep 2018*

Advisors: Preeti Sivasankar, Ph.D., Alyssa Panitch, Ph.D.

Bachelor of Technology, Biotechnology, University of Pune *May 2013*

WORK EXPERIENCE

Biology Intern, Symic Bio *Jan 2018 – Jun 2018*

- Designed and conducted in-vitro and ex-vivo studies for mechanism of action data for drug discovery and optimization programs resulting in data set used to choose lead candidate.
- Expanded and maintained mammalian cell cultures to support 5 different projects in 3 disease indications.
- Developed and executed cell based assays to evaluate and advance novel compounds in various therapeutic indications such as fibrosis and cardiovascular diseases
- Designed and executed complex multiplexing immunologic assays for in vitro and ex vivo imaging
- Designed and executed complex traditional and competitive binding ELISAs using liquid handling systems
- Initiated and managed collaboration with neighboring university to expand in vitro analytical capabilities for the company's research team

RESEARCH EXPERIENCE

Graduate Research Assistant, Purdue University *Aug 2013 – Present*

- Engineered an interpenetrating 3 dimensional collagen - hyaluronic acid hydrogel for vocal fold wound healing
- Developed tools and methods to culture cells in 3 dimensions and conduct in-vitro cell based assays such as immunofluorescence, gene expression, proliferation and viability

- Performed fluorescence assisted cell sorting (FACS) to embed pure populations of breast cancer stem cells in 3D hyaluronic acid hydrogels to test mechanically driven epithelial to mesenchymal transition of cancer stem cells
- Engineered a physiologically relevant vocal fold fibroblast-epithelial cell coculture model to test therapeutics
- Tested the anti-fibrotic effects of MK-II inhibitor peptides on activated fibroblasts
- Developed methods to characterize hydrogels such as rheology, cryo-SEM, swelling and degradation

NSF I-Corps Entrepreneurial Lead, Purdue University *Aug 2016 – Dec 2016*

- Performed over 80 customer discovery interviews to find a product market fit for an autologous artificial skin graft using Lean LaunchPad
- Developed and validated value propositions, key resources, key activities, cost structures, revenue streams and partners using how to build a startup's business model canvas
- Evaluated regulatory affairs such as IND filing involved in commercializing biologics and medical devices

Undergraduate Researcher, University of Pune *May 2011 – May 2013*

- Designed and validated agarose-guar gum biopolymer matrices for immobilization of yeast to enchance continuous ethanol production by 17% in comparison to standard fermentation techniques
- Investigated and screened alternative soil microbial resources for production of shikimic acid, precursor for Tamiflu

RESEARCH SKILLS

Cell Culture: Mammalian Cell Lines, Primary Cells, 3-D Cell Culture, Coculture, Cancer Cells

Ex-Vivo: Tissue Dissections, Sectioning and Handling, Imaging

Microscopy: Confocal, Light, Fluorescent, Cryo-SEM, Birefringence

Molecular Biology: DNA and RNA Extraction, qRT-PCR, SDS-PAGE, Western Blots

Immunoassays: ELISA, MSD, Antibody Optimization, Binding Assays, FACS

Cell Based Assays: Proliferation, Cytotoxicity, Apoptosis, Migration, Inhibition

Hydrogels: Hyaluronic Acid, Collagen, Laminin, Matrigel gels

Bioconjugation: Organic Synthesis, Polymer Synthesis, Modification and Characterization

Characterization: NMR Spectroscopy, Rheometry, HPLC, Live-Dead and Cell Based Assays

Software Skills: SoftMax Pro, ImageJ, MSD WorkBench, GraphPad PRISM, Minitab, Adobe Illustrator and Photoshop, MS Word, MS Excel, MS Powerpoint

PUBLICATIONS

- **Walimbe T.**, Calve S., Panitch A., Sivasankar MP. "Incorporation of Type I and III Collagens in Tunable Hyaluronan Hydrogels for Vocal Fold Tissue Engineering". *In writing.*
- Liu X., **Walimbe T.**, Schrock WP., Zhang W., Sivasankar MP. (2017) "Acute Nanoparticle Exposure to Vocal Folds: A Laboratory Study", *Journal of Voice*. Volume 31, Issue 6, 662 – 668
- **Walimbe T**., Panitch A., Sivasankar MP. (2017) "A review of Hyaluronic Acid and Hyaluronic Acid Hydrogels for Vocal Fold Tissue Engineering", *Journal of Voice*. Volume 31, Issue 4, 416 – 423
- **Walimbe T.**, Panitch A., Sivasankar MP. (2016) "An In-vitro Scaffold-free Epithelial-Fibroblast Coculture Model for the Larynx", *The Laryngoscope*. Volume 127, Issue 6, 185 – 192

PRESENTATIONS

- **Walimbe T.,** Silva Garcia JM., Panitch A., Calve S., Solorio L. (2017) "Assessing the Effect of Stiffness on CD44 Expression of Highly Tumorigenic Breast Cancer Stem Cells." BMES National Meeting. Cancer Mechanobiology. Poster Presentation.
- **Walimbe T.**, Panitch A, Sivasankar MP. (2016) "Hyaluronic Acid Based Vocal Fold Tissue Engineering: A Review." 45th Voice Foundation Annual Symposium: Care of the Professional Voice. Podium Presentation.
- **Walimbe T.**, Panitch A., Sivasankar MP. (2016) "An In-Vitro Scaffold-Free Epithelial-Fibroblast Coculture Model for the Vocal Folds." Combined

Otolaryngology Spring Meetings: 96th Annual Meeting of the American Broncho-Esophagological Association. Podium Presentation.

- **Walimbe T.**, Kosinski A., Panitch A., Sivasankar MP. (2015) "RGD Concentration Alters Vocal Fold Fibroblast Gene Expression in 2D and 3D Systems." BMES National Meeting. Tissue Engineering. Poster Presentation.
- **Walimbe T.**, Thakar T., and Kulkarni S. (2012) "Immobilization of Yeast in a Novel Biopolymer Matrix for Enhancing Ethanol Production." 9th BRSI Convention and International Conference on Industrial Biotechnology. Poster Presentation.
- Godbole M., **Walimbe T.**, Thakar T., Patil R., Raut A., and Kate S. (2012) "Prospecting Alternative Soil Microbial Resources for Production of Shikimic Acid, Precursor of Tamiflu." 9th BRSI Convention and International Conference on Industrial Biotechnology. Poster Presentation.

LEADERSHIP AND SERVICE ACTIVITES

Purdue Biomedical Engineering Graduate Student Association

Professional Development Head | May 2016 – May 2017

Vice President, Ombudsman | May 2015 – May 2016

Treasurer | May 2014 – May 2015

Purdue Women In Engineering Program

Graduate Women's Gatherings Leadership Team | May 2015 – May 2017

Access Engineering Leadership Team | May 2015 – August 2015

ACHIEVEMENTS AND AWARDS

- Culture Hero, Symic Bio: For conquering disease with edgy science and disciplined execution of research
- Best Poster Award: Health and Disease: Science, Technology, and Culture Graduate Student Poster Competition
- Graduate Student Travel Award: Purdue Graduate Student Government (PGSG)
- University Valedictorian, University of Pune